TRC2102

Effect of Aggregate-Binder Compatibility on Performance of Asphalt Mixtures in Arkansas

Zahid Hossain, Ph.D., P.E.
Andrew F. Braham Ph.D., P.E.

Department of Civil Engineering, Arkansas State University
Department of Civil Engineering, The University of Arkansas

Final Report

August 2023

TRC2102

Effect of Aggregate-Binder Compatibility on Performance of Asphalt Mixtures in Arkansas

Zahid Hossain, Ph.D., P.E.
Andrew F. Braham Ph.D., P.E.

Department of Civil Engineering, Arkansas State University
Department of Civil Engineering, The University of Arkansas

Final Report

August 2023

Arkansas Department of Transportation

Notice of Nondiscrimination

The Arkansas Department of Transportation (ARDOT) complies with all civil rights provisions of federal statutes and related authorities that prohibit discrimination in programs and activities receiving federal financial assistance. Therefore, the Department does not discriminate on the basis of race, sex, color, age, national origin, religion (not applicable as a protected group under the Federal Motor Carrier Safety Administration Title VI Program), disability, Limited English Proficiency (LEP), or low-income status in the admission, access to and treatment in the Department's programs and activities, as well as the Department's hiring or employment practices. Complaints of alleged discrimination and inquiries regarding the Department's nondiscrimination policies may be directed to Civil Rights Officer Joanna P. McFadden (ADA/504/ Title VI Coordinator), P. 0. Box 2261, Little Rock, AR 72203, (501) 569-2298, (Voice/TTY 711), or the following email address: joanna.mcfadden@ardot.gov.

Free language assistance for Limited English Proficient individuals is available upon request.

This notice is available from the ADA/504/Tittle VI Coordinator in large print, on audiotape and Braille

Disclaimer:

The contents of this report reflect the views of the authors, who are responsible for the facts and the accuracy of the data presented herein. The contents do not necessarily reflect the official views or policies of ARDOT and they assume no liability for the contents or use thereof. This report does not constitute a standard, specification, or regulation. Comments contained in this report related to specific testing equipment and materials should not be considered an endorsement of any commercial product or service; no such endorsement is intended or implied.

Effect of Aggregate-Binder Compatibility on Performance of Asphalt Mixtures in Arkansas

By

Zahid Hossain, Ph.D., P.E.
Professor of Civil Engineering, Arkansas State University (A-State)

Andrew F. Braham, Ph.D., P.E.
Professor of Civil Engineering, University of Arkansas (UARK)

Prepared For
Arkansas Department of Transportation (ARDOT)

August 4, 2023

Final Report

Acknowledgments

This document presents the findings of the ARDOT-sponsored *TRC 2102, Effect of Aggregate-Binder Compatibility on Performance of Asphalt Mixtures in Arkansas*. The authors would like to show their gratitude to the ARDOT for providing financial assistance during this research project. The authors are grateful for the assistance of those who took part in the research project, including the ARDOT employees from the Systems Information and Research Section and the State Materials Laboratory. The authors also acknowledge the talents and efforts of graduate research assistants Md. Rafiue Islam, Mohammad Oyan, Abu Sayed Akid, and David Murphy, and several research assistants at A-State and UARK. Industry partners and material suppliers are also greatly appreciated for their roles in the successful completion of this project.

Technical Report Documentation Page

1. Report No.	2. Government Accession No.	3. Recipient's Catalog No.
4. Title and Subtitle Effect of Aggregate-Binder Compatibility on Performance of Asphalt Mixtures in Arkansas		5. Report Date August 2023 6. Performing Organization Code
7. Author(s) Zahid Hossain, 0000-0003-3395-564X, https://orcid.org/0000-0003-3395-564X Andrew Braham, 0000-0001-7994-5290, https://orcid.org/0000-0001-7994-5290		8. Performing Organization Report No.
9. Performing Organization Name and Address Arkansas State University, 2105 East, Aggie Rd, Jonesboro, AR 72401 University of Arkansas, 1 University of Arkansas, Fayetteville, AR 72701		10. Work Unit No. (TRAIS) 11. Contract or Grant No. TRC2102
12. Sponsoring Agency Name and Address Arkansas Department of Transportation 10324 Interstate 30, Little Rock, AR 72209		13. Type of Report and Period Covered Final Report 14. Sponsoring Agency Code
15. Supplementary Notes [Provided by agency]		

16. Abstract

The main objectives of this study were to assess compatibility among different types of binders and aggregates and to determine the maximum amount of sandstone aggregates in asphalt concrete surface mix (ACHM). To this end, three Performance Grade (PG) binders (PG 64-22, PG 70-22, and PG 76-22), each from six different sources were evaluated in the laboratory. Four types of aggregates (limestone, sandstone, novaculite, and dolomite), each from two different sources, were evaluated for their physical and mechanical properties. A total of 144 loose mixtures were subjected to the Texas Boiling Test (TBT). Five ACHM plant mixtures were evaluated by conducting performance tests such as dynamic modulus, Hamburg Wheel Tracking, Illinois Flexibility Index Test, Indirect Tensile Cracking Test (IDEAL-CT), and Tensile Strength Ratio. Furthermore, six ACHM mixtures with varying amounts of sandstone were prepared and tested in the laboratory. Sandstone aggregates were more absorptive than the others. Hard binders (e.g., PG 70-22) binders were found to possess higher adhesion energy than soft binders (PG 64-22). However, the performance properties of the binders were found to be crude-source dependent. The ACHM mixtures with high sandstone were found to be more susceptible to moisture damage and cracking. The tested binders, aggregates, and binder-aggregate systems were ranked based on their performance properties. t is recommended to set a maximum absorption of aggregates to 2%. The pH measurements of aggregates and binders can be incorporated into the QC/QA protocols to understand their compatibility, and the TBT can be followed to determine the moisture resistance of asphalt mixtures. Asphalt producers are suggested to use the most compatible aggregates and binders, based on the compatibility database provided in this report. It is also recommended to set the maximum level of sandstone in surface ACHM at 60%.

17. Key Words Asphalt Concrete, Compatibility, Moisture Resistance, Sandstone, Durability	18. Distribution Statement No restrictions. This document is available to the public through the National Technical Information Service, Springfield, VA 22161.		
19. Security Classification (of this report) Unclassified	20. Security Classification (of this page) Unclassified	21. No. of Pages 110	22. Price

Form DOT F 1700.7 (8-72) Reproduction of completed page authorized

SI* (MODERN METRIC) CONVERSION FACTORS

APPROXIMATE CONVERSIONS TO SI UNITS

Symbol	When You Know	Multiply By	To Find	Symbol
		LENGTH		
in	inches	25.4	millimeters	mm
ft	feet	0.305	meters	m
yd	yards	0.914	meters	m
mi	miles	1.61	kilometers	km
		AREA		
in^2	square inches	645.2	square millimeters	mm^2
ft^2	square feet	0.093	square meters	m^2
yd^2	square yard	0.836	square meters	m^2
ac	acres	0.405	hectares	ha
mi^2	square miles	2.59	square kilometers	km^2
		VOLUME		
fl oz	fluid ounces	29.57	milliliters	mL
gal	gallons	3.785	liters	L
ft^3	cubic feet	0.028	cubic meters	m^3
yd^3	cubic yards	0.765	cubic meters	m^3
		NOTE: volumes greater than 1000 L shall be shown in m^3		
		MASS		
oz	ounces	28.35	grams	g
lb	pounds	0.454	kilograms	kg
T	short tons (2000 lb)	0.907	megagrams (or "metric ton")	Mg (or "t"
		TEMPERATURE (exact degrees)		
°F	Fahrenheit	5 (F-32)/9 or (F-32)/1.8	Celsius	°C
		ILLUMINATION		
fc	foot-candles	10.76	lux	lx
fl	foot-Lamberts	3.426	$candela/m^2$	cd/m^2
		FORCE and PRESSURE or STRESS		
lbf	poundforce	4.45	newtons	N
lbf/in^2	poundforce per square inch	6.89	kilopascals	kPa

APPROXIMATE CONVERSIONS FROM SI UNITS

Symbol	When You Know	Multiply By	To Find	Symbol
		LENGTH		
mm	millimeters	0.039	inches	in
m	meters	3.28	feet	ft
m	meters	1.09	yards	yd
km	kilometers	0.621	miles	mi
		AREA		
mm^2	square millimeters	0.0016	square inches	in^2
m^2	square meters	10.764	square feet	ft^2
m^2	square meters	1.195	square yards	yd^2
ha	hectares	2.47	acres	ac
km^2	square kilometers	0.386	square miles	mi^2
		VOLUME		
mL	milliliters	0.034	fluid ounces	fl oz
L	liters	0.264	gallons	gal
m^3	cubic meters	35.314	cubic feet	ft^3
m^3	cubic meters	1.307	cubic yards	yd^3
		MASS		
g	grams	0.035	ounces	oz
kg	kilograms	2.202	pounds	lb
Mg (or "t")	megagrams (or "metric ton")	1.103	short tons (2000 lb)	T
		TEMPERATURE (exact degrees)		
°C	Celsius	1.8C+32	Fahrenheit	°F
		ILLUMINATION		
lx	lux	0.0929	foot-candles	fc
cd/m^2	$candela/m^2$	0.2919	foot-Lamberts	fl
		FORCE and PRESSURE or STRESS		
N	newtons	0.225	poundforce	lbf
kPa	kilopascals	0.145	poundforce per square inch	lbf/in^2

*SI is the symbol for the International System of Units. Appropriate rounding should be made to comply with Section 4 of ASTM E380.
(Revised March 2003

Table of Contents

List of Tables

List of Figures

List of Equations

List of Abbreviations and Acronyms

AASHTO	American Association of State Highway and Transportation Officials
ACHM	Asphalt Concrete Hot Mix
AFM	Atomic Force Microscope
APA	Asphalt Pavement Analyzer
ARDOT	Arkansas Department of Transportation
A-State	Arkansas State University
ASTM	American Society of Civil Engineers
BBR	Bending Beam Rheometer
CR	Compatibility Ratio
DMT	Derjaguin-Muller-Toporov
DSR	Dynamic Shear Rheometer
FHWA	Federal Highway Administration
HMA	Hot Mix Asphalt
HWT	Hamburg Wheel Tester
IDEAL-CT	Indirect Tensile Asphalt Cracking Test
IDT	Indirect Tension
I-FIT	Illinois Flexibility Index Test
OCA	Optical Contact Analyzer
PATTI	Pneumatic Adhesion Tensile Testing Instrument
PAV	Pressure Aging Vessel
PFQNM	Peakforce Quantitative Nanomechanical Mapping
PG	Performance Grade
RAP	Reclaimed Asphalt Pavement
RTFO	Rotational Thin Film Oven
RV	Rotational Viscometer
SD	Sessile Drop
SFE	Surface Free Energy
TBT	Texas Boiling Test
TRC	Transportation Research Committee
TSR	Tensile Strength Ratio
UARK	University of Arkansas

Executive Summary

The Arkansas Department of Transportation (ARDOT) engineers are concerned about the use of certain aggregates (i.e., sandstone) for preparing surface asphalt concrete hot mix (ACHM) and they are presumably incompatible with some asphalt binders. Such incompatibility can be associated with either chemical or adhesive bond failures between aggregate and binder. The ACHM prepared from incompatible asphalt binders and aggregates is highly prone to stripping that can cause other premature damages such as potholes, interlayer failures, and cracking. Also, the excessive amount of highly absorptive aggregates (e.g., sandstone) can potentially result in dry or brittle mixtures that can cause constructability and durability issues. In the current ARDOT specifications, the amount of limestone or gravel included in ACHM is limited due to skidding resistance concerns. There is no such limit on sandstone.

The main objective of this study was to recommend implementable guidelines that ensure the use of durable and compatible aggregate-binder systems in the asphalt concrete surface mix (ACHM) design for its enhanced performance in the field. To this end, three Performance Grade (PG) binders, namely, PG 64-22, PG 70-22, and PG 76-22, each from six different sources, were collected and tested in the laboratory through physical and rheological measurements such as penetration, viscosity, pH, optical contact angle (OCA), and atomic force microscope (AFM) analysis. Four types of aggregates (limestone, sandstone, novaculite, and dolomite), each from two different sources, were collected and tested for their physical and mechanical properties such as absorption, LA abrasion, pH, and OCA. Loose mixture samples prepared with different types of aggregate and binders were subjected to the Texas Boiling Test (TBT). Five ACHM plant mixture samples (12.5 mm and 9.0 mm) with different types of aggregates and binders were collected, and their performance was evaluated in the laboratory by conducting tests such as Hamburg Wheel Tracking, Illinois (I-FIT), Indirect Tensile Asphalt Cracking Tests (IDEAL-CT), and Tensile Strength Ratio (TSR). Furthermore, six ACHM mixtures [NMS of 12.5 mm and 9.0 mm; each with low (40%), medium (63%), and high (86%) percentages of sandstone] were prepared and evaluated in the laboratory.

All tested aggregates were basic (pH >7.0), and they comfortably met the ARDOT's LA abrasion requirement (% of loss < 40). In general, sandstone aggregates were found to be highly porous and absorptive (up to 3.7%). All tested asphalt binders were found acidic (pH < 7.0), and they met the viscosity requirements for pumping (i.e., viscosity ≤3 Pa.s at 135°C). Rheological and performance properties of tested asphalt binders were founds to be highly crude-source dependent. In general, polymer modified PG 70-22 and PG 76-22 binders were more viscous than PG 64-22 binders. The surface free energy (SFE)-based compatibility ratio data suggested dolomites and limestone mixtures would be more compatible with aggregate-binder systems than the others. The TBT results suggested that any aggregate-binder combination that could retain more than 85% of asphalt after the test, could be designated as a moisture-damage-resistant mixture. The percentage retention within the range of 70 and 85 could be improved by adding an anti-stripping agent to mixtures. Typically, percent retention increased with binder grade. The addition of binders recovered from reclaimed asphalt pavement (RAP) increased the stiffness of the virgin binder, which was evident from the penetration and viscosity test data. The RAP binder mostly increased the virgin binder's pH, yet remained acidic. The AFM test results suggested that it could be used as a viable tool for determining the moisture damage and examining the surface morphology and molecular-level properties of asphalt binders.

The tested binders have been ranked based on penetration, viscosity, work of cohesion, and pH values. An overall rank has been assigned to each tested binder by considering the equal weight of each test result. The aggregates were ranked based on properties such as absorption, abrasion resistance, and pH. Similar to binders, an overall rank was assigned to each tested aggregate by considering the equal weight of each test result. The binder-aggregate systems were ranked based on surface free energy (SFE) parameters such as compatibility ratio and wet adhesion energy and retained asphalt binder percentage observed after the Texas Boiling Test. The ranking databases provided in this report can serve as an important tool for selecting the most compatible aggregate-binder system for preparing surface ACHM.

Dynamic modulus data of plant mixtures did not follow any particular trend. Furthermore, the dynamic modulus test results of laboratory mixtures did not show consistent results across the various levels of sandstone. The Hamburg Wheel Tracking test captured the impact of anti-strip agents, as mixtures with anti-strip agents had lower rut depth than identical mixtures without anti-strip agents. High levels of sandstone showed significantly poorer results in terms of moisture susceptibility and rutting than medium and low levels of sandstone without anti-strip agents for all laboratory mixtures. The TSR data showed that the high levels of sandstone showed the worst results, by 10-25%, versus the medium and low levels of sandstone results. This indicates that the high levels of sandstone increase moisture susceptibility and rutting susceptibility. This could be attributed to the high level of absorption characteristics of sandstone that contains enormous micropores and results in moisture intrusion in the mixture. High absorptive sandstone aggregates are also suspected to have less effective binder in the mixture, which in turn reduces the bonding between aggregate and binder. The Flow Number test did not show consistent results across the various levels of sandstone. The IDEAL-CIT and I-FIT data indicated that the highest level of sandstone showed the worst results, by 20-40%, versus the medium and low levels of sandstone results.

Finally, the following are recommended for possible implementations: (i) since sandstone has significantly more absorption than other types of aggregates, it is recommended to set a maximum absorption of aggregates to 2%; (ii) since acidity plays a major role in getting compatible aggregates and binders in the asphalt mixtures (i.e., acidic binders are more compatible with basic aggregates, and vice versa), the ARDOT may include pH measurements of aggregates and binders in their QC/QA protocols; (iii) As a quick test of moisture resistance, the ARDOT may incorporate the TBT to determine adhesion between asphalt and aggregate; (iv) the ACHM producers are suggested to use the most compatible aggregates and binders, summarized in Appendix A; and (v) it is recommended to set the maximum level of sandstone in surface ACHM at 60%.

1 Introduction

This report provides an overview of the problem statement, objectives, scope, and findings of the Arkansas Department of Transportation (ARDOT) sponsored Transportation Research Committee (TRC) project #2102, which has been collaborative efforts between Arkansas State University (A-State) and the University of Arkansas (UARK).

1.1 Problem Statement

There have been some problems with the use of certain aggregates around the State of Arkansas (e.g., some sources of the northeast and west-central Arkansas aggregates) for asphalt mixtures that caused significant durability and performance issues in recent years. In particular, aggregates from some sources (quarries) are suspected to be problematic as they are presumably incompatible with some asphalt binders used in products such as surface asphalt concrete hot mix (ACHM). Such incompatibility can be associated with either chemical or adhesive bond failures between aggregate and binder. In practice, contractors (hot mix plant operators) use aggregates in producing asphalt mixtures without knowing the compatibility between aggregates and binders. Asphalt mixtures prepared from certain asphalt binders and aggregates (e.g., sandstone) are highly prone to stripping that can cause significant premature moisture damage issues (e.g., potholes, moisture-induced interlayer failures, premature cracking, etc.) in the field. Also, the excessive amount of highly absorptive aggregates (e.g., sandstone) can potentially result in dry or brittle mixtures that can cause constructability and durability issues such as difficulty in obtaining specified compaction, early oxidation, premature cracking, and stripping. The compatibility issues are further augmented when an excessive amount of absorptive aggregates (e.g., sandstone) are used in the mixture. In the current ARDOT specification, the amount of limestone or gravel included in ACHM is limited due to skidding resistance concerns. There is no such limit on sandstone. In addition, the increased use of reclaimed asphalt pavement (RAP) in recent years and subsequent adjustment of the amount of asphalt binder in the mixture makes it further dry.

The aggregate compatibility and durability-related issues can be mitigated by using appropriate asphalt binders in consideration of their chemical properties (e.g., acidic or basic), which are

mostly dependent on binders' crude sources. For instance, acidic aggregates (e.g., granite or gravel) are usually more prone to strip from acidic binder than basic aggregates such as limestone. Particular chemical polar compounds of asphalt binder are absorbed by aggregates, and the absorption is aggregate-dependent. Some of these polar materials are desorbed by water more easily than others depending on the specific aggregate-binder combination. Therefore, there is a need to investigate the effect of aggregate-binder compatibility on changes in durability and performance characteristics of asphalt mixtures based on comprehensive evaluations that consider multiple factors involved, including a range of aggregate and binder types used in Arkansas. Further, there is a necessity to set a limit for sandstone aggregates to be used in the surface ACHM. Additionally, the effects of anti-stripping agents, air voids, and RAP in the aggregate-binder compatibility and performance of surface ACHM need to be evaluated for constructing durable surface ACHM.

1.2 Objectives

The primary objective of this study is to recommend implementable guidelines and test protocols that ensure the use of durable and compatible aggregate-binder systems in the mix design phase for enhanced mixture performance in the field. This study requires comprehensive evaluations considering multiple critical factors, including a range of aggregate and binder types used in Arkansas. Specific objectives of the proposed study are:

(i) Evaluate rheological (e.g., viscosity) and chemical properties (e.g., polarity and surface free energy) of asphalt binders,

(ii) Evaluate physical and mechanical (e. g., absorption and durability) and chemical (e.g., polarity and surface free energy) properties of aggregates,

(iii) Develop a database of compatible aggregate-binder systems,

(iv) Recommend suitable test method(s) to screen incompatible aggregates/binders and recommend changes, if any, to the ARDOT specifications,

(v) Evaluate selected asphalt plant-produced surface ACHM samples containing different types of aggregates,

(vi) Evaluate laboratory-produced surface ACHM samples with varying amounts of absorptive (sandstone) aggregates, and

(vii) Recommend the maximum amount of sandstone aggregates to be used in surface ACHM.

1.3 Tasks and Scope

To fulfill the aforementioned objectives of the project, the research team has executed several tasks, which are: conduct a thorough literature review, select and collect test samples (asphalt binders, additives, aggregates, and mixtures), process test materials, evaluate the properties of asphalt binders, evaluate the properties of aggregates, evaluate the compatibility of aggregates and binder systems, investigate the performance properties of asphalt mixtures, analyze test data, and produce deliverables.

This study has been limited to testing aggregates, binders, and asphalt mixture samples in the laboratory. These test samples have been collected from different ARDOT-approved sources throughout Arkansas. In addition, asphalt mixture samples with varying amounts of sandstone have been prepared in the laboratory for their performance evaluation.

The plans, activities, financial statuses, progress, and findings of the project have been provided to the ARDOT periodically in the form of a kick-off meeting, 10 quarterly reports, and meetings with the Project Manager. Technical details and implementable recommendations have been provided to the ARDOT in the form of Benchmark and Implementation reports, respectively. In terms of project management, the team met (virtual and in-person) on a biweekly basis to discuss project plans, activities, and accomplishments in the two years of the project. Afterward, the team communicated through virtual meetings, e-mail exchanges, phone calls, and face-to-face meetings as needed. The team also met the Project Manager of the project quarterly. The project has been completed within the budget.

1.4 Organization of the Report

The current chapter (Chapter 1) provides the problem statement, objectives, tasks, and scope of the project. To accomplish the objectives of this study, the research team has conducted a comprehensive literature review pertinent to the project and the findings are provided in Chapter 2 of this project. With the help of the ARDOT Research and Materials Division, the research team has collected all test materials (binders, aggregates, mixtures, and RAP) needed for the project. These materials have been processed for conducting appropriate laboratory tests, which are elaborated on in Chapter 3 of this report. Test results and findings of aggregates, asphalt binders, and asphalt mixture samples are provided in Chapter 4. Chapter 5 provides additional discussions of test results of asphalt binders and aggregates, and compatibility databases. The conclusions and recommendations of this study are provided in Chapter 6, which is followed by Acknowledgments (Chapter 7) and a list of references (Chapter 8). This report also contains an appendix (Appendix A), which summarizes compatibility databases along with pertinent information.

2 Literature Review

2.1 Asphalt Binders and Aggregates

The surface energy is an important parameter in determining the moisture resistance of asphalt mixes. One of the objectives is to determine the contact angles directly on the asphalt binder as well as on aggregates using a sessile drop (SD) device. From the measured contact angles, the surface free energy (SFE) of asphalt binder and aggregates will be estimated. The SFE data will provide an idea about the moisture resistance of different asphalt mixes. Knowledge gained from reviewing pertinent literature will help the research team understand the sample preparation and test procedure for measuring contact angle using an SD device along with other literature reviews on this topic. The findings of the current study can also be compared with existing literature and make meaningful conclusions and recommendations.

Koc and Bulut (2014) measured the contact angles of selected asphalt binders and aggregates using a sessile drop (SD) device. Afterward, the SFE components of both binders and aggregate were estimated from the measured contact angles. In this study, SFE values of five different aggregates and one asphalt binder have been determined. Three different liquids: water, diiodomethane, and ethylene glycol were used during contact angle measurement. The SFE data obtained using the SD method were compared with that of the Wilhelmy Plate (WP) method for asphalt binders and the Universal Sorption Device (USD) method for aggregates. The SFE of aggregates from the SD agreed with that found in the literature but disagreed with that of the USD. The asphalt binders' SFE results from SD were in close agreement with that of the WP.

Rahmani et al. (2018) measured SFE components of aggregate, and asphalt binder (unaged, aged, and modified). Afterward, the moisture sensitivity of asphalt mixes was investigated based on the findings from SFE. A total of eight different asphalt mixes including two types of asphalt binder with different penetration grades and two types of aggregates were investigated in different test conditions (dry and wet). The SD test was conducted to determine the SFE of aggregate and asphalt binder. Also, a modified Lottman indirect tensile test (AASHTO T283) was conducted to determine the moisture sensitivity of hot mix asphalt (HMA). Results indicated that aging of asphalt binders might increase the debonding energy, adhesion-free energy, and

cohesion-free energy for asphalt mixes made of higher penetration grade binder (85-100) and might decrease for lower penetration grade binder (60-70). Results also indicated that the aging effect should be considered while determining the SFE of asphalt binder.

Allen et al. (2013) predicted the macroscale and composite nanoscale viscoelastic behavior of asphalt binder and HMA using a combination of AFM imaging and nanoindentation. In this study, the importance of performing AFM image processing in determining the macroscale and composite nanoscale viscoelastic behavior of asphalt binder and hot mix asphalt HMA was shown. Three different asphalt binders were selected based on crude source, chemical composition, etc., and were aged using a rolling thin film oven (RTFO) and a pressure aging vessel (PAV). A constant of 5nN tip force was applied on the asphalt sample for 4 secs during the creep test and a total of 250 data points were collected during this period. From the obtained results, it has been found that relaxation modulus values decrease with the increase in scale length.

Rashid and Hossain (2016) analyzed the mechanistic properties and morphology of Ground Tire Rubber (GTR) modified binders using PeakForce Quantitative Nanomechanical Mapping (PFQNM™). To characterize asphalt materials at micro-and nano- levels, an AFM can play an important role. Different mechanistic properties such as adhesion, modulus of elasticity, hardness, and energy dissipation of asphalt binder were measured using AFM. The AFM samples were prepared by placing the preheated asphalt binder on a clean glass plate and afterward heated in the oven at 165 °C for 15 minutes. Each test specimen was scanned in three different areas 5×5 μm, 10×10 μm, and 20×20 μm. Indentations by sharp tips were made on various points of the sample and a force-displacement curve was used for further analysis. Results indicated that the mechanistic properties of asphalt binder get changed due to the modification by GTR.

Hossain et al. (2020) investigated the variation in SFE of asphalt binders due to rejuvenation and aging. In this study, the contact angle between the asphalt binder (control, aged, and rejuvenated) and three probe liquids (distilled water, Glycerol, and Formamide) was measured using an SD device. SFE has three components: (1) Lifshitz–van der Waals components, (2) Lewis acid components, and (3) Lewis basic components. It has been found that the Lifshitz–van der Waals components were comparatively much higher than those from acidic and basic components in the case of the aged binders and the binders with rejuvenators. The moisture

damage resistance was found higher for limestone-based asphalt concrete mixture compared to that of asphalt concrete mixture with granite.

Howson et al. (2011) studied the impact of material characteristics and additives on the SFE and the resulting bond between asphalt binders and aggregates. In this study, SFE has been measured on asphalt binders (unmodified, polymer-modified, aged) and 11 aggregates. Also, the impact of water pH has been examined on SFE and water-aggregate adhesive bonds. It was found that resistance to moisture damage was found to be increased for the modified binder (antistripping). The pH of the water was found to be increased with the contact of aggregate. However, there was no significant change in SFE due to the change in the pH value.

2.2 Asphalt Mixture

Asphalt mixtures (also known as Hot Mix Asphalt, HMA, or Asphalt Concrete Hot Mix, ACHM) are the most widely utilized pavement material because of their availability, ease of installation, and capability to deal with dynamic loads. The make-up of an asphalt mixture can be seen in Figure 1, shown as the aggregate skeleton (Fu et al. 2010). This image shows how the asphalt binder is meant to hold together the mineral aggregate contained in the asphalt mixture. This bond between the aggregate and binder must be maintained if the pavement is to continue to perform over time. The asphalt mastic, the mix of asphalt cement and fine aggregate particles (mineral fillers), partially fills the voids between the skeleton formed by large aggregates. Mineral fillers (3–14% by the weight of the total mixture) are meant to be coated by asphalt binder (about 5% by the weight of the total mixture) to form the asphalt mastic phase, which bonds with the aggregates. Over time as moisture enters the system, it may wear away the adhesive and cohesive bonds present in the asphalt binder. The rate of this deterioration is affected by the selection of materials in the mixture.

While the selection of aggregate within an asphalt mix design is of high importance, it is not the only civil engineering material that depends heavily on the selection of the species of aggregate, and properties thereof. Portland Cement concrete is another widely used material, in which recent research has pointed out the importance of the effects of the aggregate used within it. A joint study (Bentz, 2017) performed by the National Institute of Standards and Technology (NIST)

and the Federal Highway Administration (FHWA) explored the effects of the usage of different aggregates on the desirable qualities of concrete (compressive strength, flexural strength, modulus of elasticity, etc.). The results of this study showed that the species of aggregate can have a significant impact on the strength of concrete. This research noted that much of the incompatibility between aggregate and paste (cement, water, and fine aggregate), is mostly due to the modulus of elasticity of the aggregate and the CTE (coefficient of thermal expansion) of the aggregate. It was also noted that this incompatibility causes interfacial stresses and microcracking at the interface of the aggregate and paste. Even though Portland Cement Concrete is vastly different than HMA, the elasticity and chemical properties of an aggregate could also have an impact on the performance of an asphalt mixture as well.

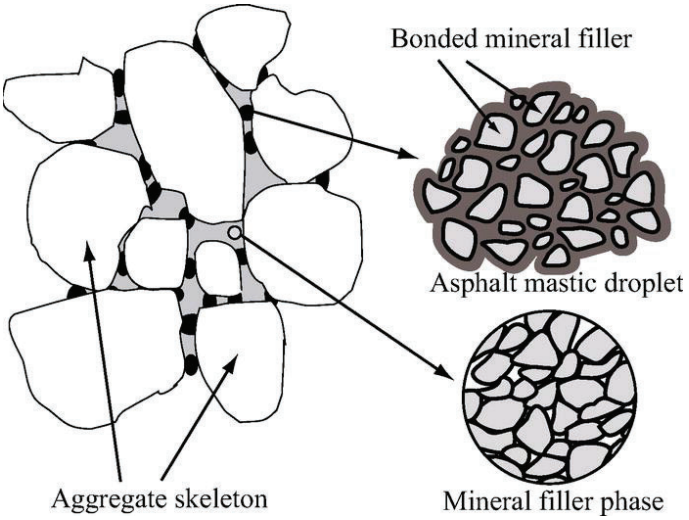

Figure 1. Aggregate Skeleton (Fu et al. 2010).

Moisture damage is one of the most common forms of damage to asphalt pavement. Moisture damage occurs when water weakens the adhesive bond between the aggregate and the binder, or the cohesive bond holding the binder together. This phenomenon is commonly referred to as stripping because it results in the asphalt binder stripping away from the aggregate. Research has shown that the physical and chemical properties of aggregates significantly affect the moisture sensitivity of an asphalt mixture. However, it is very difficult to understand and quantify the level of contribution to this issue from the aggregate, the filler, and the binder.

Much of the notable research in the past few years was built on the ideas of the research performed by Copeland et al. (2007). This research was performed on binders to test for their adhesive properties with or without moisture conditioning. The results of this research noted that dry samples tended to fail cohesively (a failure within the asphalt binder or asphalt mastic), while moisture-conditioned samples tended to fail adhesively (a failure between the asphalt binder/mastic and the aggregate). In addition to this, it is noted that moisture decreases the adhesive properties of binders. From this, it can be determined that the adhesive bond between the aggregate and the binder significantly affects the overall moisture resistance of asphalt pavement.

Over the past fifteen to twenty years, a lot of research has been deeply studying the effects of certain aggregate properties on the performance of asphalt mixtures. One foundational study on the subject (McCann et al. 2005) noted that moisture damage is very difficult to attribute to a single predictor variable since there are so many different possible causes or variables within an asphalt mixture. The researchers looked into eleven different predictor variables for SHRP aggregates and binders. The goal of this research was to perform a regression analysis on these different variables to find which factors are most consequential to the moisture resistance of a mixture. According to this study, the most important aggregate property for predicting moisture sensitivity is acid insolubility, followed by pore ratio and surface area.

There has been a lot of other useful research on the effect of aggregate properties on the performance of asphalt mixtures. This study (Horgnies et al. 2011) is focused on the interaction between the mineralogy of the aggregates and the adhesion force measured at the interface between bitumen and aggregate. Granite and dolomite were the two aggregates tested. A peel test was used to study the adhesive bond between the aggregate and binder, then the failure plane was analyzed with spectrometry (X-ray Photoelectron Spectroscopy [XPS] and Energy-dispersive X-ray [EDX]) to analyze the surface composition where the bond failed adhesively. This research indicated that alkali-feldspars induce weak adhesive bonds. This research also found dolomite to be a better-performing aggregate than granite regarding bond strength.

A lot of research has focused on analyzing the mineralogical composition of aggregates and whether these minerals can be indicative of performance in asphalt mixtures. This study (Zhang

et al. 2015) evaluated two different limestones and two different granites and performed the pull-off, Pneumatic Adhesion Tensile Testing Instrument (PATTI), and peel tests. Each of these tests was used to analyze the failure surface of the bond. Test specimens were moisture-conditioned to analyze the moisture resistance of the adhesive bond created between the aggregate and binder. This study hoped to isolate mineralogical compositions that could indicate moisture sensitivity. The results of this study found that the minerals quartz and anorthite are detrimental to moisture resistance and that calcite is a moisture-resistant mineral. This study also found that limestone seems to form a more moisture-resistant bond than granite.

Another piece of important research (Cala & Caro, 2021) encapsulates many of the ideas presented in previous studies focused on the effects of aggregate composition. This study aimed to create a quantitative model to predict the adhesion between aggregate and asphalt based on aggregate chemistry. This testing studied seven different siliceous aggregates and two calcareous aggregates. Pull-off testing was performed to compare each of these. The results of this study found that aggregate chemistry is more influential to moisture susceptibility than dry adhesion and that higher concentrations of siliceous compounds result in lesser moisture resistance of a mixture. This lines up with the previous studies, knowing that many of the indicated poor-performing minerals (quartz, feldspar, anorthite, etc.) are in fact, siliceous.

It is also important in the literature review to study research performed on the test methods that will be utilized for asphalt mixtures. One study (Yan et al. 2020) tested six different plant-produced asphalt mixtures gathered from around the country. These mixtures were used to compare the semicircular beam flexibility index (SCB-IFIT), unnotched semi-circular beam (SCB), and cracking index (IDEAL-CT) tests on each of the different mixtures. The findings of this study saw that the IFIT test had higher variability than the unnotched and the IDEAL-CT tests. They also found that there is a high correlation between the flexibility index (IFIT) and IDEAL-CT. The cracking index values also correlated with the fatigue of mixtures in the field.

Conceptually it has been noted by research that the most evident performance issues caused by aggregate properties will relate to moisture damage. So, it is important to study the available literature on moisture sensitivity tests. Chung Do et al. (2018) analyzed the differences between the tensile strength ratio (TSR) (AASHTO T 283) and other commonly used test methods that

study the moisture sensitivity of mixtures. Four different base mixtures with varying levels of the anti-stripping agent were studied. Three of these mixtures had granite, and the fourth had limestone. The takeaways from this study concluded that the TSR can be used to measure moisture damage, however, the ratio should not be used alone. The moisture-conditioned strength of the specimen should be used along with the tensile strength ratio to compare the moisture resistance of specimens. This study also concluded that binder aging has a significant impact on the moisture sensitivity of specimens.

Another important test to perform for not only moisture damage testing but also testing for rutting sensitivity is the Hamburg wheel tracking test. One study (Tsai et al. 2016) was performed to analyze and study the Hamburg-Wheel Tracking Device (HWTD) and its usage with HMA. This study investigated several different mixtures and tested also to find the accuracy and relevance of the HWTD. It was concluded that the cylindrical specimen geometry better constrained shear flow. It also concluded that care should be taken to minimize the gap width between the two cylindrical specimens, or the specimens should be bonded together to prevent localized failure from large peak loadings at the joint.

Another very important test to perform on HMA mixtures is the dynamic modulus. This test indicates the cracking and rutting potential of a mixture. However, this test method utilizes a very complex form of analysis, time-temperature superposition. Because of the complexity of this process, it will be important to study literature that can assist in accurately performing this analysis. One such study (Yang et al. 2017), investigated three common testing geometries utilized for this test method (the uniaxial, indirect tensile [IDT], and torsion bar configurations). Since the uniaxial configurations cannot be performed on cores gathered from already placed pavements, it is important to be able to correlate the results of the other configurations to the uniaxial configuration. This study examined field sections from 10 different places in Arkansas. This study found that the seed values for time-temperature superposition recommended in AASHTO R62 often lead to illogical coefficients in the master curve. This research recommends adding additional parameters to the Solver function in excel.

A second study (Bhasin et al. 2004) followed up on the National Cooperative Highway Research Program (NCHRP) Project 9-19, which recognized the dynamic modulus, flow time, and flow

number tests as the top three candidates for a simple performance test to identify mixtures susceptible to permanent deformation. This study analyzed 12 different mixtures using the dynamic modulus, flow time, flow number, asphalt pavement analyzer (APA), and the HWTD tests. After this testing, it was concluded that the best correlations for permanent deformation were found between the flow time and flow number and the APA and HWTD tests. This study also recommended that with the dynamic modulus test, it is important to understand that it is a stiffness test related to the designed thickness of pavement layers. Therefore, it is not always indicative of rutting resistance but still provides extremely useful information when comparing different mixtures.

3. Research Methodologies

In consultation with the ARDOT, sources of test materials (aggregates, binders, and asphalt mixture) have been identified. They have been collected for further processing and laboratory testing. Sources of these test materials and steps involved in the processing and testing of these materials are elaborated on next.

3.1 Aggregates

Table 1 shows the nomenclature of eight aggregate samples collected and tested in this study. Samples of four major types of aggregates, namely, sandstone, novaculite, limestone, and dolomite were collected. Each type of these aggregates was collected from two different sources and tested to determine their routine properties such as specific gravity, abrasion resistance, and pH contents.

Table 1. Nomenclature of Aggregates Used in This Study

Aggregate Type	Aggregate Source	Nomenclature
Sandstone	Duffield Quarry (Blackstone Construction)– Gum Log Quarry, Russellville, AR; 2 miles west on Hwy 326	SS1
Sandstone	APAC-Central - Jenny Lind,	SS2
Novaculite	Gravel Mountain Quarries, Bismarck, AR; 9 miles west on Hwy 347	NV1
Novaculite	Redstone Construction - Little Rock Quarry, Little Rock, AR; I-430	NV2
Limestone	Benton County Stone - Mill Creek Quarry, Bella Vista, AR; At Bella Vista	LS1
Limestone	APAC Central - Sharp's Quarry, Lowell, AR; Junction of Puppy Creek Road and Wagon Wheel Road at I-540	LS2
Dolomite	Martin Marietta - Propst Pit #4, Black Rock, AR; 4 miles north on Hwy 63	DM1
Dolomite	Vulcan Materials. Black Rock, AR; 3 miles north on Hwy. 63	DM2

3.1.1 Specific Gravity and Absorption (AASHTO T 85)

Specific gravity and absorption of selected aggregates have been evaluated as per AASHTO T 85 (Figure 2). The aggregates were sieved through a mechanical sieve shaker. The amount of sample required for the tests depends on the nominal maximum aggregate size (NMAS) of the

aggregates. The required amounts of samples were washed and dried in the oven at 110 ± 5°C. Samples were cooled and immersed in water in a bucket for about 15 hrs. The sample was removed from the bucket and the excess water was drained out. A towel was used (rolling, shaking, and rolling) to remove surface-free water and make it saturated surface dry (SSD). The weight of the SSD sample was measured in the air as well as in water using a specific gravity bench. Afterward, the sample was put back in the oven at 110 ±5°C for 24 hours until a constant mass was obtained. The sample was then cooled, and the dry weight of the sample was measured. Each sample had three specimens, and the average values of the corresponding test results of the three specimens were reported as the specific gravity and absorption.

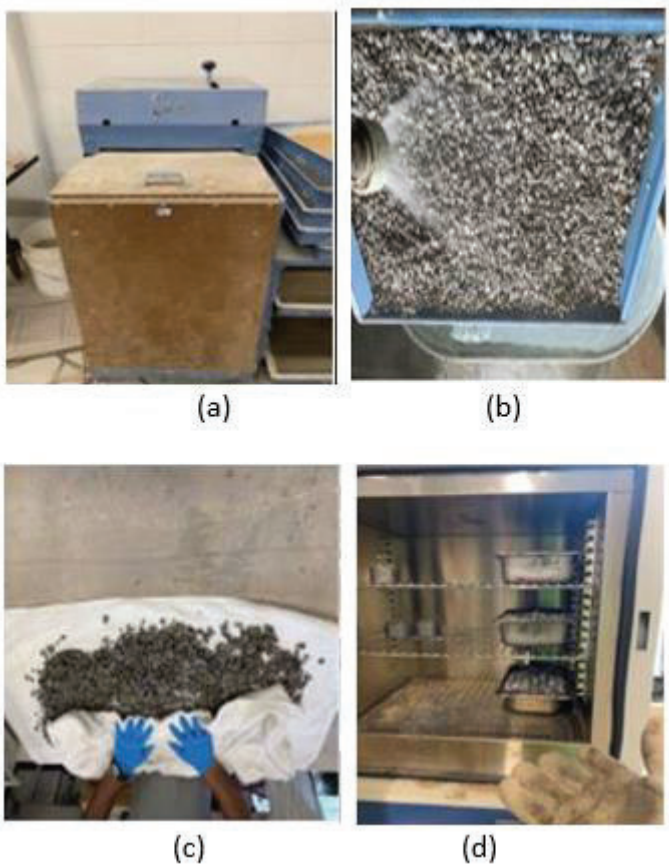

Figure 2. Major Steps Involved in Specific Gravity And Absorption Tests of Aggregates: (a) Sieving, (b) Soaking, (c) Making Saturated Surface Drying, and (d) Drying in the Oven.

3.1.2 Los Angeles (LA) Abrasion Resistance (AASHTO T 96)

The LA abrasion resistance of aggregates has been evaluated as per AASHTO T 96. A total of 5000 gm of mineral aggregate was taken (Grading B and C) for one specimen. A total of three replicate

specimens were tested from each type of aggregate. The sample was washed and dried at 110 ± 5°C for 24 hours to ascertain a constant mass. The aggregates were mixed and placed in the Los Angeles testing machine containing the required number of steel charges as shown in Figure 3. The aggregate was subjected to a rotational speed of 30 to 33 r/min for 500 revolutions. The sample was discharged from the machine and sieved through the No. 12 sieve. The sample retained on the No. 12 sieve was washed and dried at 110 ± 5°C for 24 hours to get a constant mass. Then, the LA Abrasion loss was estimated.

Figure 3. LA Abrasion Test of Aggregate.

3.1.3 pH Content

About 2000 gm of coarse aggregate was taken for one specimen. It was then placed in a 1-gallon jug. An equal amount of deionized water was added to it. The mixture was covered with a lid to prevent contamination and evaporation and was kept in there for 30 minutes. The mixture was then agitated, and the agitation was repeated at 2 hours and 4 hours. Then the mixture was kept undisturbed for 20 hours. Afterward, a sufficient amount of solution was removed from the mixture and filtered through a coarse filter paper. In the meantime, a pH meter was calibrated using a buffer solution (pH =7.0). Then the pH of the mixture solution was measured. Figure 4 shows a pictorial view of the pH setup.

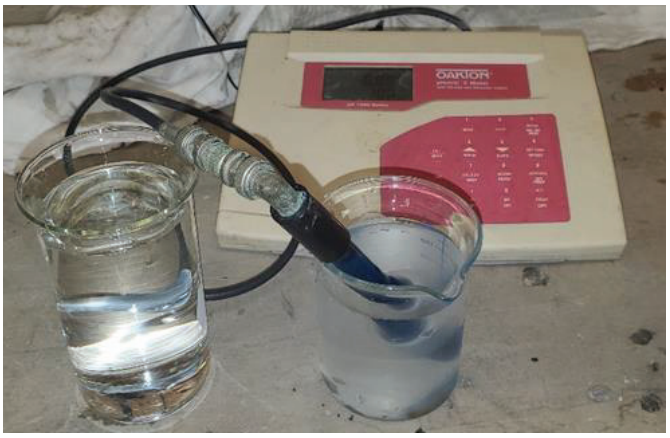

Figure 4. Snapshot of pH Measurement of Aggregates.

3.2 Asphalt Binders

Table 2 shows the nomenclature of the three types of ARDOT-approved Performance Grade (PG) asphalt binders collected and tested in this study. Each type of PG binder was collected from six different sources, thus a total of 18 binder samples were collected directly from refineries.

Table 2. Nomenclature of Asphalt Binders Used in This Study

Binder Type	Binder Source	Nomenclature
PG 64-22	Ergon Asphalt and Emulsion, Inc. Memphis, TN	S1B1
	Marathon Petroleum Corporation Memphis, TN	S2B1
	Coastal Energy Corporation Willow Springs, MO	S3B1
	Ergon Asphalt and Emulsion, Inc. Vicksburg, MS	S4B1
	Holly Frontier Refining & Marketing LLC Catoosa, OK	S5B1
	Lion Oil Company Memphis, TN	S6B1
PG 70-22	Ergon Asphalt and Emulsion, Inc. Memphis, TN	S1B2
	Marathon Petroleum Corporation Memphis, TN	S2B2
	Coastal Energy Corporation Willow Springs, MO	S3B2
	Ergon Asphalt and Emulsion, Inc. Vicksburg, MS	S4B2
	Holly Frontier Refining & Marketing LLC Catoosa, OK	S5B2
	Lion Oil Company Memphis, TN	S6B2
PG 76-22	Ergon Asphalt and Emulsion, Inc. Memphis, TN	S1B3
	Marathon Petroleum Corporation Memphis, TN	S2B3
	Coastal Energy Corporation Willow Springs, MO	S3B3
	Ergon Asphalt and Emulsion, Inc. Vicksburg, MS	S4B3
	Holly Frontier Refining & Marketing LLC Catoosa, OK	S5B3
	Lion Oil Company Memphis, TN	S6B3

3.2.1 Rotational Viscosity (RV) (AASHTO T 316.)

The RV test of asphalt binders was conducted per AASHTO T 316. The spindle, sample chamber, and viscometer environmental chamber were preheated. The unaged asphalt binder was also heated until fluid enough to be poured into the sample chamber. Generally, less than 10.5 gm of liquid asphalt binder was taken for each specimen. A total of three specimens were tested for each sample of an asphalt binder. The testing temperatures were 135°C, 150°C, 165°C, and 180°C. The test specimen was poured into the viscometer's environmental chamber and the cylindrical spindle was submerged. The test temperature was set at 135°C. The test specimen was kept inside the environmental chamber for approximately 30 minutes to equilibrate the temperature of the sample with that of the environmental chamber. Then the 10-minute test period started. The motor was started during this period. A total of 3 readings were taken at 10, 11, and 12 minutes. Afterward, the temperature was raised from 135°C to 150°C. When the environmental chamber shows the desired temperature, the counting of the 10-minute test period starts. The motor was started during this period. Again, a total of 3 readings were taken at 10, 11, and 12 minutes. The same steps were followed for testing temperatures of 165°C and 180°C. The apparatus required for the RV test is given in Figure 5.

Figure 5. Apparatus for RV Test.

3.2.2 pH Value (Acid Number)

About 5 gm of asphalt binder was taken as a sample into a 250 mL flask, and about 30 mL of toluene was added to it. The solution was heated slowly to dissolve the asphalt binder. It was then cooled down to room temperature and transferred to a 250 mL separatory funnel. About 15 mL of de-ionized water was added to the toluene-asphalt solution. The separatory funnel was shaken for 2 minutes and put into a clamp. In this process, two layers of the solution developed: the top layer was toluene and the bottom layer was aqueous. The aqueous layer was extracted into a glass beaker. Then the aqueous layer was transferred into a steel tube and was centrifuged for 2 minutes. Then again about 15 ml of deionized water was added to the toluene solution for the second time. Then, the separatory funnel was shaken for 2 minutes and the aqueous layer was extracted into a glass beaker and centrifuged. Two aqueous layers were then combined and filtered (filter paper) into a beaker and pH was measured. Before measuring the pH, a pH meter was calibrated using a buffer solution with a pH value of 7.0. Figure 6 shows some of the steps involved in the pH test.

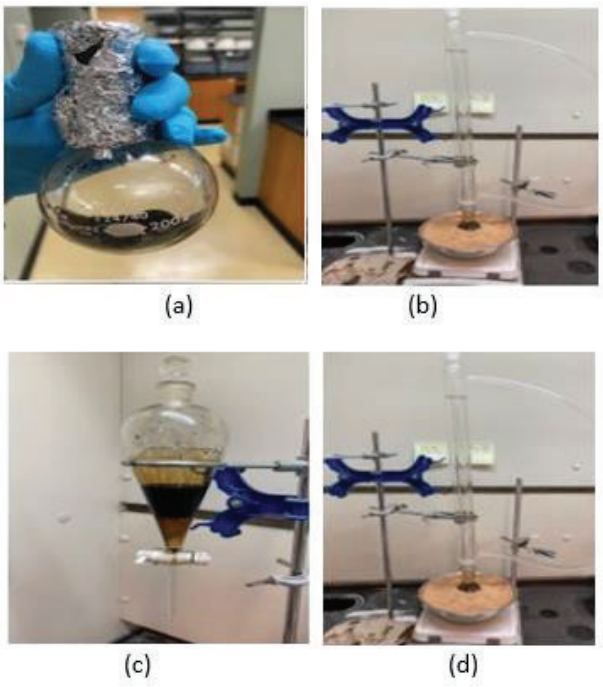

Figure 6. pH Test of Asphalt Binder: (a) About 5 gm of Asphalt Binder, (B) Slowly Heating Asphalt With Toluene, (C) Development of Aqueous (Bottom) and Toluene-Asphalt (Top) Layers, and (D) Measuring pH.

3.2.3 Sessile Drop (SD) (Optical Contact Angle) Test

A sessile drop test is conducted to measure the optical contact angles (OCAs) of asphalt binders and aggregates with different reference solvents. The reference solvents used in this study to measure OCA were water, ethylene glycol (EG), and formamide (FM). The use of these three liquids can be found in the literature (Little and Bhasin, 2006; Hossain et al. 2019, Hossain et al. 2021, Oyan et al. 2022). The experimental setup is shown in Figure 7. First, a tiny drop of solvent was placed on the sample. The volume of the drop was 3 µL for binder samples and 5 µL for aggregate samples. For each drop, more than 100 readings of contact angles between the sample and reference solvent were determined. At least three different drops of a solvent were placed across the samples to capture the angles. This process is repeated for two other solvents. The SFE parameters (work of adhesion, work of cohesion, compatibility ratio, etc.) were then measured by the Good-Van Oss-Chaudhury theory and the Young-Dupre equation (Van Oss et al. 1987). The three different SFE components: a monopolar acidic component (Γ^+), a monopolar basic component (Γ^-), and an apolar or Lifshitz-van der Waals (Γ^{LW}) components were calculated by using the contact angles. The SFE components of the three reference solvents are tabulated in Table 3.

The acid-base component of the total SFE is denoted as Γ^{AB} and is calculated by Equation 1.

$$\Gamma^{AB} = 2\sqrt{(\Gamma^+\Gamma^-)}$$

Equation 1. Relationship Between Acid-Base Components of SFE

The Total SFE (Equation 2) is calculated as the summation of Γ^{LW} and Γ^{AB}.

$$\Gamma^{total} = \Gamma^{LW} + \Gamma^{AB}$$

Equation 2. Relationship Between Total and Acid-Base Components of SFE

Gibb's free energy of adhesion (ΔG_{ad}) consists of two components (Lifshitz-van der Waals and Acid-base), as shown in Equation 3.

$$\Delta G_{ad} = \Delta G_{ad}^{LW} + \Delta G_{ad}^{AB}$$

Equation 3. The Gibb's Free Energy of Adhesion

The individual components of Equation 3 are given by Equations 4 and 5.

$$\Delta G_{ad}^{AB} = -2\left\{\sqrt{(\Gamma_L^+ \Gamma_S^-)} + \sqrt{(\Gamma_L^- \Gamma_S^+)}\right\}$$

Equation 4. Expression of Acid-Base Energy

$$\Delta G_{ad}^{LW} = -2\sqrt{(\Gamma_L^{LW} \Gamma_S^{LW})}$$

Equation 5. Expression of Lifshitz-van der Waals Energy

Combining these equations, the Young-Dupre equation for the work of adhesion (W^a), can be found, as shown in Equation 6.

$$W^a = \Delta G_{ad} = \Gamma^{total}(1 + \cos\theta) = 2\left\{\sqrt{(\Gamma_L^+ \Gamma_S^-)} + \sqrt{(\Gamma_L^- \Gamma_S^+)} + \sqrt{(\Gamma_L^{LW} \Gamma_S^{LW})}\right\}$$

Equation 6. Expression of the Young-Dupree Equation

Equation 6 was used to calculate the SFE components of asphalt binder from the measured contact angles θ using three reference liquids. Here, L and S denote the liquid (reference solvent) and solid (asphalt binder), respectively. ΔG_{ad} is also known as dry work of adhesion (ΔG_{dry}^{ad}) as water is not present in the system. However, in the presence of water, the adhesive bond energy between the aggregate-binder interface gets reduced making the stripping thermodynamically favorable. This adhesion energy is known as wet work of adhesion (ΔG_{wet}^{ad}). The magnitude of wet work of adhesion is desired to be low as it will make stripping action difficult to take place (Bhasin et al. 2006). Wet work of adhesion (ΔG_{wet}^{ad}) energies can be calculated using Equation 7, where 1, 2, and 3 represented asphalt, aggregates, and water, respectively (Hossain et al. 2015, Cheng et al. 2002

$$\Delta G_{wet}^{ad} = \Delta G_{132}^{ad} = \Gamma_{13} + \Gamma_{23} - \Gamma_{12} = 2\Gamma_L^{LW} + 2\sqrt{(\Gamma_1^{LW}\Gamma_2^{LW})} - 2\sqrt{(\Gamma_1^{LW}\Gamma_3^{LW})} - 2\sqrt{(\Gamma_2^{LW}\Gamma_3^{LW})} + 4\sqrt{(\Gamma_3^{+}\Gamma_3^{-})} - 2\sqrt{\Gamma_3^{+}}\left(\sqrt{\Gamma_1^{-}} + \sqrt{\Gamma_2^{-}}\right) - 2\sqrt{\Gamma_3^{-}}\left(\sqrt{\Gamma_1^{+}} + \sqrt{\Gamma_2^{+}}\right) + 2\sqrt{(\Gamma_1^{+}\Gamma_2^{-})} + 2\sqrt{(\Gamma_1^{-}\Gamma_2^{+})}$$

Equation 7. Expression of the Wet Work of Adhesion

Finally, the compatibility between aggregate and asphalt binder can be quantified by the ratio of $|\Delta G_{dry}^{ad}|$ and $|\Delta G_{wet}^{ad}|$ and is shown in Equation 8 (Howson et al. 2007).

$$\text{Compatibility Ratio, (CR)} = \frac{|\Delta G_{dry}^{ad}|}{|\Delta G_{wet}^{ad}|}$$

Equation 8. Expression of the Compatibility Ratio

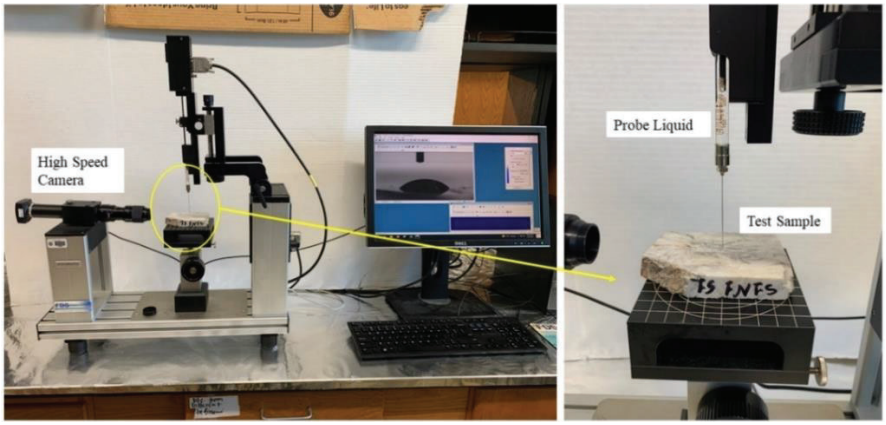

Figure 7. Experimental Setup of an OCA Device.

Table 3. Surface Free Energy Components of Reference Liquids (Hossain et al. 2015).

Liquid	$\Gamma_L^+(acid)$	$\Gamma_L^-(base)$	Γ_{LW}^L	Γ^L
Water	25.5	25.5	21.8	72.8
Ethylene glycol	1.92	47	29	48
Formamide	2.28	39.6	39	58

The OCA Sample preparation (asphalt binder): At first asphalt binder is heated in a metal can at 163 °C for a sufficient time to make it flowable. In the meantime, a clean glass plate is taped around to construct a rectangular strip in the middle (Figure 8) and heated at the same

temperature. Once the binder is flowable enough, a few drops of asphalt binder are poured on the hot and taped glass plate and dragged longitudinally with another glass plate to prepare a thin layer of binder samples. The samples are then tested within 24 to 72 hours of their preparation.

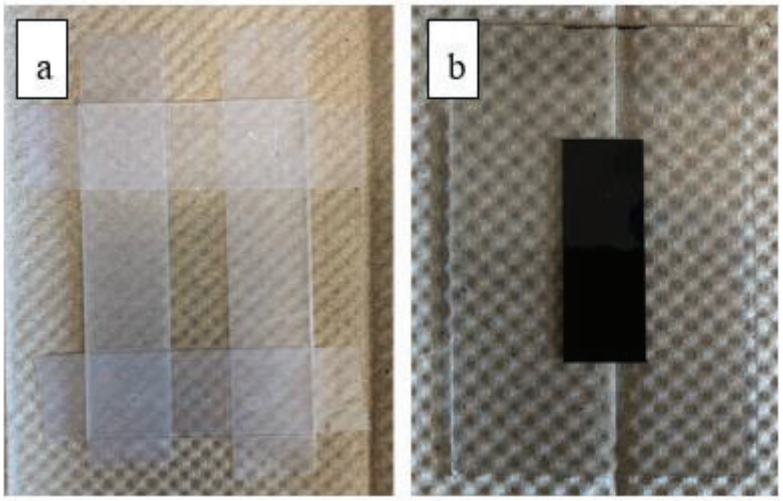

Figure 8. Sessile Drop Test Sample for OCA Measurement: (A) Taped Glass Plate and (B) Asphalt Coated Glass Plate for Test.

The OCA Sample preparation (aggregates): Big aggregate chunks (6-8 in) were collected from the quarry and cut into the desired shape (Figure 9). The transformation of a big aggregate chunk to a thick rectangular sample required to follow several steps,

- A rock-cutting saw was used to cut the aggregate chuck into small pieces with the dimensions of 3 in x 3 in x 0.5 in. During this cutting process, a continuous cool water supply was maintained to prevent the saw from overheating, thus altering the aggregate mineralogy.
- Having the desired shape, both 3 in x 3 in sides were rubbed with 230-grain size sandpaper for ten minutes. The dust was occasionally removed by spraying water on the surface. This same rubbing action was repeated for 500, 600, and 800-grain size sandpaper.
- Then, the aggregate samples were washed with distilled water and submerged in soapy water for one hour. Following this step, they were vigorously rubbed and washed with distilled water for about 30 mins.

- Afterward, the samples were oven-dried for 24 hours at 110 ± 5°C. The oven-dried samples were then cooled and stored in a Ziplock bag for testing purposes. Figure 9 shows the final aggregate samples that were used in the SD test.

Similar steps followed by other researchers can be found in the literature (Oyan et al. 2023).

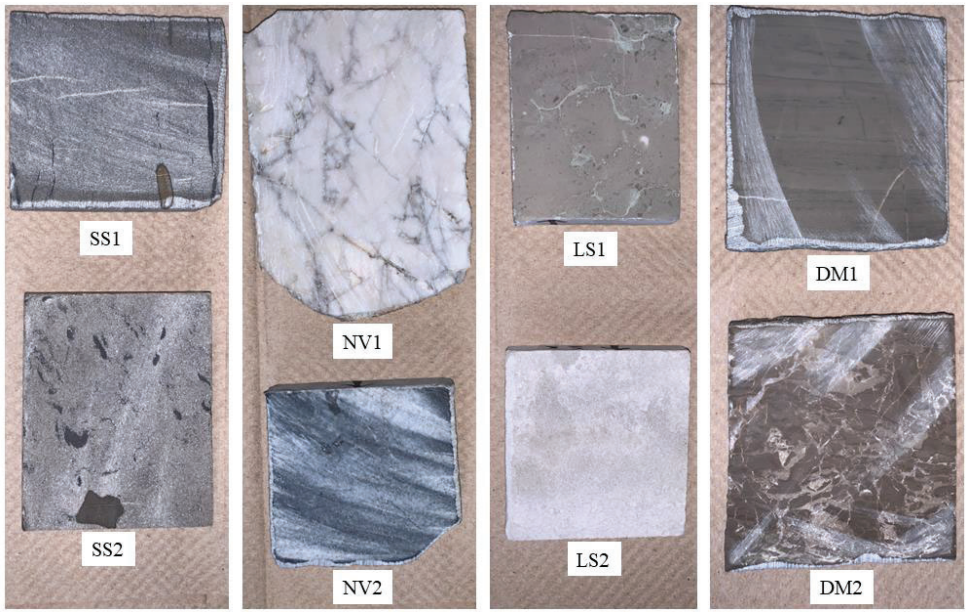

Figure 9: Aggregate Samples for SD Test.

3.2.4 Atomic Force Microscopy (AFM)

The Atomic Force Microscopy (AFM) technique has been used by multiple researchers to study the properties of asphalt binders at the micro-scale in recent years. The AFM tools can capture the microstructures presented on the asphalt binder surface and provide mechanical properties by correlating their morphological properties as well. In this study, a Dimension Icon AFM from Bruker has been used to observe the surface roughness/morphology and the mechanical properties such as the Derjaguin-Muller-Toporov (DMT) modulus, adhesion force, deformation, and dissipated energy of the asphalt binders in the laboratory. Figure 10: The AFM System Used in this Study. shows the AFM used in this study. The PeakForce Quantitative Nanomechanical Mapping (PFQNM™) mode of the AFM system has been chosen as it provides maps for the surface roughness and mechanistic properties simultaneously at the molecular level. Similar to the tapping mode, the peak force tapping provides the surface morphology and the force-

displacement curve of any point under the scan area which are analyzed through the quantitative nanomechanical mapping to find the properties of the scanned surface.

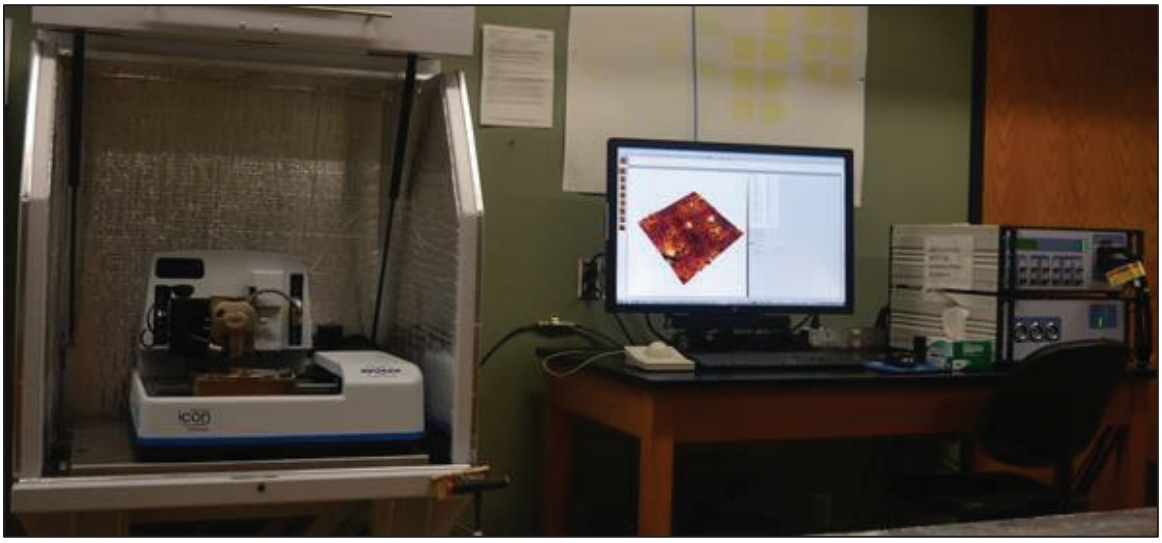

Figure 10: The AFM System Used in this Study.

To prepare the specimens for the AFM tests from the selected binder samples, the heat cast method was followed which has been used by several researchers in the characterization of asphalt binders (Hossain et al. 2017, 2020; Bagchi et al. 2021; Rashid et al. 2019; Roy and Hossain 2021; Tarefder and Zaman 2010; Dourado et al. 2012; Jahangir et al. 2015; Masson et al. 2006; Nahar et al. 2013). The major steps involved in preparing the AFM test specimens are given below.

- At first, the asphalt binder sample was heated in a preheated oven at 160 °C until it became sufficiently fluid to pour.
- A very small amount of asphalt binder, generally 2 drops, was placed on a thin glass plate 2” by 3” in size.
- Afterward, the samples with the glass plates were placed in the oven for nearly 15 minutes to create a uniform and smooth surface for the binder. However, in the case of stiff binders, like SBS, the heating time was extended until the desired result was obtained.

- The prepared specimens were then cooled at room temperature for 30 minutes and stored in a humidity-controlled desiccator for 24 hours before testing.
- The AFM tests were conducted using the prepared specimens of the asphalt binders.
- After conducting the AFM tests, the scanned maps were analyzed offline using the NanoScope version 9.0) software to quantify the roughness and mechanical properties of asphalt binders.

3.2.5 Texas Boiling Test of Loose Mix

Texas Boiling Test is a rapid method to evaluate the stripping of asphalt mixtures. This test was performed according to ASTM D3625. Four different aggregate sizes are available to prepare the asphalt mixture:

i) passing 3/8 inch Sieve and retaining on Sieve No. 4,
ii) passing Sieve No. 4 and retaining on Sieve No. 10,
iii) passing Sieve No. 10 and retaining on No. Sieve 40, and
iv) passing Sieve No. 40 and retaining on Sieve No. 80.

A mixture can be prepared with either one of these aggregate sizes or a mix of them. This study employs passing 3/8 inch retained on No. 4 sized aggregate to prepare the mix. Similar sized aggregates have already been used in the past by researchers to evaluate the moisture susceptibility of asphalt mixtures (*Hossain et al. 2020, 2021, Oyan et al. 2023*). The whole test can be divided into two major steps: preparing the asphalt mixture and boiling the mixture.

To prepare a laboratory mix, 100 gm of desired aggregates (oven-dried) was taken and put into an oven at 163°C for at least 30 min. The asphalt binder was also heated at the same temperature to make it fluid. Later, 5 gm of binder samples was poured on the aggregates and these were manually mixed. The mix was kept at room temperature for sufficient time to cool and then the aggregates were separated from one another (Figure 11).

About 500 ml of distilled water was taken in a 1000 ml beaker. The water was heated to 100°C. Once the water was boiled the loose mix was placed into it. The boiling time was ten minutes, and the mixture was stirred with a glass rod three times at an interval of three minutes. While

boiling, stripped asphalts were skimmed away to prevent recoating. Water was decanted following the boiling action. The mixture was spread on an aluminum foil to let it dry and cool to room temperature. After half an hour, the percentage of retained asphalt was visually examined with the help of a rating board developed by the Texas Transportation Institute (TTI) (Figure 12) (Kennedy et al. 1984).

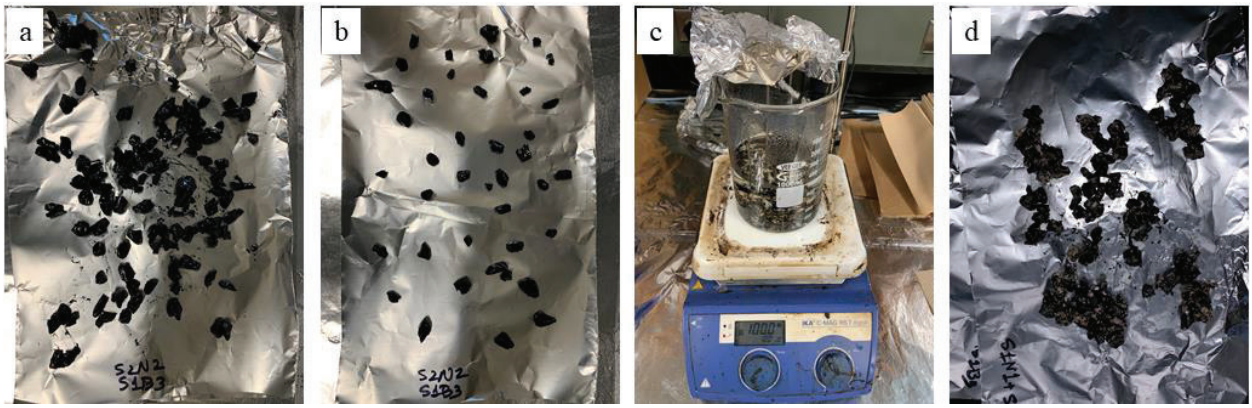

Figure 11. Texas Boiling Test; (a) Asphalt Mixture, (B) Separated Coated Aggregates, (C) Boiling the Sample, and (D) Air Drying After Boiling.

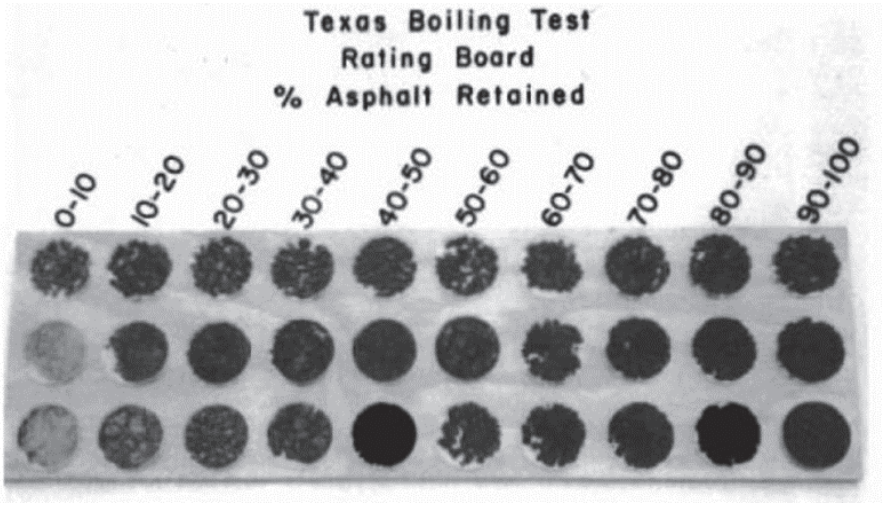

Figure 12. Rating board for Texas Boiling Test (Kennedy et al. 1984).

3.2.6 Asphalt binders collected from plant

Five asphalt mixtures and their corresponding plant binders were collected from five different plants across Arkansas. Their summary is presented in Table 4. RAP was also collected from four plants, as four of these mixtures included some percentages of RAP (Table 4. Key Features of

Collected Plant Mixtures for Binder Tests). Then, the RAP binder was extracted from RAP mixtures, which were subsequently blended with corresponding plant binders at their respective percentages.

Table 4. Key Features of Collected Plant Mixtures for Binder Tests

Plant Name	Redstone Const. Group, Inc.	APAC-Central, Inc. (Sharp quarry)	Blackstone Construction, LLC (Duffield)	Delta Asphalt of AR, Inc.	APAC-Central, Inc. (Jenny Lind)
Mix design	WMA049-19	HMA345-18	HMA428-19	HMA037-21	WMA034-21
Mix type	12.5 MM ACHM Surface	12.5 MM ACHM Surface	9.5 MM ACHM Surface	12.5 MM ACHM Surface	12.5 MM ACHM Surface
Total asphalt content, %	5.1	5.4	5.5	5.2	5.7
Binder	PG 70-22	PG 70-22	PG 70-22	PG 70-22	PG 70-22
Binder source	Marathon Petroleum Corporation Memphis, TN	Lion Oil Company (Port Place) Muskogee, OK	Marathon Petroleum Corporation Memphis, TN	Ergon Asphalt and Emulsion, Inc. Memphis, TN	Lion Oil Company (Port Place) Muskogee, OK
Mixing temp (°)	310	340	325	320	315
Compaction temp (°)	265	310	295	295	285
Anti-strip agent	Evotherm P25 (0.25%)	Evotherm P25 (0.25%)	Morlife 300 (0.25%)	NovaGrip 975 (0.25%)	Evotherm P25 (0.25%)
RAP content (%)	15	20	14	25	0
Binder nomenclature	PB1	PB2	PB3	PB4	PB5

3.2.7 Binder Recovery

The binder extraction was performed according to the AASHTO T 164 (Test Method A) specification. The solvent used in this project was n-Propyl Bromide (nPB). A centrifuge extractor

(Figure 13) was used to extract the binder + nPB solution from aggregates. Binders were then recovered from the binder + nPB solution using a rotary evaporator (Rotavapor) for further testing. First, approximately 1000 gm of loose asphalt mixtures were placed in the bowl, the weight measurement was not necessary. Later enough nPB was poured into the bowl and the mix was soaked for an hour to allow the binder to get dissolved in nPB. Afterward, the bowl was placed into the extractor and the chamber was secured. A 1000 mL glass beaker was used to receive the extracted solution. The extractor's rotation was initiated, and speed was increased slowly up to 3000 rpm. With 3000 rpm rotational speed, the solution was separated from aggregates and collected in a beaker. The device was kept running until the extract ceased its flow from the ejection pipe. The obtained solution was allowed to rest for about 15 minutes to settle the fine particles down and then carefully transferred to a flask for the recovery procedure.

Figure 13. **Centrifuge Extractor for Asphalt Binder Extraction Process.**

The recovery procedure was conducted according to the ASTM D5404 specification. The nPB was evaporated using Rotavapor and subsequently condensed to liquid in the condenser and collected in a different flask leaving the asphalt binder behind. The recovery process is depicted in Figure 14. Firstly, the flask containing the solution was firmly attached to the rotavapor and placed in a hot (95 °C) oil bath. The flask was rotated at a speed of 40 rpm and the coolant was circulated through the condenser. A vacuum pressure of 53 ± 7 mbar below the atmospheric pressure was applied to the flask, and nitrogen gas was supplied at a rate of approximately 500 mL/min. The evaporation rate was approximately 100mL/min at this point. Once the bulk amount of nPB was collected, the vacuum pressure was slowly increased up to 800 ± 7 mbar below the

atmospheric pressure. The nitrogen supply was increased to approximately 600 mL/min and the rotation speed was increased to 45 rpm. At this point, the bubble formation rate was carefully noticed. The setup was run for an additional 10 minutes once the last bubble formation was noticed. Then, the flask with asphalt binder was detached. The recovered binder was then transferred to a metal can at 163℃.

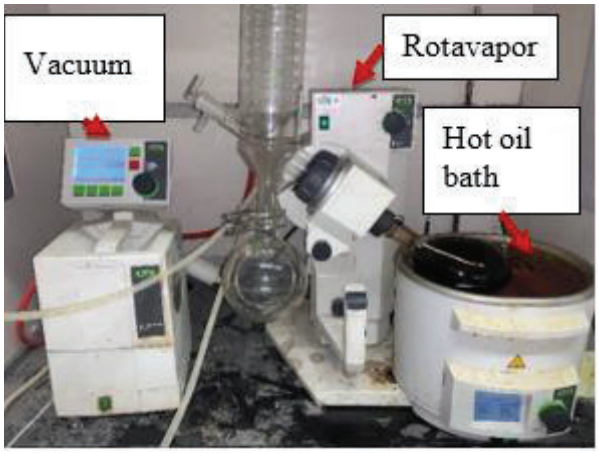

Figure 14. **The Rotary Evaporation System for Asphalt Binder Recovery Process.**

3.2.8 RAP binder blending

After enough RAP binders were recovered, they were blended with their respective plant binder following a manual blending protocol developed by Hossain et al. (2013). Researchers suggested that this manual blending protocol can simulate the large-scale field mixing mechanism in the laboratory. Besides RAP blending, researchers also followed the same blending protocol to mix additives with virgin binders (Oyan et al. 2021, 2022, Rashid et al. 2019, Bagchi et al. 2021). This laboratory blending protocol involved the following prescribed steps:

(i) The required amount of neat binder was transferred in an aluminum can and heated at the mixing temperature mentioned in the mix design (Table 4) for one hour. For example, the binder collected from the Redstone Construction Group LLC. plant was heated at 310 °F (154 °C).

(ii) The container of RAP binder was heated separately at the same temperature for one hour at the same time.

(iii) The required amount of RAP binder was poured into the base binder and stirred with a preheated clean glass rod for one minute.

(iv) The container with binder and RAP was kept in the oven at a preselected temperature for nine minutes covered with aluminum foil.

(v) The "one-minute stirring + nine-minute heating" cycle was repeated for a total count of six times, allowing 60 minutes of blending time for each mix.

(vi) The interior wall of the sample container was scraped periodically to prevent the accumulation of RAP binders on the wall.

Figure 15 shows RAP blending with asphalt following manual blending protocol. The blended asphalt binder was then allowed to cool down to room temperature for testing purposes.

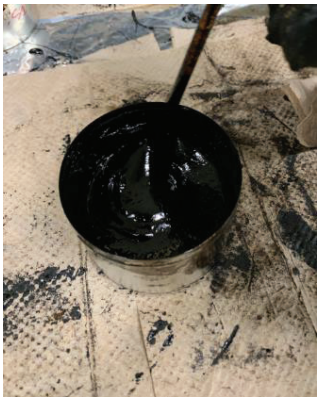

Figure 15. RAP Blending With Virgin Plant Binders.

3.3 Asphalt Mixture

As outlined in the proposal, selected performance tests have been conducted on ACHM asphalt mixtures collected from plants, in both the Lab Mix Lab Compacted (LMLC) and Reheated Plant Mix Lab Compacted (RPMLC) form.

3.3.1 Volumetrics (AASHTO T 331 & T 269)

The bulk specific gravity test and maximum specific gravity test will be conducted as per the AASHTO specifications. These tests will be performed to verify the compaction data and sample preparation. The bulk-specific gravity will be calculated using a CORELOK machine. This piece of equipment can be seen in Figure 16. The voids in mineral aggregate (VMA) and voids filled with

asphalt (VFA) will also be found in this process. The results from the volumetrics testing will also help identify any discrepancies between the lab and plant mixtures.

Figure 16. A CORELOK Machine Used in Specific Gravity Measurements.

3.3.2 Dynamic Modulus (AASHTO T 378-17 & R 84-17)

The dynamic modulus test will be performed to evaluate the viscoelastic properties of each mixture. The specimens for this test shall be 4 inches in diameter by 6 inches in height. This test will consist of sinusoidal loadings at three different frequencies (0.1 Hz, 1.0 Hz, and 10 Hz) and three different temperatures (4 ^{o}C, 20 ^{o}C, and 40 ^{o}C), per AASHTO R 84. This test will be performed without confining pressure. The results will be analyzed to create a master curve, which is described and outlined in AASHTO R 84. These results will also serve to further reveal the rutting and cracking potential of each asphalt mixture. The dynamic modulus setup can be seen in Figure 17 and is a non-destructive test.

Figure 17. Dynamic Modulus and Flow Number Test Setup.

3.3.3 Flow Number (AASHTO T 378)

The flow number test shall also be performed per AASHTO T 378, this test will further the understanding and analysis of the different elastic properties of the asphalt mixtures. This test will be performed by subjecting the asphalt specimen to repeated sinusoidal compressive loadings until a set number of loads have occurred or permanent deformations in the asphalt have reached a specific threshold. This test will be run on the same dynamic modulus sample shown in Figure 17 after the dynamic modulus testing has been completed.

3.3.4 I-FIT (AASHTO TP 124)

The intermediate temperature cracking potential of each mix will be determined from the Illinois flexibility index test (I-FIT) per AASHTO TP 124. This test will be performed on a semi-cylindrical specimen with a height of 50 mm and a 15 mm notch cut into the flat side. The specimen will be loaded at a rate of 50 mm per second until failure. The I-FIT test setup is shown in Figure 18.

Figure 18. An I-FIT Test Setup.

3.3.5 Tensile Strength Ratio (AASHTO T 283)

The tensile strength ratio test will be performed per AASHTO T 283. This test method is the recommended test for determining the mixture's moisture resistance and stripping potential. This test will be performed on six test specimens; three of the specimens will be moisture-conditioned, and the other three will be unconditioned. This test will be performed on cylindrical

specimens with a diameter of 150 mm and a thickness of 95 mm. The TSR test setup can be seen in Figure 19.

Figure 19. Tensile Strength Ratio Test Setup.

3.3.6 Hamburg Wheel-Track Testing (AASHTO T 324)

The rutting and moisture susceptibility will be determined through the Hamburg Wheel-Tracking Test, per AASHTO T 324. This test will be performed on samples prepared by a Superpave gyratory compactor and then cut to size. The specimens will be submerged in a water bath at 64 ^{o}C and repetitively loaded using a steel wheel for 20,000 passes. The resulting plot from this data will be analyzed to determine the stripping resistance of the mixture at high temperatures. The Hamburg Wheel Tracking Test can be seen in Figure 20.

Figure 20. Hamburg Wheel-Track Testing Setup.

3.3.7 IDEAL – CT (ASTM D8225)

The indirect tensile asphalt cracking (IDEAL-CT) test will be performed at intermediate temperatures. This recently developed method will be used to predict the field cracking performance of the mixture. The results of this method are used to calculate a cracking index, in which, the higher the value, the better the cracking resistance. This test will be conducted using samples that do not need to be cut or notched in sample preparation. A summary of all of the test methods that will be explored can be seen in Table 5.

Table 5: Summary of mixture test methods

Testing Method Name	Specification No.
Bulk Specific Gravity	AASHTO T 331
Dynamic Modulus & Flow Number	AASHTO T 378 & R 84
I-FIT	AASHTO TP 124
Tensile Strength Ratio	AASHTO T 283
Hamburg Wheel-Track Testing	AASHTO T 324
IDEAL-CT	ASTM D8225-19

4 Test Results

4.1 *Aggregates*

4.1.1 Specific Gravity and Absorption

Specific gravity and absorption test results of all aggregates were presented in Figure 21 and, Figure 22, respectively. Three replicate specimens were tested for each type of aggregate. The average specific gravity values and their standard deviations are presented in these figures. DM2 and SS2 had the highest and lowest bulk-specific gravity, respectively. Overall, the absorption is less than 2% for all the aggregates except SS1. This SS1 (sandstone from Gum Log Quarry) had an absorption value of nearly 4%. On the other hand, LS1 had the least absorption value.

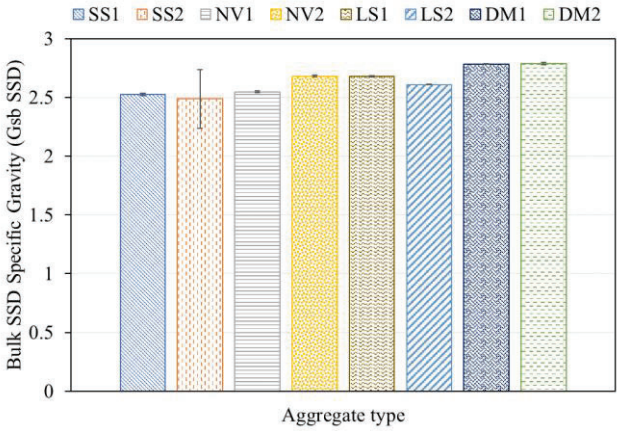

Figure 21: Specific Gravity Values of Tested Aggregates.

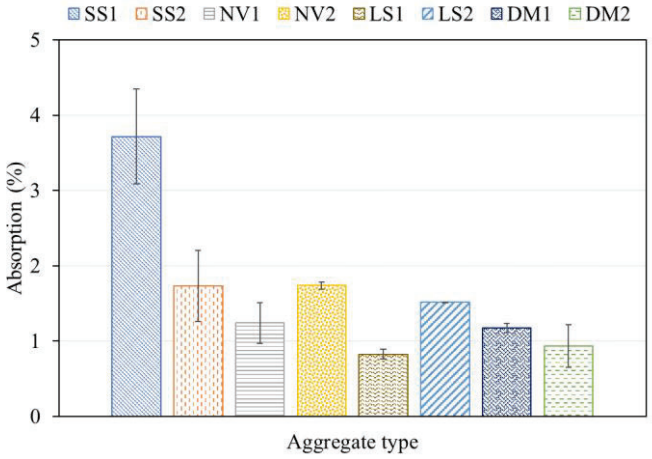

Figure 22: Absorption (%) Values of Tested Aggregates.

4.1.2 Los Angeles (LA) Abrasion Resistance

All aggregates were tested for LA Abrasion resistance, and their results are presented in Figure 23. In general, all the aggregates have an abrasion loss of less than 40% (the ARDOT requirement). NV1 showed the lowest % loss and SS2 showed the highest % loss in the LA abrasion test.

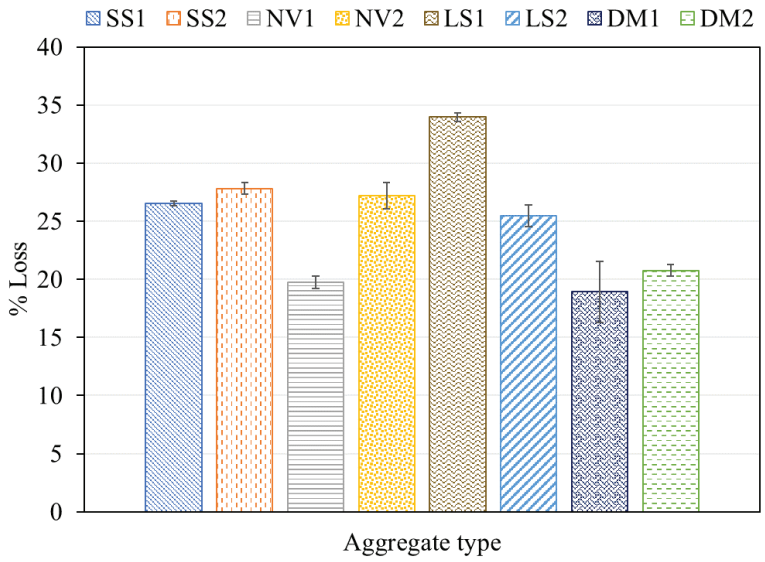

Figure 23: Percent Loss in LA Abrasion Resistance Test.

4.1.3 pH Content

All the aggregates were tested for pH and the test results were given in Figure 24. All the tested aggregates were found basic and all had pH values greater than 8.

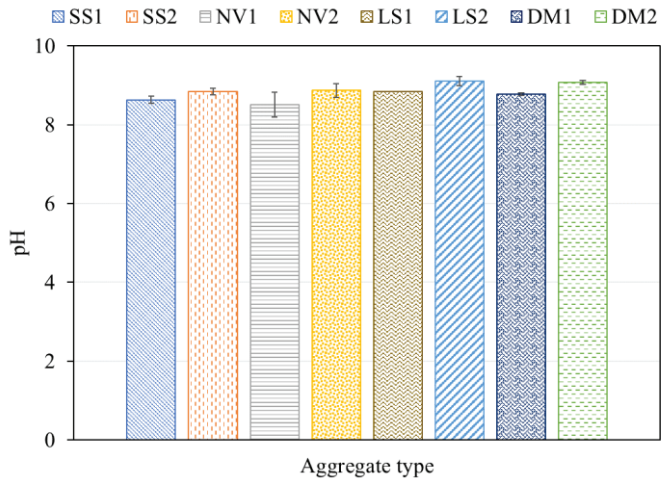

Figure 24: Measured pH Value of Tested Aggregates.

4.1.4 Sessile Drop (SD) (Optical Contact Angle) Test: Aggregate Samples

Contact angles for all aggregates were measured in the SD test and the results were shown in Figure 25. The highest contact angles were observed for water and the lowest angles were measured for formamide except for the NV1 sample. High variability in measured contact angles was assumed to be the result of irregular size and distribution of porous network and mineralogical heterogeneity.

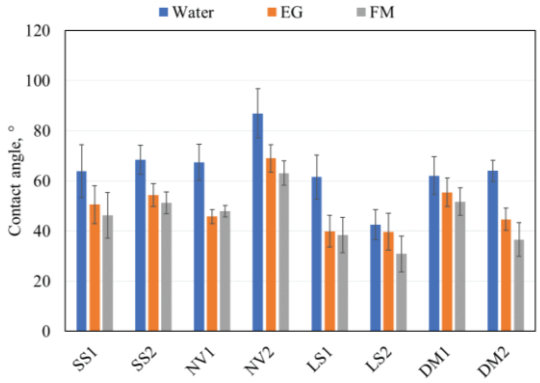

Figure 25: Contact Angles of all Aggregate Samples With Reference Liquids.

Three SFE components: a monopolar acidic component (Γ^+), a monopolar basic component (Γ^-), and an apolar or Lifshitz-van der Waals (Γ^{LW}) were eventually calculated and presented in Figure 26. Apolar Lifshitz-van der Waals (Γ^{LW}) components were the major contributor to total SFE. However, the higher basic component was also observed for all aggregates except NV2. All Source 2 aggregates had higher total SFE values compared to their Source 1 aggregates except sandstone samples. A similar trend was observed for cohesive energy values for all aggregates (Figure 27).

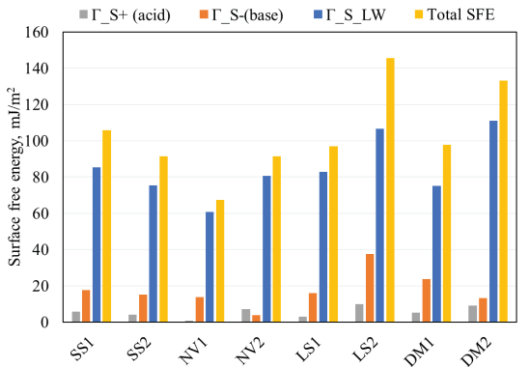

Figure 26: Surface Free Energy (SFE) Components of all Tested Aggregate Samples.

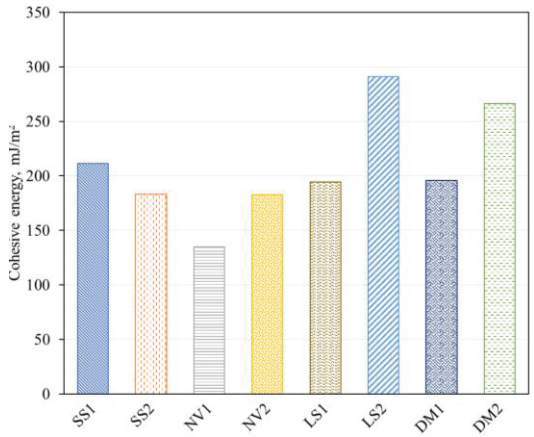

Figure 27: Cohesive Energy Values of all Tested Aggregate Samples.

4.2 Asphalt Binders

4.2.1 Penetration Test

Penetration test results of all binder source samples are presented in Figure 28. For Sources 1, 2, 4, and 6, the penetration number decreased as the binder grade increased.

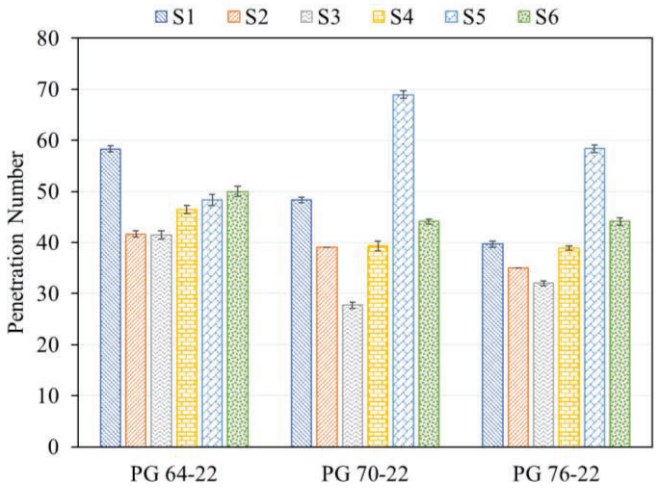

Figure 28: Penetration Test Results of Tested Asphalt Binders.

4.2.2 Rotational Viscometer (RV)

The RV test data are presented in Figures 29 through 31 for S1 through S6 asphalt binders. The viscosity data will be an indicator of moisture resistance as a binder with higher viscosity is expected to have better stripping resistance (Hossain et al. 2015). None of the viscosity measurements exceeded the Superpave criterion (≤ 3000 mPa. at 135 °C) besides S5B3.

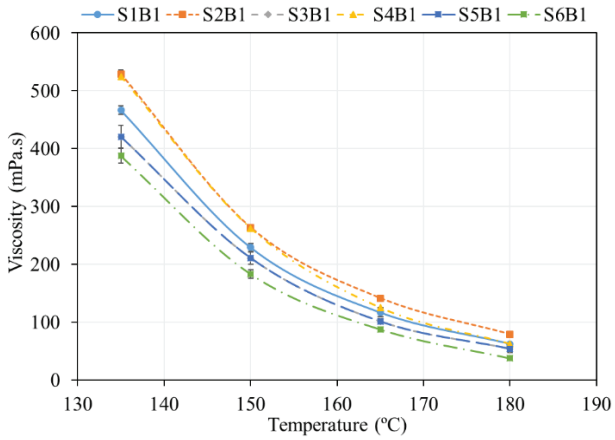

Figure 29: Viscosity Temperature Curves of PG 64-22 Binders From Different Sources.

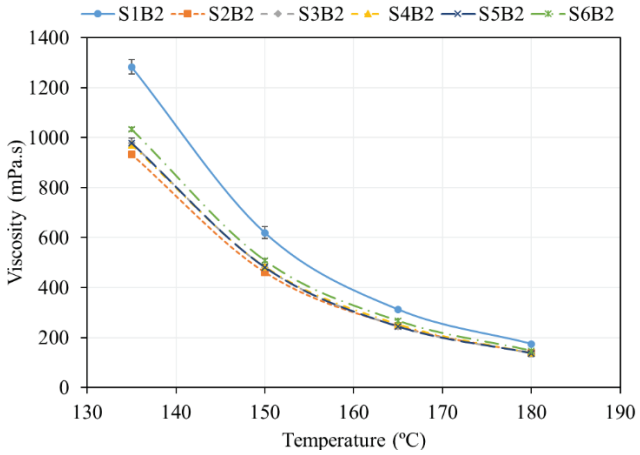

Figure 30: Viscosity Temperature Curves of PG 70-22 Binders From Different Sources

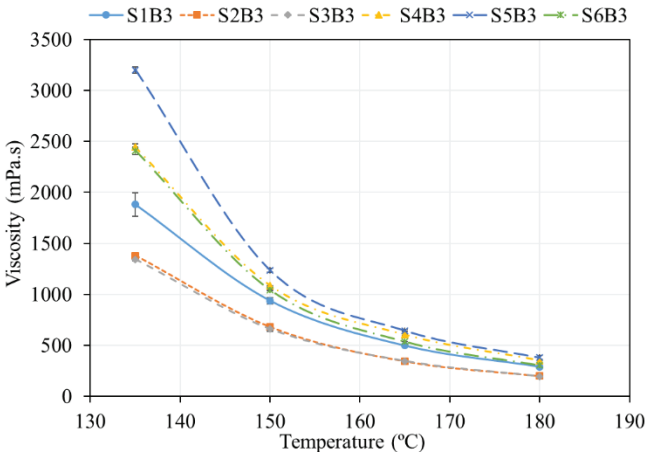

Figure 31: Viscosity Temperature Curves of PG 76-22 Binders From Different Sources.

4.2.3 Acid number (pH)

The acid number test was performed on binder samples from S1 through S6, and the results are presented in Figure 32. All the binders had pH values less than 7. Source 4 binders were found to be more acidic, and source 6 binders were the least acidic. Overall, pH did not vary significantly with the binder's grade except for source 4 binders.

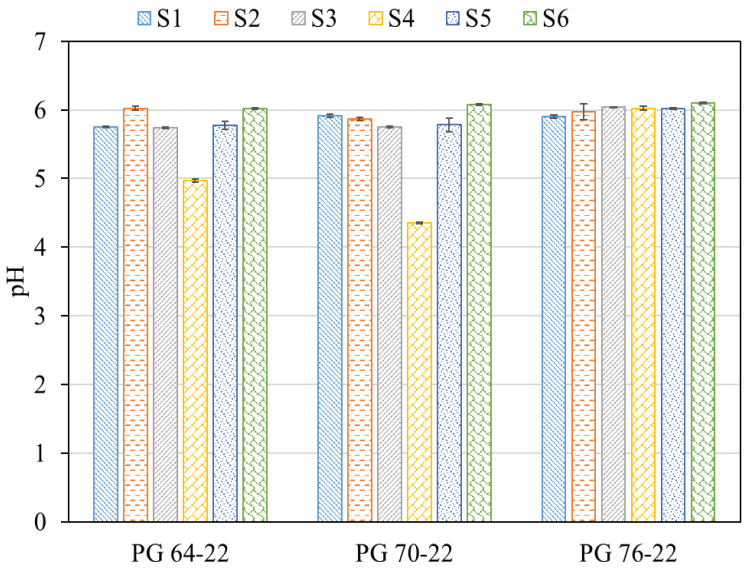

Figure 32: Measured pH Value of Asphalt Binders.

4.2.4 Sessile Drop (SD) (Optical Contact Angle) Test: Asphalt Binder

Contact angles for all asphalt binders with three reference liquids were measured and shown in Figure 33. Three SFE components were also calculated from the measured contact angles and presented in Figure 34. All the binder samples had higher contact angles with water compared to other liquids. While calculating SFE, the Lifshitz-van der Waals (Γ^{LW}) component was found to be the largest among all three components. Figure 34 showed that Source 2 binders had the lowest total SFE values. As cohesive energy is twice as much of total SFE, a similar trend was observed in Figure 35. No other trend had been observed in this figure.

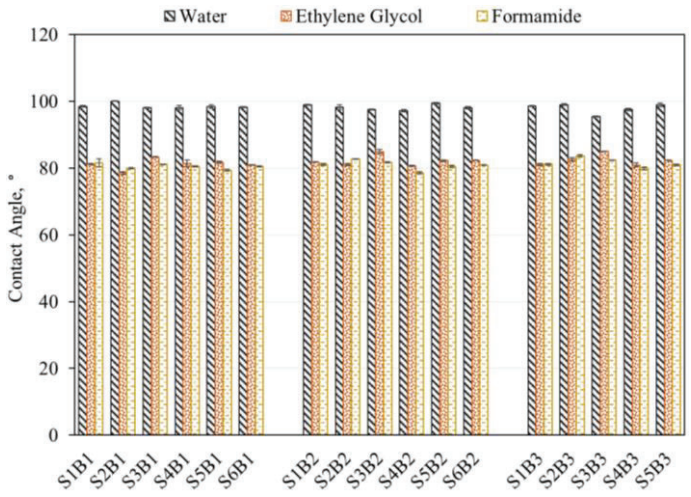

Figure 33: Contact Angles of All Asphalt Binders With References Liquids.

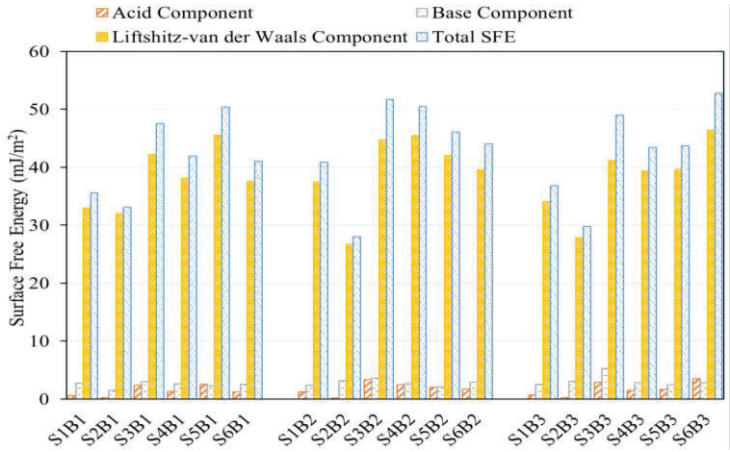

Figure 34: Surface Free Energy (SFE) Components of All Tested Asphalt Binders.

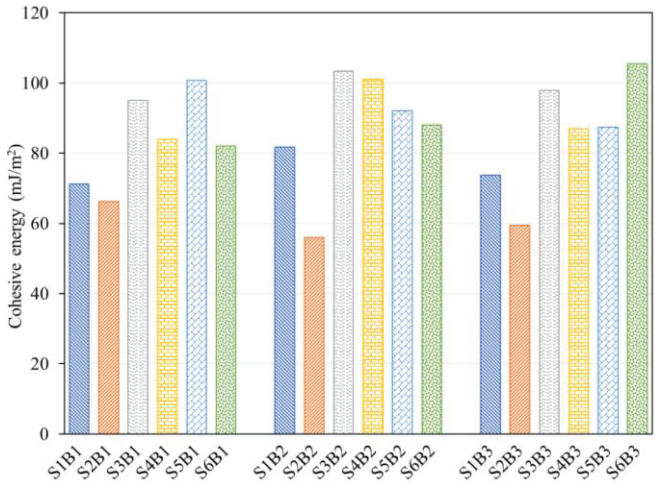

Figure 35: Cohesive Energy Values of All Tested Asphalt Binders.

4.2.5 Dry and wet adhesion bond energies

Both dry and wet work of adhesion values between aggregate and asphalt binder were presented in Figure 36. Figure 36 (a) through (c) presented dry adhesion energy values of aggregate-binder systems. The lowest dry adhesion energy was calculated for the S2B2-NV1 system (86.5 mJ/m^2). All the tested binders had the lowest dry adhesive bond energy with NV1. The highest dry adhesion energy (174.5 mJ/m^2) was calculated for the S6B3-LS2 system. The effect of aggregate source on dry work of adhesion was obvious in Figure 36 (a) through (c). Like Figure 27, Source 2 novaculite, limestone, and dolomite, and Source 1 sandstone showed higher dry adhesion energy values compared to fellow aggregates. A higher dry work of adhesion value indicates a stronger bond as more energy will be required to initiate separation at the interface.

Figure 36 (d) through (f) shed some light on the wet work of adhesion. Work of adhesion in the presence of water was expected to decrease substantially compared to dry conditions (Little and Bhasin 2006, Hossain et al. 2015). Unlike dry work of adhesion, these figures showed that the lowest wet work of adhesion was found for the S2B2-LS2 system (7.39 mJ/m^2), and the highest value was observed for the S5B1-NV2 system (55.7 mJ/m^2). Thus, limestone (source 2) would be expected to be better moisture resistant than novaculite (source 2). The effect of the source was also obvious. For sandstone, novaculite, and dolomite; Source 2 samples showed higher wet work of adhesion. Higher wet work of adhesion values indicates more energy dissipation in the presence of water i.e., the reaction will be more thermodynamically favorable (Hossain et al. 2021). Thus, for all these three aggregate types, Source 1 samples would show higher moisture damage resistance than Source 2 samples. For limestone, the Source 2 sample would show better moisture damage resistance than the Source 1 sample.

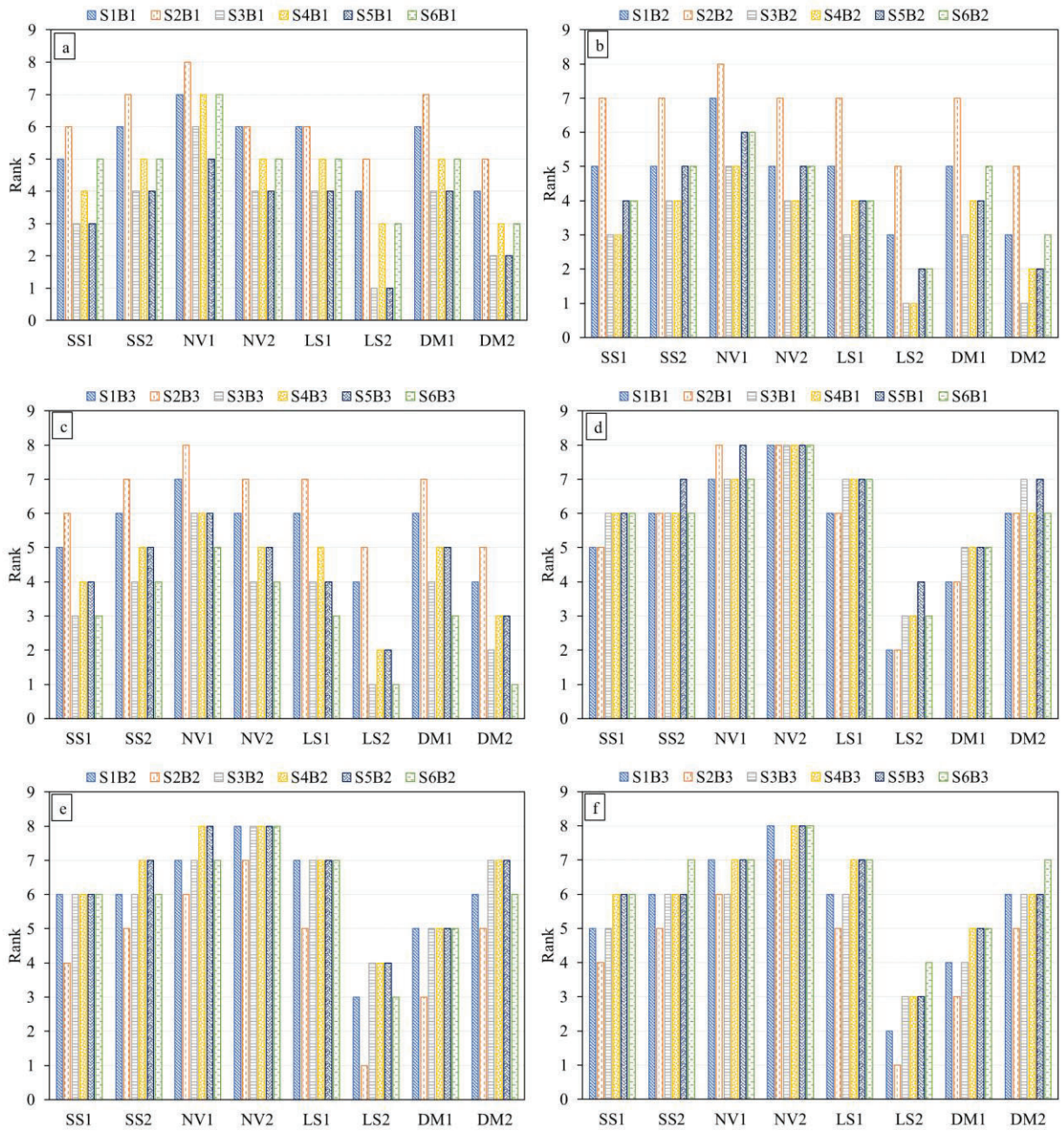

Figure 36: Work of Adhesion Between Aggregate-Binder Systems, Dry Work of Adhesion (a) PG 64-22, (b) PG 70-22, and (c) PG 76-22; Wet Work of Adhesion (d) PG 64-22, (e) PG 70-22, and (f) PG 76-22.

4.2.6 Texas Boiling Test

Texas Boiling test was performed for all the binder-aggregate systems, and results are shown in Figures 37 through 39. Figure 37 shows that SS2, LS1, DM1, and DM2 performed well i.e., they showed a good % of asphalt retention. Figure 38 shows the percent asphalt retention of mixtures prepared from PG 70-22 binders and aggregate samples. In this aggregate-binder system, SS2, LS1, and DM1 showed good % of asphalt retention (> 50%). Figure 39 shows a similar trend that was observed for PG 64-22 binder samples in Figure 37. Besides, all aggregate samples showed a very good % of asphalt retention (> 70%) with S4B3 binder.

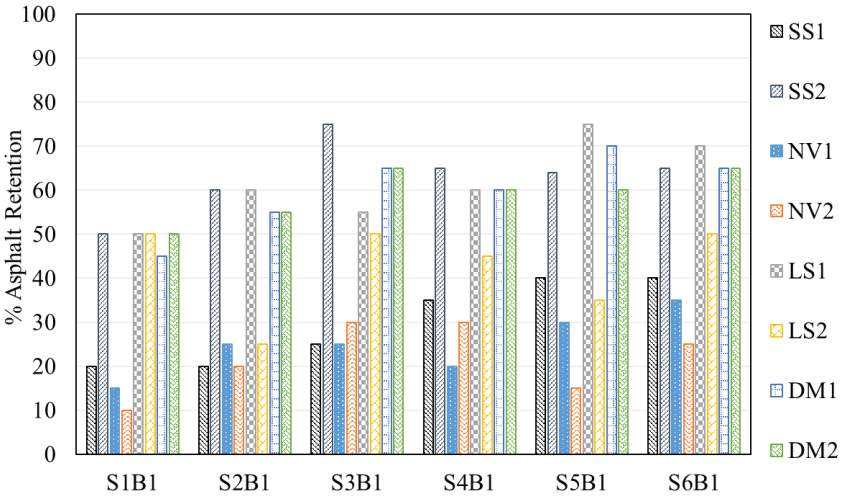

Figure 37: Texas Boiling Test Results for PG 64-22 Binders.

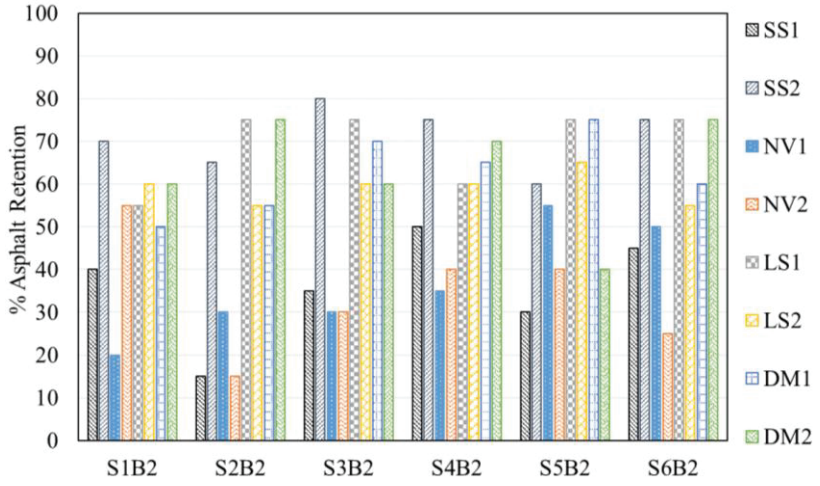

Figure 38: Texas Boiling Test Results for PG 70-22 Binders.

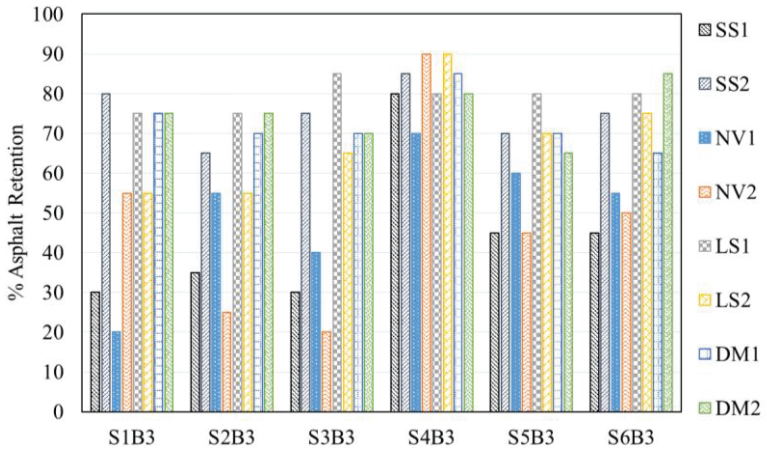

Figure 39: Texas Boiling Test Results for PG 76-22 Binders.

4.2.7 AFM Tests Results of Binders

As indicated earlier, a Dimension Icon AFM from Bruker has been used to observe the surface roughness/morphology and the mechanical properties, including the DMT modulus, adhesion force, deformation, and dissipated energy of the asphalt binders.

Figure 40 through 45 show the morphology (surface roughness) of PG 64-22, PG 70-22, and PG 76-22 binder samples from different sources cured at 3 and 7 days. Three different distinct phases such as dispersed (catena), interstitial (peri), and matrix (Perpetua) were present in asphalt binder samples. The maximum number of 'bee structures' was found for the S1, S2, and S3 sources' asphalt binder, which can be due to the high molecular mobility of the binder. On the other hand, the lowest number of 'bee structures' was observed for the S4 source's binder, indicating the molecular mobility hindrance and a high degree of association.

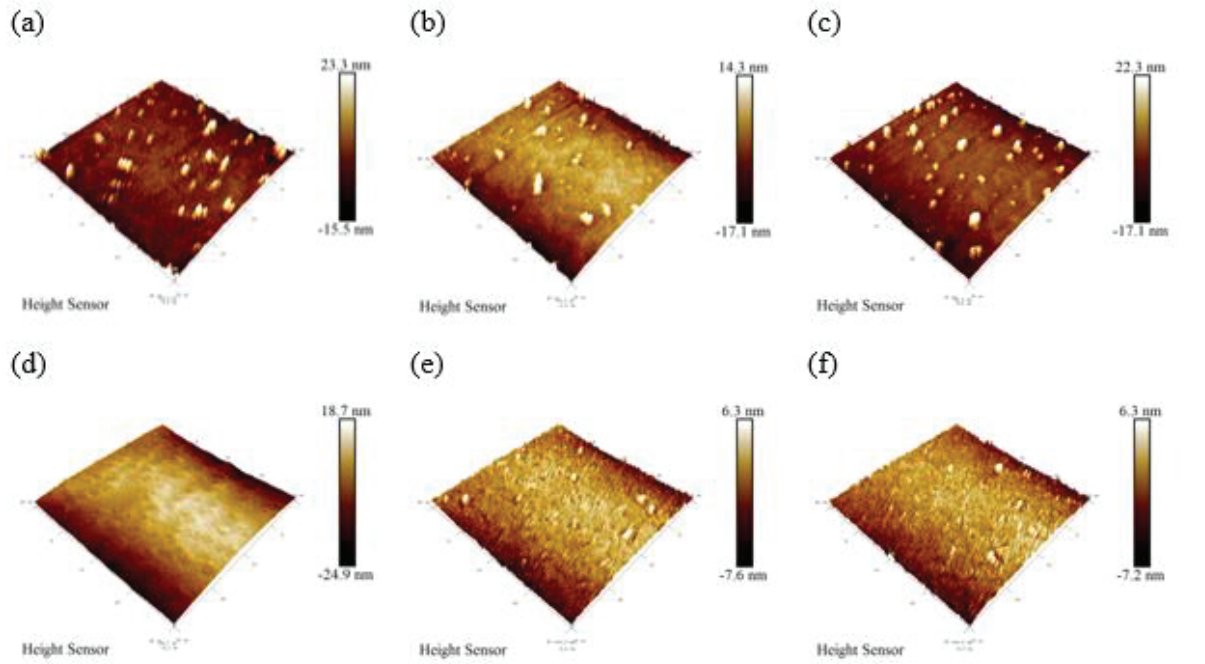

Figure 40: Morphology of PG 64-22 Binder Samples at 3 days: (a) S1B1 (b) S2B1 (c) S3B1 (d) S4B1 (e) S5B1, and (f) S6B1.

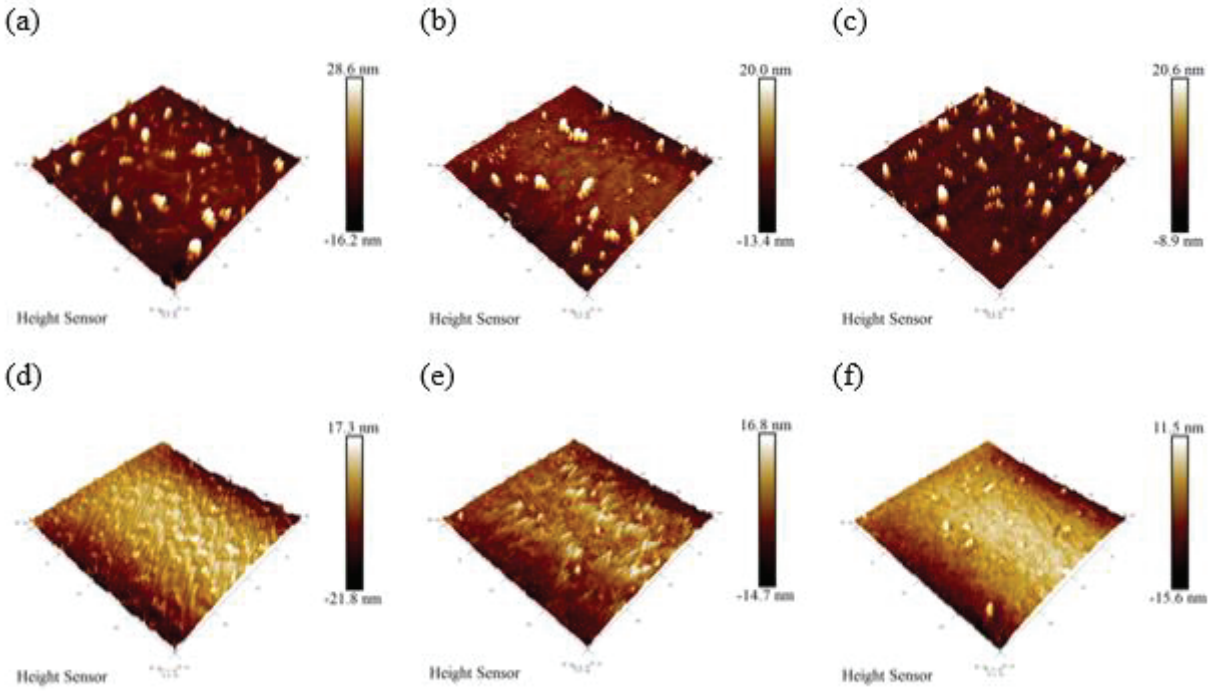

Figure 41: Morphology of PG 64-22 Binder Samples at 7 days: (a) S1B1 (b) S2B1 (c) S3B1 (d) S4B1 (e) S5B1, and (f) S6B1.

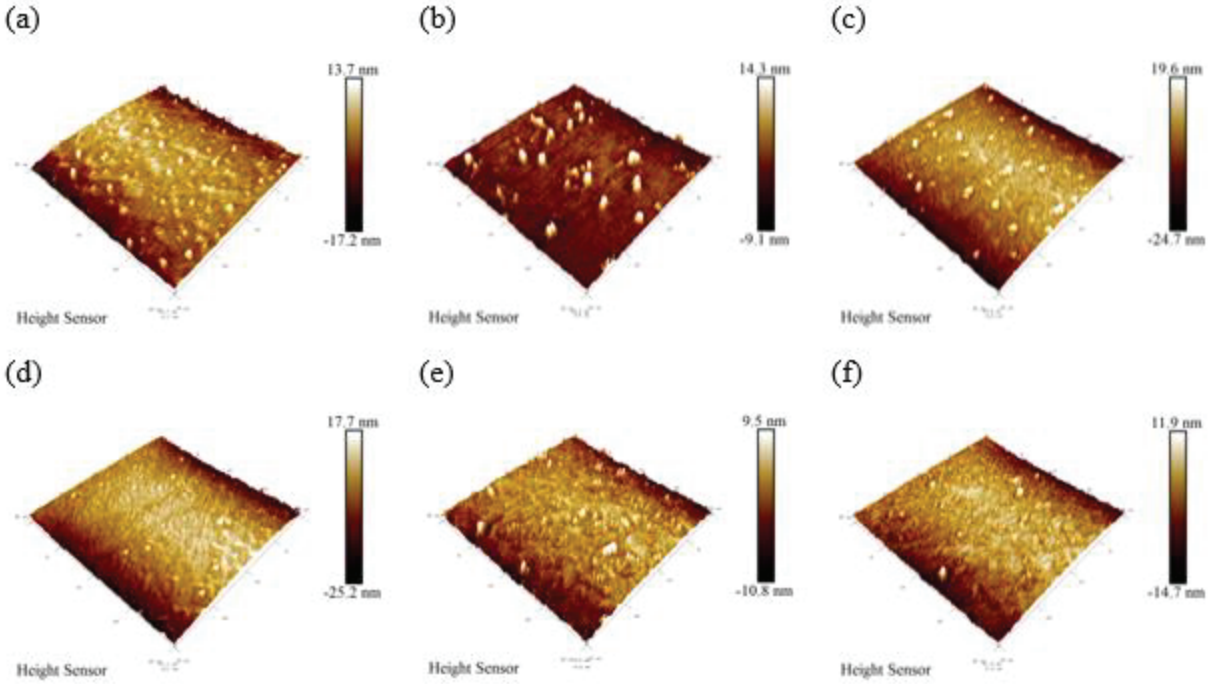

Figure 42: Morphology of PG 70-22 Binder Samples at 3 days: (a) S1B1 (b) S2B1 (c) S3B1 (d) S4B1 (e) S5B1 and (f) S6B1.

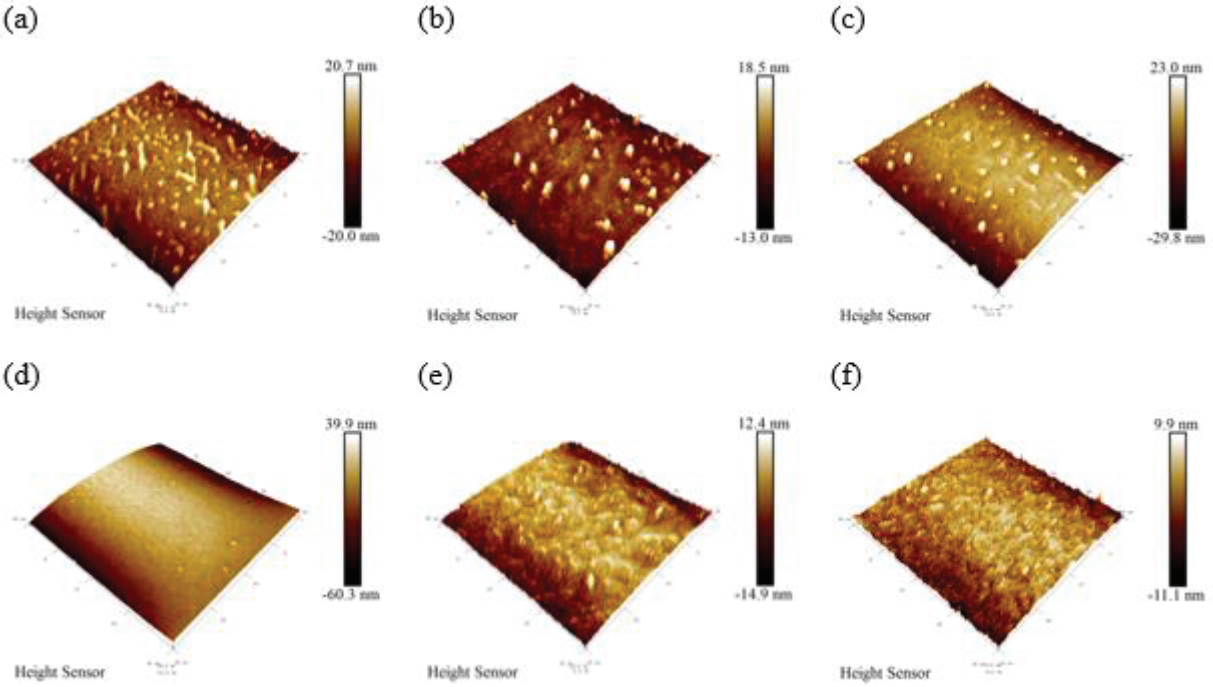

Figure 43: Morphology of PG 70-22 Binder Samples at 7 days: (a) S1B1 (b) S2B1 (c) S3B1 (d) S4B1 (e) S5B1, and (f) S6B1.

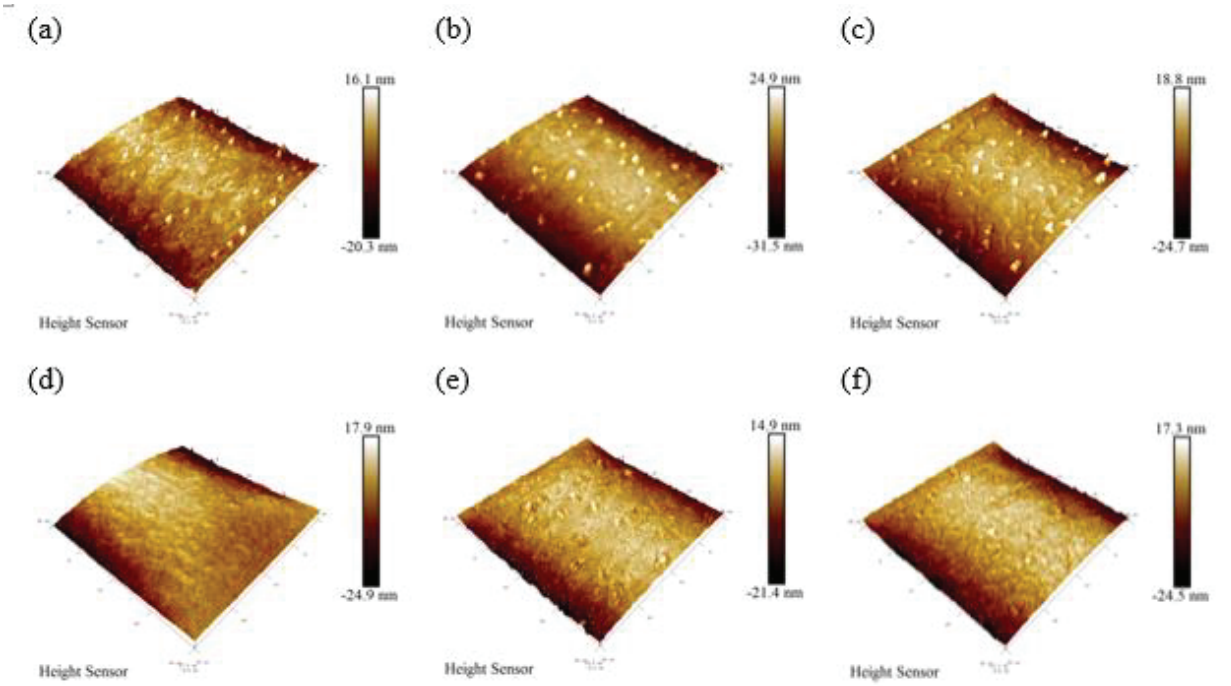

Figure 44: Morphology of PG 76-22 Binder Samples at 3 days: (a) S1B1 (b) S2B1 (c) S3B1 (d) S4B1 (e) S5B1, and (f) S6B1.

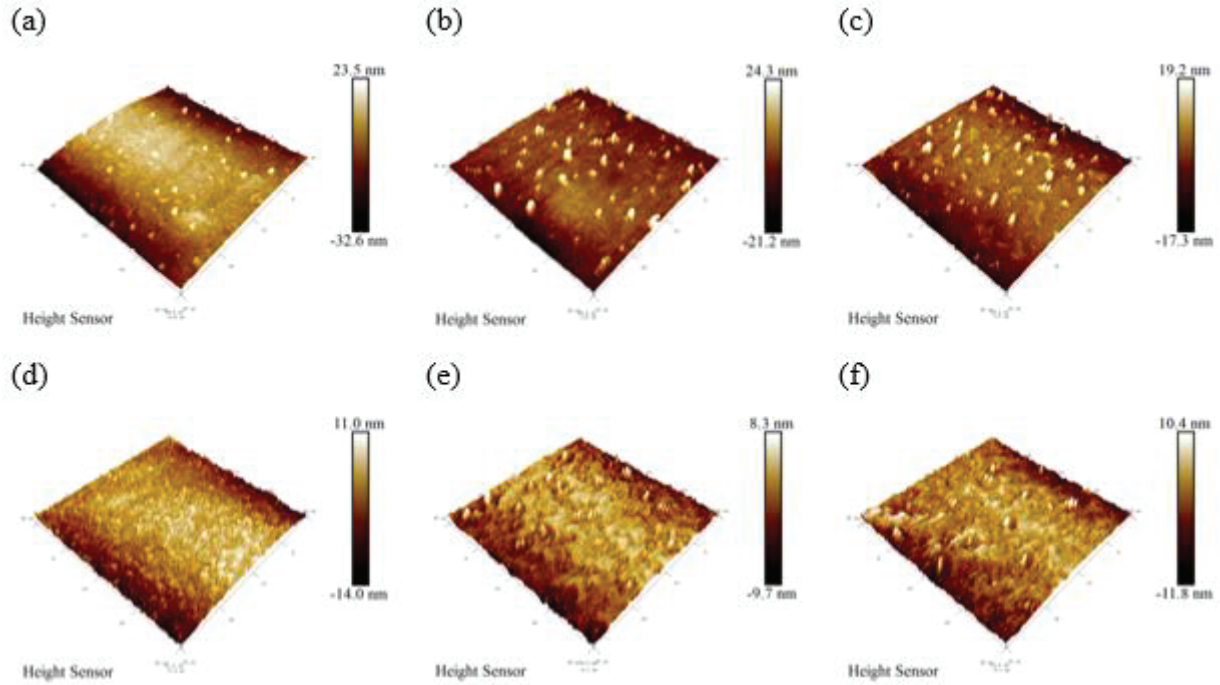

Figure 45: Morphology of PG 76-22 Binder Samples at 7 days: (a) S1B1 (b) S2B1 (c) S3B1 (d) S4B1 (e) S5B1, and (f) S6B1.

A summary of the DMT modulus data of asphalt binder samples is shown in Table 6. The maximum DMT modulus (765 MPa) was obtained for the S2B3 binder; in contrast, the S5B1 asphalt binder sample showed the lowest DMT modulus (125 MPa). The DMT modulus of the asphalt binder samples was lower in the matrix phase compared to the dispersed and interstitial phases. In general, the DMT modulus increased with the binder grade, thus indicating a stiffer binder.

Table 6: Summary of DMT Modulus (MPa) of Asphalt Binder Samples

Binder type	Binder name	3-day average value	3-day in dispersed and interstitial phase	3-day in the matrix phase	7-day average value	7-day in dispersed and interstitial phase	7-day in Matrix phase
PG 64-22	S1B1	233	159-229	136-160	236	176-228	168-211
PG 64-22	S2B1	190	156-171	109-145	196	144-178	81.3-108
PG 64-22	S3B1	192	122-164	94.9-111	216	172-205	133-152
PG 64-22	S4B1	294	243-276	168-252	209	166-182	130-154
PG 64-22	S5B1	125	113-115	96.1-98.3	189	162-163	73.6-98.3
PG 64-22	S6B1	132	102-124	89.5-92.4	159	112-145	89.8-139
PG 70-22	S1B2	282	228-245	162-209	335	267-309	227-303
PG 70-22	S2B2	224	183-207	105-144	245	209-239	147-211
PG 70-22	S3B2	367	230-350	222-252	442	317-380	195-325
PG 70-22	S4B2	154	120-151	95.7-131	254	222-243	73.7-186
PG 70-22	S5B2	232	209-221	175-186	505	385-457	230-378
PG 70-22	S6B2	328	274-302	161-252	373	261-334	188-364
PG 76-22	S1B3	745	401-567	260-350	292	212-278	106-207
PG 76-22	S2B3	634	445-538	196-324	765	488-608	333-582
PG 76-22	S3B3	256	162-185	110-166	501	309-380	239-279
PG 76-22	S4B3	268	234-254	157-188	635	360-560	219-225
PG 76-22	S5B3	256	197-230	142-193	217	170-192	103-120
PG 76-22	S6B3	130	93.5-121	77.6-103	354	211-261	113-170

Table 7 presents the summary of the adhesion force of different asphalt binder samples. The S3B1 asphalt binder sample exhibited the maximum adhesion force (788 nN) among all asphalt binders, indicating higher resistance against moisture damage. Contrarily, the minimum adhesion force (139 nN) was found for the S5B2 binder, which can be due to the presence of moisture that has eroded the asphalt binder. The dispersed and interstitial phases had higher adhesion force (112-668 nN) compared to the matrix phase (31.3-297 nN) for all the binder samples.

Table 7: Summary of Adhesion Force (nN) of Asphalt Binder Samples

Binder type	Binder name	3-day average value	3-day in dispersed and interstitial phase	3-day in the matrix phase	7-day average value	7-day in dispersed and interstitial phase	7-day in the matrix phase
PG 64-22	S1B1	480	325-405	44.9-69.7	626	433-582	140-297
PG 64-22	S2B1	599	421-557	41.6-80.3	554	315-527	59-98.1
PG 64-22	S3B1	788	444-668	86.3-162	348	243-261	131-223
PG 64-22	S4B1	504	356-466	31.3-43.5	585	457-487	71.5-121
PG 64-22	S5B1	392	352-389	68.3-78.6	693	594-632	104-139
PG 64-22	S6B1	291	215-245	49.2-59	492	388-449	91.5-165
PG 70-22	S1B2	479	271-382	80.4-112	734	524-661	67.5-139
PG 70-22	S2B2	529	382-452	87.1-146	668	471-590	104-148
PG 70-22	S3B2	579	465-557	85.8-260	605	490-545	77-140
PG 70-22	S4B2	591	530-575	66.8-113	506	420-452	110-124
PG 70-22	S5B2	220	165-206	51.1-78.6	139	114-134	39.5-79.2
PG 70-22	S6B2	514	418-473	103-117	415	338-359	90.2-130
PG 76-22	S1B3	664	517-632	106-158	693	562-641	125-208
PG 76-22	S2B3	701	528-650	103-152	541	405-490	127-207
PG 76-22	S3B3	594	307-379	117-215	355	185-279	70-132
PG 76-22	S4B3	499	401-452	115-151	653	541-586	112-227
PG 76-22	S5B3	355	307-319	112-142	141	112-125	46.6-53.4
PG 76-22	S6B3	385	265-333	107-162	198	138-176	41.6-59.5

The summary of the deformation values of asphalt binder samples is shown in Table 8. Among all asphalt binders, the lowest deformation (0.975 nm) was observed for the S4B1 binder; contrarily, the highest deformation (5.15 nm) was found for the S5B1 binder. The dispersed and interstitial phases in asphalt binder samples showed higher deformation (0.605-4.06 nm) compared to the matrix phase (0.339-3.23 nm).

Table 8: Summary of Deformation (nm) of Asphalt Binder Samples

Binder type	Binder name	3-day average value	3-day in dispersed and interstitial phase	3-day in the matrix phase	7-day average value	7-day in dispersed and interstitial phase	7-day in the matrix phase
PG 64-22	S1B1	1.87	0.848-1.36	0.569-0.738	2.09	1.44-1.99	0.868-1.2
PG 64-22	S2B1	1.18	0.605-1.07	0.339-0.514	1.41	0.798-1.32	0.602-0.696
PG 64-22	S3B1	1.7	0.973-1.84	0.445-0.687	1.48	0.908-1.12	0.676-1
PG 64-22	S4B1	0.975	0.887-0.961	0.731-0.918	2.25	1.58-1.68	1.16-1.33
PG 64-22	S5B1	1.42	1.32-1.4	1.27-1.3	5.15	2.55-3.06	1.19-1.35
PG 64-22	S6B1	1.51	1.44-1.45	1.27-1.44	2.66	2.05-2.55	1.65-2.08
PG 70-22	S1B2	3.11	1.59-2.83	0.94-1.44	4.35	3.1-3.52	0.962-1.71
PG 70-22	S2B2	1.53	0.95-1.41	0.976-1.27	2.32	1.94-2.14	1.34-1.92
PG 70-22	S3B2	1.65	1.15-1.55	0.747-0.838	2.29	1.88-2.2	0.67-1.49
PG 70-22	S4B2	1.99	1.63-1.83	1.29-1.51	2.95	1.61-2.8	1.08-1.74
PG 70-22	S5B2	2.66	2.05-2.53	1.45-1.61	3.65	2.9-3.15	2.08-2.34
PG 70-22	S6B2	5.06	2.07-4.06	1.08-1.68	4.35	2.82-3.63	2.45-3.23
PG 76-22	S1B3	2.85	2.1-2.59	1.29-1.67	2.83	1.65-2.19	1.02-1.68
PG 76-22	S2B3	3.07	1.39-2.75	1.21-1.52	2.92	1.23-1.99	0.798-0.969
PG 76-22	S3B3	2.9	2.39-2.64	1.11-2.09	2.44	1.7-2.28	1.23-1.59
PG 76-22	S4B3	2.87	2.25-2.78	1.63-2.31	2.68	2.29-2.44	1.85-1.93
PG 76-22	S5B3	4.74	3.33-3.73	1.83-2.13	3.26	2.47-3.06	1.46-1.54
PG 76-22	S6B3	4.28	2.53-3.27	1.21-2.29	4.45	2.44-2.97	1.07-1.88

Table 9 represents the summary of the dissipation values of different asphalt binder samples. Among all asphalt binders, the S5B3 asphalt binder sample showed the minimum dissipation value (47,292 eV); in contrast, the maximum dissipation value (43,8888 eV) was observed for the S1B3 binder. The dispersed and interstitial phases exhibited the dissipation of 35,785-427,031 eV and the matrix phase showed the dissipation of 10,821-160,966 eV.

Table 9: Summary of Dissipation Energy (eV) of Asphalt Binder Samples

Binder type	Binder name	3-day average value	3-day values in dispersed and interstitial phase	3-day values in the matrix phase	7-day average value	7-day values in dispersed and interstitial phase	7-day values in the matrix phase
PG 64-22	S1B1	209273	139710-174472	20814-41080	285453	192755-261483	52387-133691
PG 64-22	S2B1	284002	217395-269577	46192-62163	252898	145732-243406	33940-75334
PG 64-22	S3B1	401374	257421-352132	62139-121993	122437	78572-110474	60897-94936
PG 64-22	S4B1	287873	216475-269964	17222-24722	289842	237850-268444	39561-72471
PG 64-22	S5B1	212735	194775-195524	29278-32014	345399	326571-330524	56115-86549
PG 64-22	S6B1	140452	84089-99315	13172-15113	270960	233433-261725	67905-87415
PG 70-22	S1B2	265976	182009-219808	40685-90569	408930	300653-353601	38684-49630
PG 70-22	S2B2	292046	217770-250200	74879-104037	370107	253259-302754	63964-146622
PG 70-22	S3B2	302142	178835-268358	43854-152730	321069	252450-280840	51505-62472
PG 70-22	S4B2	322582	287265-299770	35818-68172	351869	290308-295958	94722-148316
PG 70-22	S5B2	86644	57269-76622	18348-22981	50081	39215-47799	20481-36495
PG 70-22	S6B2	246635	212561-242904	41251-48062	175075	141123-160115	22458-78448
PG 76-22	S1B3	370812	320919-362339	69002-118231	438888	379940-427031	50419-160966
PG 76-22	S2B3	393004	292541-369043	64522-116135	253773	189537-241921	79846-128391
PG 76-22	S3B3	309000	175756-219476	11674-93689	139723	92184-104335	24507-39111
PG 76-22	S4B3	321874	268530-308831	87186-130443	339839	274319-306435	32338-127640
PG 76-22	S5B3	181247	147445-163531	63907-80378	47292	35785-42845	10821-16355
PG 76-22	S6B3	220874	179378-197718	67240-74935	61745	49513-60368	11147-24195

4.3 Asphalt Binders (Plant)

4.3.1 Penetration Test

Penetration numbers for all virgin and RAP-modified plant binders are shown in Figure 46. The penetration number decreased after blending them with RAP. Thus, RAP stiffened the virgin binder. PB5 only showed a single bar as the corresponding mixture was not originally modified by RAP. The highest reduction was observed for the PB1 binder (11.6), and the lowest reduction was observed for the PB2 binder (4.5). The reduction in penetration number had a positive relation with virgin binders' penetration number.

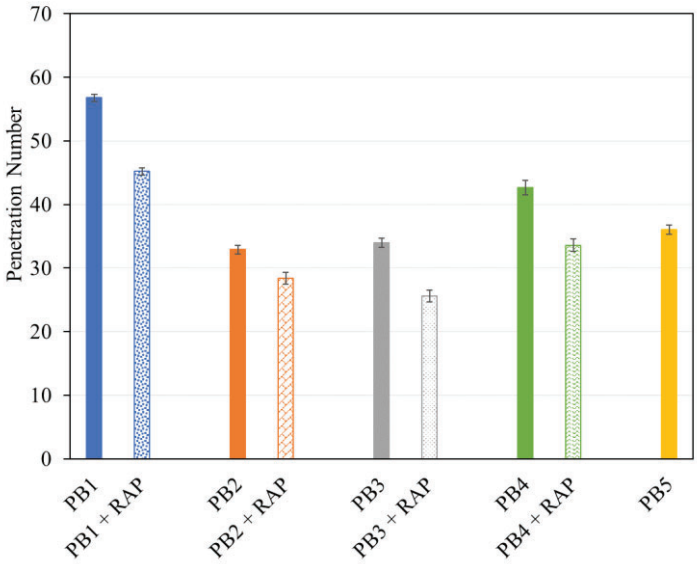

Figure 46: Changes in Penetration Number of Plant Binders With and Without RAP.

4.3.2 Rotational Viscometer (RV)

The changes in viscosity with temperature are shown in Figure 47. RAP addition reduced the viscosities at all tested temperatures; thus, binders became more viscous due to RAP modification. The reduction was higher at lower test temperatures. The highest and lowest increase in viscosities at 135 ℃ were observed for PB3 binder (251.67 mPa.s), and PB4 binder (147.22 mPa.s), respectively.

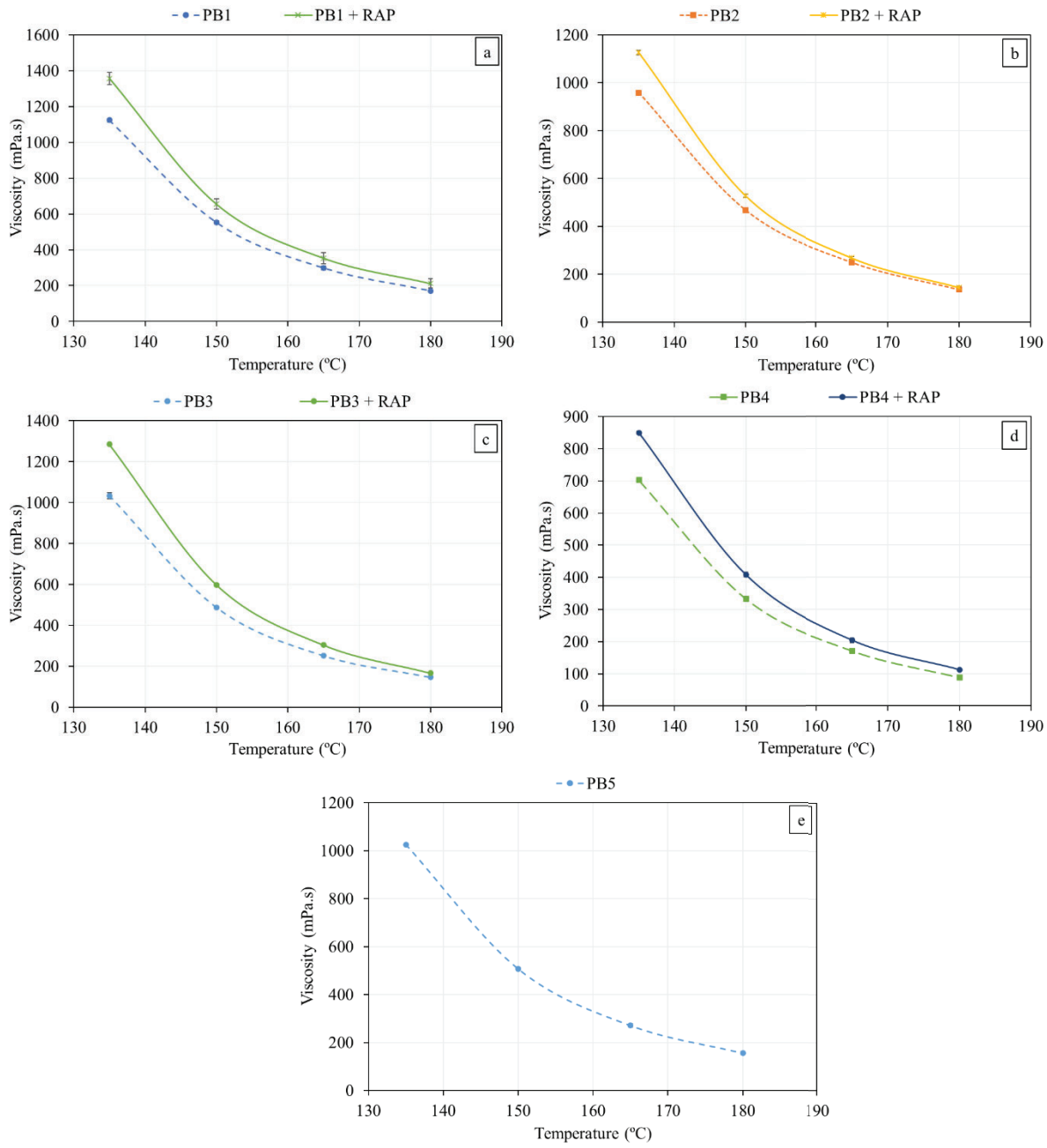

Figure 47: Variation in Viscosities With Temperature of Plant Binders With and Without RAP.

4.3.3 Acid number (pH)

The pH values of both RAP-modified and virgin binders are shown in Figure 48. The pH value increased for PB1 and PB4 binders after they were modified by RAP. For the two other binders, pH values did not change even after adding RAP to them.

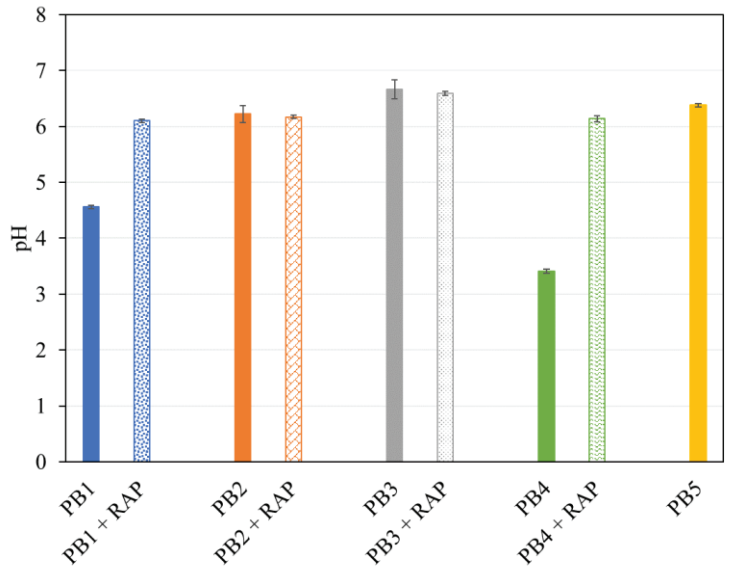

Figure 48: Changes in pH of Plant Binders With and Without RAP.

4.3.4 Sessile Drop (SD) (Optical Contact Angle) Test: Plant binders

The same reference liquids water, ethylene glycol (EG), and formamide (FM) were used in the Sessile Drop test. This test was performed on both modified and unmodified plant binders. Contact angles of all binder samples obtained with those liquids are shown in Figure 49. As seen in this figure, water produced the highest contact angles compared to other liquids for all binder samples.

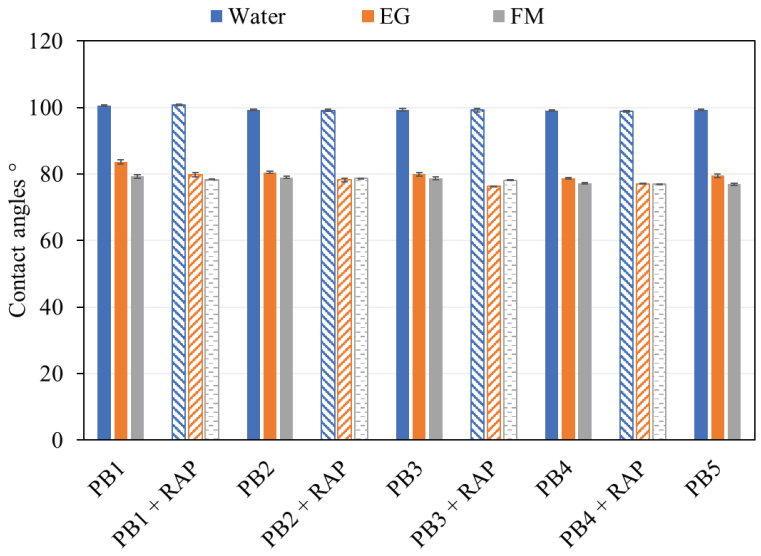

Figure 49: Changes in Contact Angles of Plant Binders With and Without RAP.

Three SFE components: a monopolar acidic component (Γ^+), a monopolar basic component (Γ^-), and an apolar or Lifshitz-van der Waals (Γ^{LW}) and total SFE were calculated and presented in Figure 50. It was observed that all three SFE components decreased due to RAP addition, which was consistent in all plant binders. The reduction was highest for the Γ^{LW} component and lowest for the Γ^+ component. Thus, total SFE values for all RAP-modified binders were lower than their corresponding unmodified binders. Work of cohesion was also calculated from total SFE and shown in Figure 51. As the work of cohesion is twice as much as total SFE, a similar trend was also observed for the former. Thus, crack initiation would occur in RAP-modified binders earlier compared to unmodified binders.

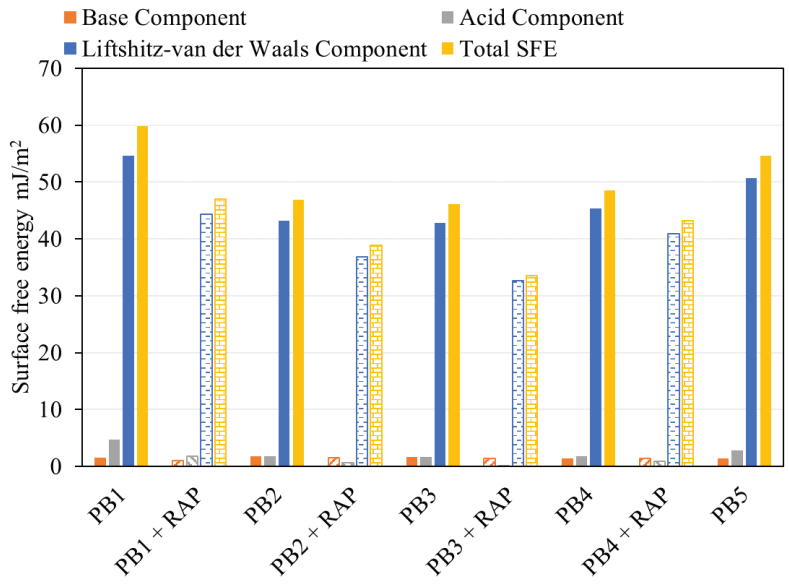

Figure 50: Total SFE and its Components of Plant Binders Before and After RAP Modification.

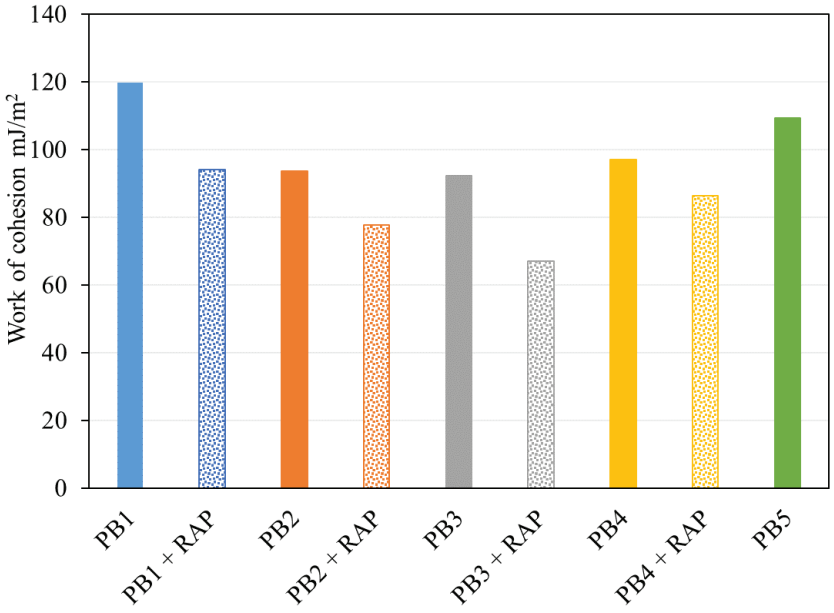

Figure 51: Work of Cohesion of Plant Binders Before and After RAP Modification.

4.4 Reheated Plant Mix Lab Compacted (RPMLC) Asphalt Mixture

The Hamburg Wheel Tracking Test, Illinois Flexibility Index Test, IDEAL-CT Test, Tensile Strength Ratio, and Dynamic Modulus test methods have been performed and data analysis has been completed analysis for the Delta Paragould, APAC-Sharp's, Redstone, and Jenny Lind, Plant Mix

Lab Compacted (RPMLC) Asphalt mixtures. Unless otherwise stated, three replicates were tested for each mixture on each test.

4.4.1 Hamburg-Wheel Track Testing

This test method was performed per AASHTO T 324. Three pairs of samples were prepared and tested using the Smart Tracker machine. The samples were placed in the machine, where they were conditioned in a 50°C water bath for 45 minutes. The device then ran a steel wheel back and forth across the sample for 20,000 passes. The rutting depth is measured at each pass. The average results from each mixture can be seen in the figure below. It should be noted that each of these mixtures contains an anti-stripping agent and all performed well with less than 4.0 mm of rutting after 20,000 passes. The results are presented in Figure 52.

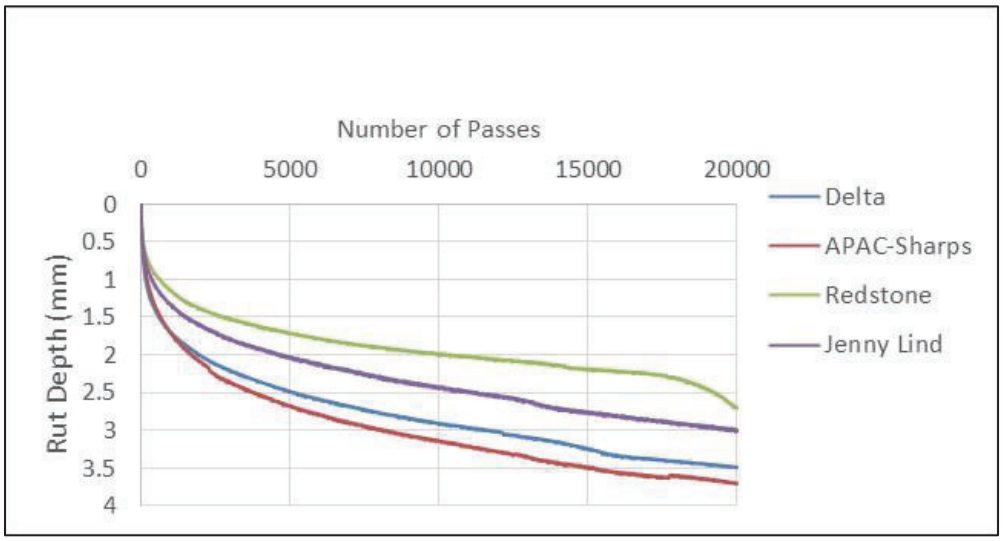

Figure 52: Hamburg-Wheel Track Testing Results.

4.4.2 Illinois Flexibility Index Test

This test is performed per AASHTO TP 124. This test is a semi-circular bend test performed with notched samples. The specimens are then conditioned at 25°C for 2 hours before the test is performed. The data received from testing is analyzed to find the flexibility index of the mixture.

The results can be seen in the figures below and are an average of four replicates. A typical sample has been plotted for each of the different mixtures. The analysis of the data performed per AASHTO TP 124 accounts for the peak loading, the area under the curve, and the post-peak-load slope. The three of these in combination are meant to quantify the strength and flexibility of a mixture. The final results of this analysis can be found in Table 10. The graphical plot is presented in Figure 53.

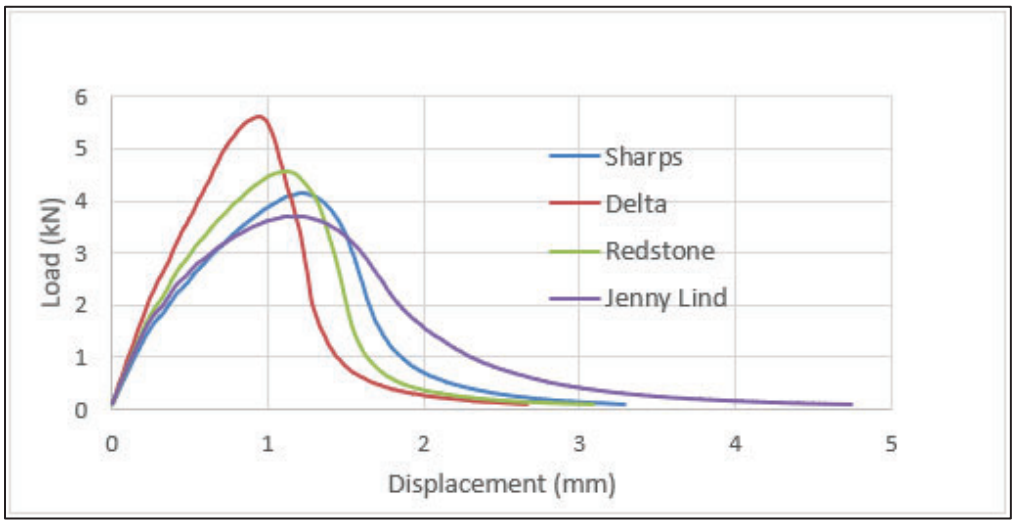

Figure 53: A graphical Plot of Illinois Flexibility Index Test Results.

Table 10: Analysis of Illinois Flexibility Index Test Results

Asphalt Mixture	Average Peak Load (kN)	Std. Dev. of Peak-Load (kN)	Average Post-Peak-Load Slope	Std. Dev. of Post-Peak-Load Slope	Average Flexibility Index	Std. Dev. of Flexibility Index
Delta	5.39	0.40	-20.82	10.9	1.27	0.41
Sharp's	3.96	0.15	-6.64	1.51	2.55	0.87
Jenny Lind	3.50	0.16	-3.41	0.39	6.93	0.83
Redstone	4.39	0.23	-10.56	3.25	3.56	3.06

4.4.3 IDEAL-CT Test

This test is performed per ASTM D8225 – 19. A plot of test results is shown in Figure 54. This test is performed on 2500 gm samples prepared from SGC specimens. The test specimens are not to be cut for this test. The specimen is conditioned at 25°C for 2 hours, then placed into the load frame and tested. The results from this test were analyzed in order to find the cracking index of the sample. The analysis outlined by the ASTM specification considers the peak loading and the slopes of the load line displacement curve to analyze the strength and flexibility of each specimen. Representative specimens from each mixture are plotted below, and the final results are also tabulated in Table 11.

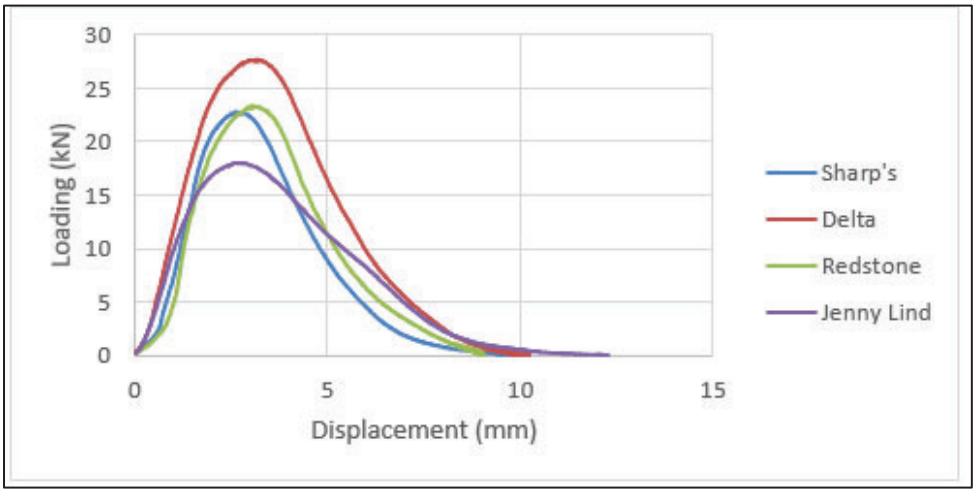

Figure 54: A graphical Plot of IDEAL-CT Test Results.

Table 11: Analysis of IDEAL-CT Test Results

Mixture:	Avg. CT (index)	Std. Dev.
Delta	48.68	18.16
Sharps	32.76	7.85
Redstone	38.21	7.28
Jenny Lind	71.62	7.12

4.4.4 Tensile Strength Ratio

This test is performed per AASHTO T 283. Six samples must be prepared for this test. Three of these samples undergo a very harsh moisture conditioning process in which the specimens are saturated to 70-80%, then placed in a 0°C freezer for 16 hours, then they are placed in a 60°C water bath for 24 hours. The moisture-conditioned samples are then compared to the unconditioned samples. The ratio of the strength of the conditioned samples to the unconditioned samples is the Tensile Strength Ratio. Per recommendations from Chung Do et al. 2018, the tensile strength ratio and the average moisture-conditioned strength shall be recorded for each mixture. The results of the three mixtures are recorded in Table 12.

Table 12: Analysis of Tensile Strength Ratio Test Results

Mixture	Average of Moisture Conditioned Strength (kPa)	Std. Dev. of Moisture Conditioned Strength (kPa)	Average Tensile Strength Ratio
Delta	1504.40	21.62	0.76
Sharps	1207.08	110.39	0.90
Redstone	1372.93	16.01	0.89
Jenny Lind	1191.26	46.03	0.83

4.4.5 Dynamic Modulus (AMPT)

This test is performed per AASHTO T 378 and AASHTO R 84 and the results are presented in Figure 55. In this test, samples are prepared to be 100 mm in diameter by 150 mm in height. These specimens are each tested in an Asphalt Mixture Performance Tester (AMPT) at three different temperatures (4°C, 20°C, and 40°C). At each temperature, the sample is loaded at different frequencies (10 Hz, 1 Hz, and 0.1 Hz). The results from each of the specimens are averaged, and time-temperature superposition is performed on the results in order to generate a 'Master Curve'; this process is outlined in AASHTO R 84. The resulting master curve can be seen below. The curves shown in Figure 55 help to determine the cracking and rutting potential of a mixture.

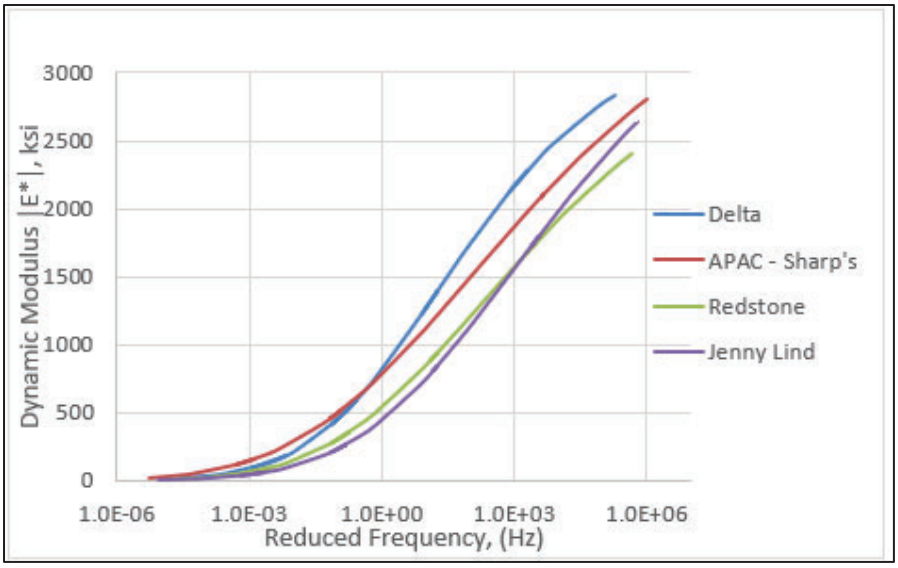

Figure 55: A graphical Plot of Dynamic Modulus Test Results.

4.5 Laboratory Asphalt Mixtures

4.5.1 Lab-Mix Sample Preparation

The lab mixes for this study will be based on the sandstone mixes gathered from Duffield and APAC-Jenny Lind. Each of these mixes has been tested at their designed level of sandstone (86% and 63% respectively), and then they have been tested with altered levels of sandstone in the mixture. So, each of these mixes has been tested at 86% sandstone, 63% sandstone, and 40% sandstone. ½" limestone chip (APAC-Sharps) will be substituted into the mixtures to make up for the removed sandstone. In order to prepare these samples, a new binder content had to be estimated for each of the new aggregate blends. This was done using the process for determining a trial binder content outlined by the *Asphalt Institute's* SP-2 (1996) document. This process outlines using Equations 9 through 13 to estimate this value.

$$G_{se} = G_{sb} + 0.8(G_{sa} - G_{sb})$$

Equation 9. Asphalt Institute Recommended Relationship Between G_{se} with G_{sa} and G_{sb}

$$V_{ba} = \frac{P_s*(1-V_a)}{(\frac{P_b}{G_b}+\frac{P_s}{G_{se}})} * (\frac{1}{G_{sb}} - \frac{1}{G_{se}})$$

Equation 10. Expression to Estimate V_{ab}

$$V_{be} = 0.176 - 0.0675(S_n)$$

Equation 11. Expression to Estimate V_{be} Form S_n

$$W_s = \frac{P_s*(1-V_a)}{(\frac{P_b}{G_b}+\frac{P_s}{G_{se}})}$$

Equation 12. Expression to Estimate W_s

$$P_{bi} = \frac{G_b*(V_{be}+V_{ba})}{(G_b*(V_{be}+V_{ba}))+W_s} * 100$$

Equation 13. Expression to Estimate P_{bi}

Regarding Equation 9, it is documented that this value of 0.8 is subject to change based on the absorptiveness of an aggregate at the discretion of the designer. Instead of this, 0.8 was treated as a variable and calculated based on four of the known binder contents associated with the properties of the aggregate blends. This multiplier was then plotted against the absorption values of the associated aggregate blends in order to calculate a relationship between the two. This relationship can be seen in Figure 56. This relationship was then used to better estimate binder values in the lab mixes with varied levels of sandstone.

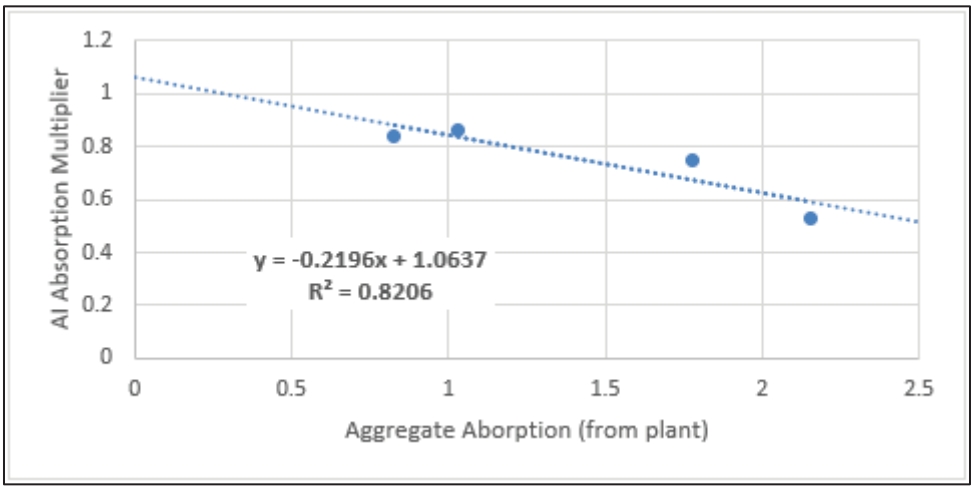

Figure 56: Regression Plot of Absorption Values of The Associated Aggregate Blends.

The following test methods have been completed on all six of the lab mix lab compacted specimens (LMLC). Three of these mixes were based on the Jenny Lind mix design, and the other

three were based on the Duffield mix design. Within each of these groupings of mixes, the amount of sandstone was varied and replaced by limestone from APAC-Sharps. The details of each of these mixes can be found in Table 13, where 'A' represents mixes based on the Jenny Lind mix, and 'B' represents the mixes based on the Duffield mix. 'L', 'M', and 'H' abbreviate low, medium, and high respectively, to notate the sandstone content in the mixture.

Table 13: Lab Mix Details

Mix:	NMAS	% Sandstone	% Limestone	% River Gravel	% RAP
Mix AL	12.5 mm	40%	41%	19%	N/A
Mix AM	12.5 mm	63%	18%	19%	N/A
Mix AH	12.5 mm	86%	8%	6%	N/A
Mix BL	9.5 mm	40%	46%	N/A	14%
Mix BM	9.5 mm	63%	23%	N/A	14%
Mix BH	9.5 mm	86%	N/A	N/A	14%

4.5.2 Dynamic Modulus:

The dynamic modulus was performed on the lab mixtures following the same steps for the plant mixtures. The final master curve can be seen in the figure below (Figure 57). Also on this figure is a zoomed-in portion that can be used to more easily rank the specimen's resistance to rutting and cracking, based on their respective portions.

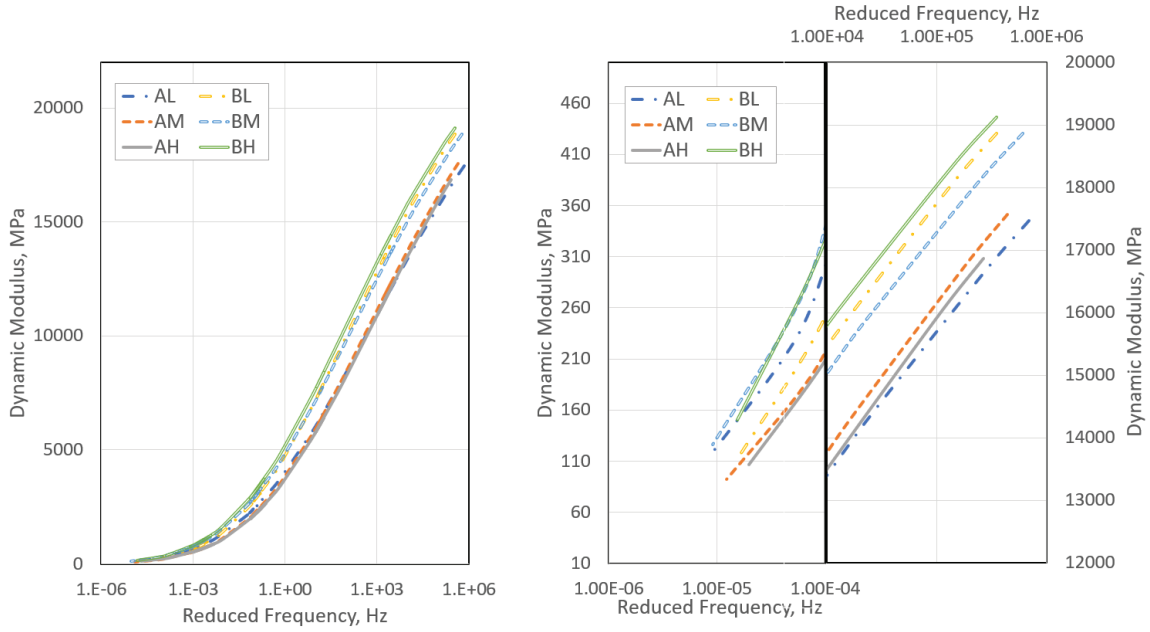

Figure 57: Dynamic Modulus Test on Lab Mixtures.

4.5.3 Hamburg Wheel Track Testing

The Hamburg Wheel Tracking test was performed similarly to how it was performed for the plant mix specimens. The main reason for the difference in the results below (Figure 58) is the lack of an anti-stripping agent present in the lab mixtures. We can also see that the mixtures from 'B' perform similarly to how they performed with anti-strip (for the plant mix specimens), however, literature has suggested that this is because of the presence of RAP in this mix design (Rafiq et al. 2020). Conversely, mixtures from 'A' did not perform well, especially with the medium and higher levels of sandstone, with rutting over 8.0 mm.

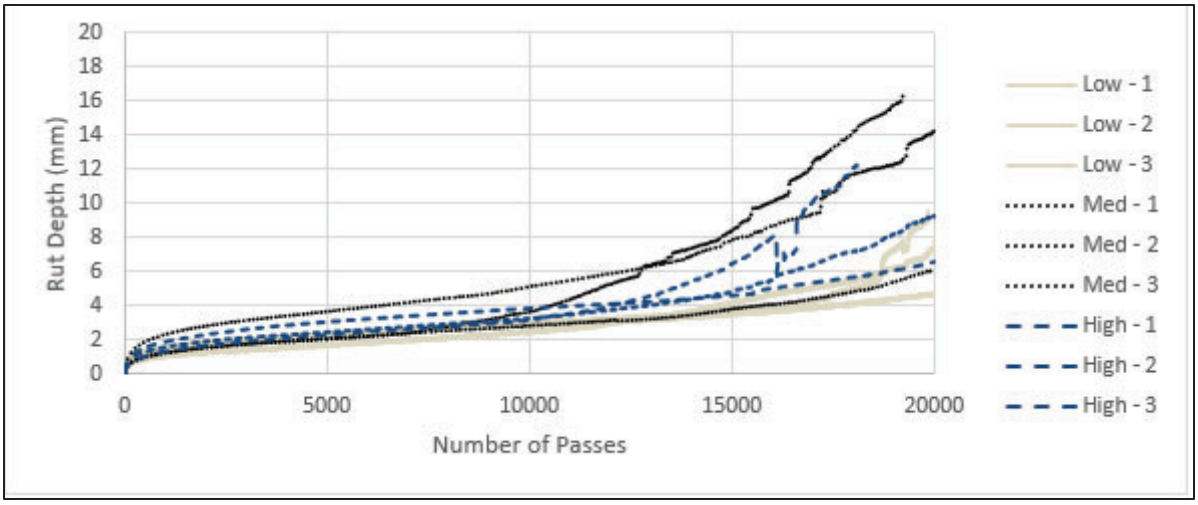

(a)

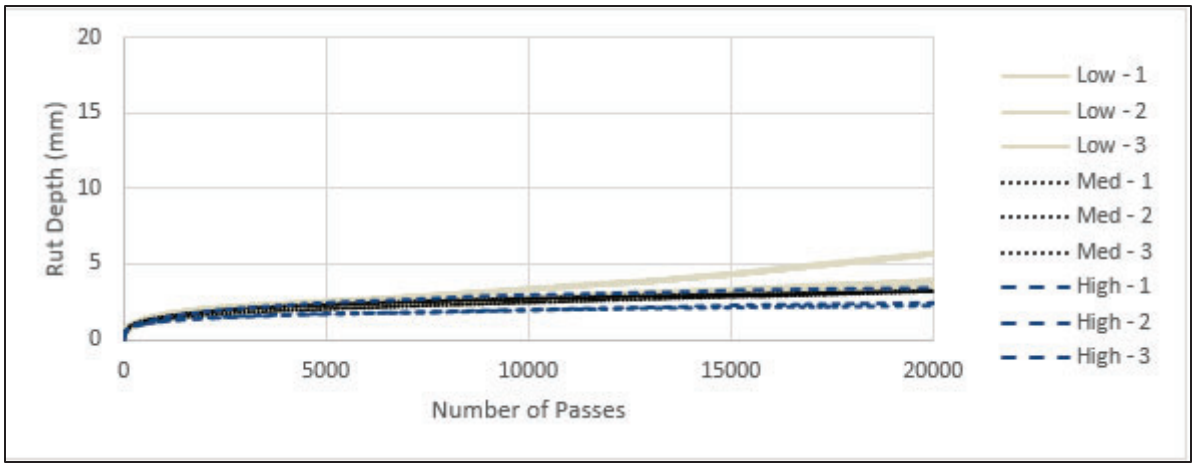

(b)

Figure 58: Hamburg Wheel Track Testing on: (a) Mix A and (b) Mix B.

4.5.4 Tensile Strength Ratio

The tensile strength ratio was performed on the LMLC specimens similarly to how it was performed on the RPMLC specimens. The lack of anti-strip in these specimens should affect the results of this test method as well. The results can be seen in Figure 59. It is seen that the TSR value with high sandstone is significantly lower than with low or medium sandstone content. This can be possibly due to the high micropores and abruption characteristics of the sandstone, which has an enormous capacity to carry or hold water while conditioning the samples.

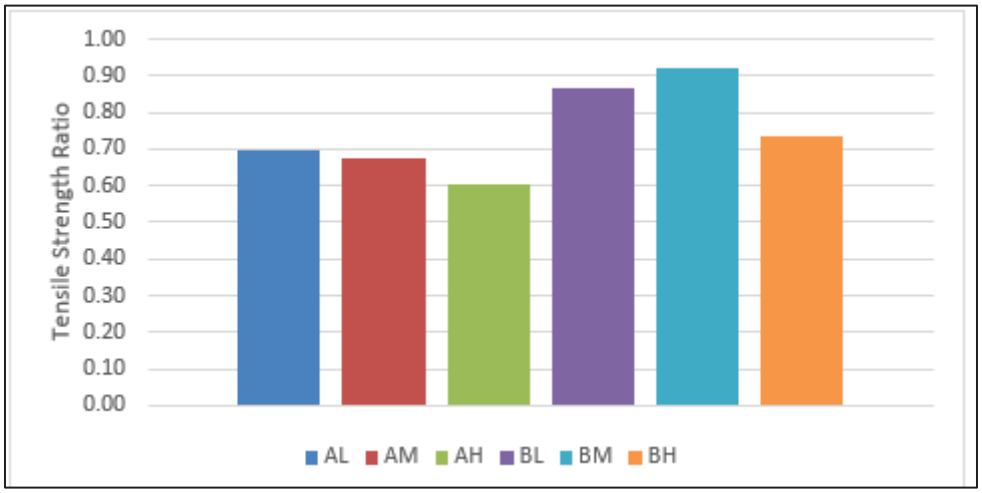

Figure 59: Tensile Strength Ratio Test Results.

4.5.5 Cracking Tests

The IDEAL-CT test was performed per ASTM D8225, this method was also performed similarly to the PMLC specimens. The final results for this method can be found in Table 14. Also, the results of the IFIT test (AASHTO TP 124) are shown in Table 14.

Table 14: IDEAL-CT Test Results

Mixture	CT Index Avg.	CT Index Std. Dev.	Flexibility Index Avg.	Flexibility Index Std. Dev.
AL	59.47	11.96	2.33	0.89
AM	58.22	9.95	1.81	0.47
AH	46.03	5.23	3.93	1.30
BL	48.32	33.35	3.58	1.93
BM	49.53	14.67	3.46	1.82
BH	26.07	3.94	0.99	0.63

4.5.6 Flow Number

The Flow Number test was performed per AASHTO T 378. This test method is sometimes referred to as a dynamic creep test. It subjects a dynamic modulus specimen to a haversine loading at a frequency of 1 Hz until the termination conditions are met (10,000 cycles or 50,000 microstrains).

The resulting flow number is determined by the AMPT to be the point of inflection where the specimen begins to deform at a faster rate. These results are used to determine the rutting resistance of a mixture; they can be seen in the figure below (Figure 60).

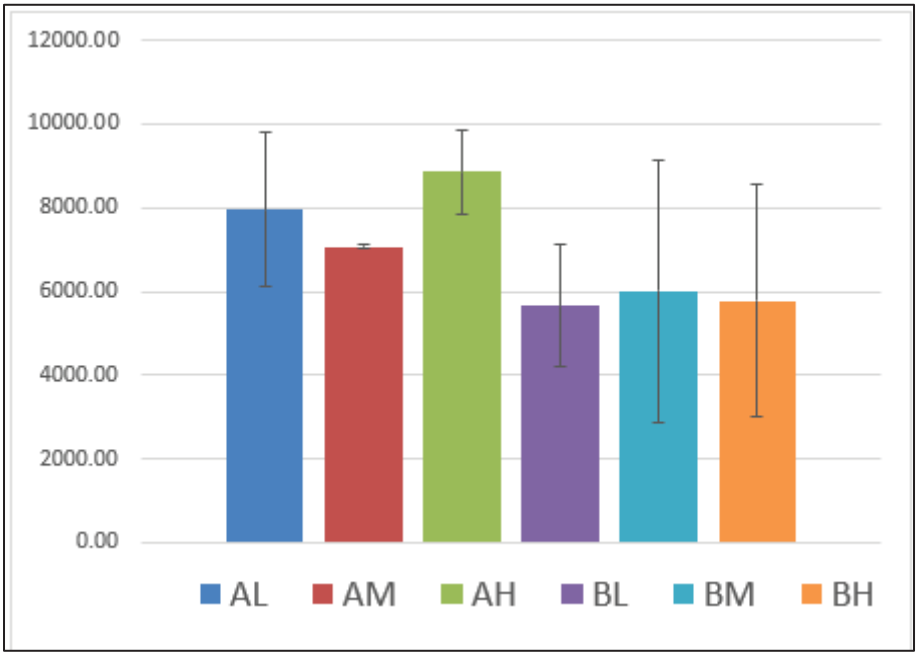

Figure 60: Flow Number Test Results.

5 Discussions

5.1 Ranking based on Compatibility Ratio (CR)

Table 15 shows relative Compatibility Ratio (CR) values between aggregate-binder systems from SFE data. This relative ranking was developed based on the minimum of all CR values (Eq. 2). Researchers suggested CR values less than 0.5 indicate very poor compatibility and are rated as "D"; similar CR values between 0.5 and 0.75 are rated as "C" (poor), and values between 0.75 and 1.5 are rated as "B" (good), and CR values above 1.5 are rated as "A" (very good) (Kandhal and Koehler 1984; Hossain et al. 2015). Table 5 also shows that 65 combinations were rated as A, 43 combinations were rated as B, 11 combinations were rated as C, and 25 combinations were rated as D. All the LS2, and DM1 samples were rated as A, all the NV1, and NV2 mixtures were rated as either C or D except for S3B3 binder, where they demonstrated good compatibility ("B" rating). It could also be observed that SS1 mixtures obtained an overall better rating compared to SS2 mixtures.

Table 15: Compatibility Ratio Calculated From SFE Data (A = Best, D = Worst)

Binder/Aggregate Samples	SS1	SS2	NV1	NV2	LS1	LS2	DM1	DM2
S1B1	A	B	D	D	B	A	A	A
S2B1	B	C	D	D	C	A	A	B
S3B1	A	B	C	C	B	A	A	A
S4B1	A	B	D	D	B	A	A	A
S5B1	B	B	D	C	B	A	A	B
S6B1	A	B	D	D	B	A	A	A
S1B2	B	B	D	D	B	A	A	A
S2B2	A	B	D	D	B	A	A	A
S3B2	A	B	C	C	B	A	A	A
S4B2	B	B	D	C	B	A	A	A
S5B2	B	B	D	D	B	A	A	B
S6B2	A	B	D	C	B	A	A	A
S1B3	A	B	D	D	B	A	A	A
S2B3	A	B	D	D	B	A	A	A
S3B3	A	A	B	B	A	A	A	A
S4B3	A	B	D	D	B	A	A	A
S5B3	B	B	D	D	B	A	A	A
S6B3	A	B	C	C	B	A	A	A

5.2 Ranking based on tested parameters

Based on the test results obtained in this study, a relative ranking was formed for aggregate and binder samples as well as aggregate-binder systems. Aggregates ranking followed a scale from 1 to 8, where 1 is the best and 8 would be the least suited aggregates. Similarly, asphalt binders were rated on a scale of 1 to 18, where 1 was the most suited and 18 was the least preferable binders. To rank the aggregates, different aggregate parameters were weighted according to their relative importance in the mixtures' performance. In this regard, pH, soundness, abrasion resistance, absorption, and specific gravity values were given a weight value of 0.3, 0.3, 0.15, 0.15, and 0.1, respectively. Likewise, for asphalt binders, penetration, viscosity (at 135 ℃), pH, and work of cohesion values were given a weight of 0.1, 0.2, 0.3, and 0.4, respectively. A similar ranking of asphalt binders and aggregates can be found in the literature; however, the researchers granted equal weight to all parameters used in the ranking (Hossain et al. 2020, Oyan et al. (2023). The ranks of the tested aggregates and asphalt binder samples are presented in Table 16 and Table 17, respectively. It is obvious that among eight aggregates, DM2, LS2, and DM1 are found to be the most preferred aggregates. Among 18 binder samples, S2B2, S3B1, and S4B1 are determined to be the most competent samples.

Table 16: Ranking of Aggregates Samples (Lower Is Better)

Sample	Specific gravity	Absorption	Abrasion	Soundness	pH	Work of cohesion	Relative ranking
SS1	7	8	5	1	7	3	4
SS2	8	6	7	2	4	6	6
NV1	6	4	2	4	8	8	8
NV2	3	7	6	3	3	7	5
LS1	4	1	8	7	5	5	7
LS2	5	5	4	8	1	1	2
DM1	2	3	1	5	6	4	3
DM2	1	2	3	6	2	2	1

Table 17: Ranking of Asphalt Binder Samples (Lower Is Better)

Sample Name	Penetration	RV	pH	Work of cohesion	Overall Relative ranking
S1B1	16	4	5	15	8
S2B1	9	6	14	11	13
S3B1	8	2	3	13	2
S4B1	12	5	10	3	3
S5B1	13	2	6	14	5
S6B1	15	1	13	10	8
S1B2	14	12	2	16	7
S2B2	5	7	8	4	1
S3B2	1	9	4	18	9
S4B2	6	8	9	7	6
S5B2	18	10	7	17	10
S6B2	10	11	17	9	13
S1B3	7	15	15	6	13
S2B3	3	14	11	12	14
S3B3	2	13	16	2	11
S4B3	4	17	1	8	4
S5B3	17	18	12	5	11
S6B3	11	16	18	1	12

The mixture systems have been ranked based on dry and wet work of adhesions and the Texas Boiling test. The ranking based on dry work of adhesion is presented in

Table 18. Table 19 shows the ranking based on wet work of adhesion. Table 20 shows the ranking based on the Texas Boiling test results. Ranking based on all these three parameters follows a scale from 1 to 8 in a stepwise method. For both dry and wet adhesions ranking, the difference between the highest and lowest numerical values has been divided into eight segments and each segment has been given a unique number (rank). The individual test result is then evaluated against these segments and ranked accordingly. For dry work of cohesion, the ranking follows a descending order, and for wet work of adhesion, an ascending order is followed. Similarly, Texas Boiling Test samples have been ranked based on their percentage of asphalt retention in a

descending manner. Percent retention values above 85% are given rank 1, and values between 70 to 85% are given rank 2 (Lytton et al. 2005). Percent retention values below 70% are ranked following the segment-wise method having a segment size of 10%. A summary of each of these ranking methods is shown at the bottom of the corresponding table for readers' convenience.

Between the ranking methods of SFE (Table 19) and the Texas Boiling test (Table 20), Table 20 is preferred since it is based on test results of loose mixture samples. On the other hand, Table 19 is based on test results of binders and aggregates separately. Another reason for preferring the ranking shown in Table 20 is that this ranking system has 8 categories (1 to 8), whereas the ranking in Table 19 has only four categories (A, B, C, and D).

Overall, the SFE-based ranking and TBT-based ranking are comparable except for the SS1. The potential reason for inconsistent results between SFE-based and TBT-based ranking for SS1 could be due to the conditioning of the test samples. In the TBT test, the loose mixture is boiled (conditioned) and asphalt retention on the aggregate is observed. This means both asphalt binder and aggregates are subjected to water intrusion at a high temperature. SS1 is a sandstone aggregate from Source 1, and it has lots of micropores and high absorption characteristics, which facilitates the passage of water through the mixtures and subsequently disintegrates binder from the aggregate. On the other hand, in the SFE tests, neither asphalt binder nor aggregate is subjected to conditioning in water. The presence of water is brought into the SFE equation while determining the adhesion energy. However, intrinsic micropores are not taken into consideration in the SFE-based analysis. Only contact angles are taken into consideration while estimating the SFE. SS1 has more micropores and absorption characteristics than other aggregates. Thus, the inconsistency between SFE-based and TBT-based ranking for other aggregates is noticeable. Another important point is- the TBT-based ranking has 8 categories (1 through 8). On the other hand, the SFE-based ranking is relatively broad (A, B, C, and D) and range is very high.

Table 18: Ranking of Aggregate-Binder Systems Based on Dry Work of Adhesion (Lower is Better)

Binder/Aggregate Samples	SS1	SS2	NV1	NV2	LS1	LS2	DM1	DM2
S1B1	5	6	7	6	6	4	6	4
S2B1	6	7	8	6	6	5	7	5
S3B1	3	4	6	4	4	1	4	2
S4B1	4	5	7	5	5	3	5	3
S5B1	3	4	5	4	4	1	4	2
S6B1	5	5	7	5	5	3	5	3
S1B2	5	5	7	5	5	3	5	3
S2B2	7	7	8	7	7	5	7	5
S3B2	3	4	5	4	3	1	3	1
S4B2	3	4	5	4	4	1	4	2
S5B2	4	5	6	5	4	2	4	2
S6B2	4	5	6	5	4	2	5	3
S1B3	5	6	7	6	6	4	6	4
S2B3	6	7	8	7	7	5	7	5
S3B3	3	4	6	4	4	1	4	2
S4B3	4	5	6	5	5	2	5	3
S5B3	4	5	6	5	4	2	5	3
S6B3	3	4	5	4	3	1	3	1
Ranking steps	1	2	3	4	5	6	7	8
Dry work of adhesion (mJ/m^2) (x)	86.5≥ x ≥97.5	97.5> x ≥108.5	108.5> x ≥119.5	119.5> x ≥130.5	130.5> x ≥141.5	141.5> x ≥152.5	152.5> x ≥163.5	163.5> x ≥174.5

Table 19: Ranking of Aggregate-Binder Systems Based on Wet Work of Adhesion (Lower is Better)

Binder/Aggregate samples	SS1	SS2	NV1	NV2	LS1	LS2	DM1	DM2
S1B1	5	6	7	8	6	2	4	6
S2B1	5	6	8	8	6	2	4	6
S3B1	6	6	7	8	7	3	5	7
S4B1	6	6	7	8	7	3	5	6
S5B1	6	7	8	8	7	4	5	7
S6B1	6	6	7	8	7	3	5	6
S1B2	6	6	7	8	7	3	5	6
S2B2	4	5	6	7	5	1	3	5
S3B2	6	6	7	8	7	4	5	7
S4B2	6	7	8	8	7	4	5	7
S5B2	6	7	8	8	7	4	5	7
S6B2	6	6	7	8	7	3	5	6
S1B3	5	6	7	8	6	2	4	6
S2B3	4	5	6	7	5	1	3	5
S3B3	5	6	6	7	6	3	4	6
S4B3	6	6	7	8	7	3	5	6
S5B3	6	6	7	8	7	3	5	6
S6B3	6	7	7	8	7	4	5	7
Ranking steps	1	2	3	4	5	6	7	8
Wet work of adhesion (mJ/m^2) (x)	7.9≥ x ≥13.9	13.9> x ≥19.9	19.9> x ≥25.8	25.8> x ≥31.8	31.8> x ≥37.8	37.8> x ≥43.8	43.8> x ≥49.8	49.8> x ≥55.7

Table 20: Ranking of Aggregate-Binder Systems Based on Texas Boiling Test (Lower is Better)

Binder/Aggregate Samples	SS1	SS2	NV1	NV2	LS1	LS2	DM1	DM2
S1B1	7	4	8	8	4	4	5	4
S2B1	7	3	7	7	3	7	4	4
S3B1	7	2	7	6	4	4	3	3
S4B1	6	3	7	6	3	5	3	3
S5B1	5	3	6	8	2	6	2	3
S6B1	5	3	6	7	2	4	3	3
S1B2	5	2	7	4	4	3	4	3
S2B2	8	3	6	8	2	4	4	2
S3B2	6	2	6	6	2	3	2	3
S4B2	4	2	6	5	3	3	3	2
S5B2	6	3	4	5	2	3	2	5
S6B2	5	2	4	7	2	4	3	2
S1B3	6	2	7	4	2	4	2	2
S2B3	6	3	4	7	2	4	2	2
S3B3	6	2	5	7	1	3	2	2
S4B3	2	1	2	1	2	1	1	2
S5B3	5	2	3	5	2	2	2	3
S6B3	5	2	4	4	2	2	3	1
Ranking steps	1	2	3	4	5	6	7	8
% asphalt retention (x)	x ≥ 85	85> x ≥70	70> x ≥60	60> x ≥50	50> x ≥40	40> x ≥30	30> x ≥20	20> x ≥10

6 Conclusions and Recommendations

6.1 *Conclusions*

- Sandstone and dolomite samples were the lightest and heaviest aggregates, respectively. Variations in specific gravity between sources for all aggregates were below 5%. Source 1 sandstone showed the highest absorption value (3.72%) and all other aggregate samples had absorption values of less than 2%. Source 1 limestone and Source 2 dolomite absorbed water less than 1% of their dry weight. Thus, Source 1 sandstone was highly porous, and porosities in limestone and dolomite were very low.
- All aggregates passed the ARDOT requirement for the LA abrasion test (% of loss < 40). Variations between sources for sandstone and dolomite samples were insignificant. Test data showed that Source 1 limestone was the least durable aggregate and both Source 1 novaculite and dolomite were highly durable aggregates.
- All aggregate samples yielded similar pH and they were all basic i.e., pH >7.0.
- Overall, both dolomites and Source 2 limestone were the top three aggregates based on this study scope.
- Penetration number is inversely related to the stiffness of asphalt binder. At 25 ℃, usually, stiffness increased as binder grade increased except for Source 5 binder samples. Source 5 PG 70-22, and PG 76-22 binder samples were even softer than all PG 64-22 samples tested in this project. The difference in penetration number i.e., stiffness was minute for polymer-modified binder samples among other sources. Plant binders got stiffer upon the addition of RAP i.e., lower penetration number.

- RV test results showed that binder viscosity increased as their grade increased. All binders were compliant with Superpave viscosity criteria (viscosity < 3200 mPa.s at 135 ℃) except PG 76-22 binder samples from Source 5. Plant binders with RAP showed higher viscosities in all tested temperatures compared to respective plant binders.
- All asphalt binders were found acidic (pH < 7.0) in this study. Source 4 PG 64-22 and PG 70-22 binder samples were more acidic within their respective binder grade. Besides, variations in pH within individual binder grades were insignificant. RAP addition either increased or left unchanged the plant binder's pH yet remained acidic.
- In general, Source 2 PG 70-22, Sources 3 and 4 PG 64-22 were the top-ranked asphalt binders.
- In the Sessile Drop (SD) test, for both binder and aggregate samples water produced the highest contact angles among the three probe liquids. The other two liquids produced almost similar contact angles; however, Ethylene Glycol had higher contact angles than Formamide in most cases. Standard deviations in contact angles were higher for aggregate samples because of surface porosity and rough micro-texture. The effects of RAP on contact angles were found insignificant.
- Surface Free Energy (SFE) analysis showed Total SFE values for aggregate samples were higher than asphalt binder samples. As the work of cohesion is twice as much as Total SFE, calculated work of cohesion values was also higher for aggregate samples. For aggregate samples, Source 2 showed higher SFE than Source 1 except for sandstone. Regarding the asphalt binder, no such trend was observed. The total SFE of plant binders

was reduced when RAPs were added to them indicating a loss of work of cohesion. Lowering SFE indicates a moisture-damage-prone asphalt mixture.

- Based on dry work of adhesion energy, Source 2 limestone and dolomite, and Source 1 sandstone mixtures performed better than other aggregates. Overall, Source 1 dolomite and sandstone, and Source 2 limestone mixtures ranked at the top in terms of wet work of adhesion. The compatibility Ratio suggested both dolomites and Source 2 limestone mixtures as the most compatible aggregate-binder systems.
- Texas Boiling Test results showed that the lab mixture containing Source 1 limestone, Source 2 sandstone, and dolomites from both Sources 1 and 2 showed a good percentage of asphalt retention. In general, any aggregate-binder combination that could retain more than 85% of asphalt after the test, could be designated as a moisture-damage-resistant mixture. The percent retention within the range of 70 and 85 could be improved by adding an anti-stripping agent to mixtures. Typically, percent retention increased with binder grade. PG 76-22 binder from Source 4 was observed to be highly compatible with all the tested aggregates. Overall, Source 1 sandstone and both novaculites showed poor asphalt retention. Overall Source 2 sandstone and dolomite, and Source 1 limestone mixtures were observed to be the least moisture susceptible mixtures.
- Based on the findings, it can be concluded that an AFM can be used as a viable tool for determining the moisture damage and examining the surface morphology and molecular-level properties of asphalt binders. For surface morphology, the 'bee structures' were dominant for the S1, S2, and S3 sources' asphalt binders compared to other sources. The

higher DMT modulus, adhesion force, dissipation energy, and lower deformation were observed for the S1, S2, S3, and S4 sources' binder compared to the S5 binder.

- The Dynamic modulus was able to clearly show that the Duffield mix was more susceptible to cracking than the APAC-Sharps mixture, but the susceptibility to rutting was not as clear. In addition, the test did not show consistent results across the various levels of sandstone.
- The Hamburg Wheel Tracking test captured the impact of anti-strip agents, as mixtures with anti-strip agents had lower rut depth than identical mixtures without anti-strip agents. High levels of sandstone (86%) showed significantly poorer results than medium (63%) and low (40%) levels of sandstone without anti-strip agents for the APAC-Sharps mixture. The Duffield mix showed similar results. This indicates that the high levels of sandstone increase moisture susceptibility and rutting susceptibility.
- The Tensile Strength Ratio showed that the high levels of sandstone showed the worst results, by 10-25%, versus the medium and low levels of sandstone results. This indicates that the high levels of sandstone increase moisture susceptibility and rutting susceptibility. This could be attributed to the high level of absorption characteristics of sandstone that contains enormous micropores and results in moisture intrusion in the mixture. High absorptive sandstone aggregates are also suspected to have less effective binder in the mixture, which in turn reduces the bonding between aggregate and binder. The Duffield mix performed better than the APAC-Sharps mix.

- The IDEAL-CIT and I-FIT flexibility index, two cracking tests, indicated that the highest level of sandstone showed the worst results, by 20-40%, versus the medium and low levels of sandstone results. The APAC-Sharps mix performed better than the Duffield mix.
- The Flow Number test did not show consistent results across the various levels of sandstone. However, the APAC-Sharps mix consistently performed better than the Duffield mix.

6.2 Recommendations

- Aggregates were tested for their durability, soundness, absorption, specific gravity, acidity, and surface-free energy. Since sandstone has significantly more absorption than other types of aggregates, it is recommended to set a maximum absorption of aggregates to 2%. In future research, the chemical composition needs to be identified by FTIR (Fourier Transformation Infrared Spectroscopy) and XRD (X-ray Diffraction) as aggregates' chemistry plays a crucial role in their compatibility with asphalt binder.
- Since acidity plays a major role in getting compatible aggregates and binders in the asphalt mixtures, the ARDOT may include pH measurements of aggregates and binders in their QC/QA protocols. Typically, acidic binders are more compatible with basic aggregates, and vice versa.
- As a quick test of moisture resistance, the ARDOT may incorporate the Texas Boiling Test to determine adhesion between asphalt and aggregate.
- It is recommended that the ARDOT contractors use the most compatible aggregates and binders, summarized in Appendix A, in producing asphalt mixes.

- All of the cracking tests showed that the APAC-Sharps mix was less susceptible to cracking than the Duffield mix, but some of the rutting tests showed that the Duffield mix was less susceptible to rutting than the APAC-Sharps mix. The Hamburg Wheel Tracking Test, the Tensile Strength Ratio, the IDEAL-CT, and the Flexibility Index all showed that high levels of sandstone (86%) compromised the performance of the asphalt mixtures. However, the results of medium levels of sandstone (63%) were not consistent. Therefore, it is recommended to set the maximum level of sandstone at 60%.

7 References

- Allen, R. G., Little, D. N., Bhasin, A., & Lytton, R. L. (2013). Identification of the Composite Relaxation Modulus of Asphalt Binder Using AFM Nanoindentation. Journal of Materials in Civil Engineering, 25(4), 530-539. DOI: 10.1061/(ASCE)MT.1943-5533.0000615.
- Bagchi, T., Hossain Z, Rahaman, M.Z., Baumgardner, G. (2021). Comparing Micro-and Macro-Level Rheological Properties of Polymeric and RAP Modified Asphalt Binders. 2021.
- Bentz, D., P. (2017). Influence of Aggregate Characteristics on Concrete Performance. National Institute of Standards and Technology, NIST Technical Note 1963.
- Bhasin, A., Button, J. W., Chowdhury, A. Evaluation of Simple Performance Tests on Hot-Mix Asphalt Mixtures from South Central United States. Transportation Research Record: Journal of the Transportation Research Board (2004).
- Bhasin, A., Masad, E., Little, D., and Lytton, R. 2006. Limits on Adhesive Bond Energy for Improved Resistance of Hot-Mix Asphalt to Moisture Damage. Transp. Res. Rec., 1970(1), 2-13. https://doi.org/10.1177/0361198106197000101
- Bhasin, A. 2007. Development of Methods to Quantify Bitumen-Aggregate Adhesion and Loss of Adhesion Due to Water. Doctoral dissertation, College Station, TX: Texas A&M Univ. https://hdl.handle.net/1969.1/5934
- Cala, A., Caro, S. Predictive Quantitative Model for Assessing the Asphalt-Aggregate Adhesion Quality Based on Aggregate Chemistry. Road Materials and Pavement Design (2021).
- Cheng, D., Little, D. N., Lytton, R. L., & Holste, J. C. 2002. Use of Surface Free Energy Properties of The Asphalt-Aggregate System to Predict Moisture Damage Potential (With Discussion). Journal of The Association Of Asphalt Paving Technologists, 71.
- Chung Do, T., Phuc Tran, V., Phuc Le, V., Jong Lee, H. Mechanical Characteristics of Tensile Strength Ratio Method Compared to Other Parameters Used for Moisture Susceptibility Evaluation of Asphalt Mixtures. ScienceDirect (2018).
- Copeland, A., R., Youtcheff, J., Shenoy, A. (2007). Moisture Sensitivity of Modified Asphalt Binders: Factors Influencing Bond Strength. Transportation Research Record, No. 1998, pp. 18-28.

- Dourado, E. R., Simao, R. A., Leite, L. F. (2012) Mechanical Properties of Asphalt Binders Evaluated by Atomic Force Microscopy. Journal of Microscopy. 2012 Feb;245(2):119-28.
- Fu, P., Jones, D., Harvey, J., T., Halles, F., A. (2010). Investigation of the Curing Mechanism of Foamed Asphalt Mixes Based on Micromechanics Principles. Journal of Materials in Civil Engineering, 22:1, pp. 29-38.
- Horgnies, M., Darque-Ceretti, E., Fezai, H., Felder, E. (2011). Influence of the Interfacial Composition on the Adhesion Between Aggregates and Bitumen: Investigations by EDX, XPS, and Peel Tests. International Journal of Adhesion & Adhesives. Vol. 31. Pp. 238-247.
- Hossain Z., Elsayed, A., Bagchi, T., & Roy, S. (2020). Assessment of Compatibility of Mineral Aggregates and Binders Used In Highway Construction and Maintenance Projects, Transportation Consortium of South-Central States, Baton Rouge, LA.
- Hossain, K., Karakas A., and Hossain, Z. (2019). "Effects of Aging and Rejuvenation on Surface-Free Energy Measurements and Adhesion of Asphalt Mixtures." DOI: 10.1061/(ASCE) MT.1943-5533.0002780. American Society of Civil Engineers.
- Hossain, Z, Roy S, Rashid, F. (2020) Microscopic Examination of Rejuvenated Binders With High Reclaimed Asphalts. Construction and Building Materials. 2020 Oct 10;257:119490.
- Hossain, Z., Bairgi, B., & Belshe, M. (2015). Investigation of Moisture Damage Resistance of GTR-Modified Asphalt Binder by Static Contact Angle Measurements. Construction and Building Materials, 95, 45-53.
- Hossain, Z., Elsayed, A., & Sakib Oyan, M. N. (2021). Feasibility Assessment of Warm Mix Asphalt in Arkansas. Transportation Consortium of South-Central States, Baton Rouge, LA.
- Hossain, Z., Lewis, S., Zaman, M., Buddhala, A., & O'Rear, E. (2013). Evaluation for Warm-Mix Additive-Modified Asphalt Binders Using Spectroscopy Techniques. Journal of materials in civil engineering, 25(2), 149-159.
- Hossain, Z., Rashid, F., Mahmud, I, Rahaman M. Z. (2017). Morphological and Nanomechanical Characterization of Industrial And Agricultural Waste–Modified Asphalt Binders. International Journal of Geomechanics. 2017 Mar 1;17(3):04016084.

- Howson J., Masad E.A., Bhasin A., Branco V.C., Arambula E., Lytton R., & Little D. 2007. System of the Evaluation of Moisture Damage Using Fundamental Materials Properties. Texas Transportation Institute, TxDOT Report No. FHWA/TX-07/0- 4524-1, College Station, TX.
- Howson J., Masad E., Bhasin A., Little D., and Lytton R. (2011). Comprehensive Analysis of Surface Free Energy of Asphalts And Aggregates and the Effects of Changes in pH. https://doi.org/10.1016/j.conbuildmat.2010.11.098, Construction, and Building Materials Volume 25, Issue 5, May 2011, Pages 2554-2564.
- Jahangir, R., Little, D., Bhasin, A. (2015). Evolution of Asphalt Binder Microstructure Due to Tensile Loading Determined Using AFM and Image Analysis Techniques. International Journal of Pavement Engineering. 2015 Apr 21;16(4):337-49.
- Kandhal, P. S., & Koehler, W. C. (1984). Significant Studies on Asphalt Durability: Pennsylvania Experience. Transportation Research Record, 999, 41-50.
- Kennedy, T. W., Roberts, F. L., & Lee, K. W. (1984). Evaluating moisture Susceptibility of Asphalt Mixtures Using the Texas Boiling Test. Transportation Research Record, 968, 45-54.
- Koc, M. and Bulut, B. (2014). Assessment of a Sessile Drop (SD) Device and a New Testing Approach Measuring Contact Angles on Aggregates and Asphalt Binders, Journal of Materials in Civil Engineering 26(3):391-398, DOI: 10.1061/(ASCE)MT.1943-5533.0000852
- Little DN, Bhasin A. (2006). Using Surface Energy Measurements to Select Materials for Asphalt Pavement. NCHRP Project 9-37. Transportation Research Board, Washington, DC.
- Lytton, R. L., E. Masad, C. Zollinger, R. Bulut, and D. N. Little. 2005. Measurement of Surface Energy and its Relationship to Moisture Damage. TXDOT Rep. No. 0-4524-2. Austin, TX: Texas Transportation Institute, Texas A&M Univ, College Station, TX.
- Masson, J. F., Leblond, V., Margeson, J. (2006). Bitumen Morphologies By Phase-Detection Atomic Force Microscopy. Journal Of Microscopy. 221(1):17-29.
- McCann, M., Anderson-Sprecher, R., Thomas, K. P. Statistical Comparison Between SHRP Aggregate Physical and Chemical Properties and the Moisture Sensitivity of Aggregate-Binder Mixtures. Road Materials and Pavement Design (2005).

- Nahar, S. N., Mohajeri. M., Schmets, A. J., Scarpas, A., (2013). Van de Ven MF, Schitter G. First Observation Of Blending-Zone Morphology at Interface of Reclaimed Asphalt Binder and Virgin Bitumen. Transportation Research Record. 2370(1):1-9.
- Oyan, M. N. S., & Hossain, Z. (2021). Feasibility Study of Warm Mix Asphalt in Arkansas. In Tran-SET 2021 (pp. 304-316). American Society of Civil Engineers, Reston, VA.
- Oyan, M. N. S., & Hossain, Z. (2022). Rheological, Chemical, and Water Resistance Properties of Asphalt Binders Modified with Selected Warm Mix Additives. In Tran-SET 2022, pp. 25-34. American Society of Civil Engineers, Reston, VA.
- Oyan, M. N. S., Hossain, Z., & Elseifi, M. (2022). Evaluation of Moisture Susceptibility and Chemistry of Recovered Asphalt Binders. In Tran-SET 2022, pp. 1-8, American Society of Civil Engineers, Reston, VA.
- Oyan, M. N. S., Hossain, Z., Islam, M. R., Braham, A., & Chun, S. (2023). Relative Compatibility Analysis of Aggregate-Binder Systems in Arkansas against Stripping. Journal of Materials in Civil Engineering, 35(9), 04023285. https://doi.org/10.1061/JMCEE7.MTENG-15772
- Rafiq, W., Napiah, M. B., Sutanto, M. H., Alaloul, W. S., Zabri, Z. N. B., Khan, M. I., Musarat, M. A. (2020) Investigation on Hamburg Wheel-Tracking Device Stripping Performance Properties of Recycled Hot-Mix Asphalt Mixtures. Multidisciplinary Digital Publishing Institute – Materials Journal.
- Rahmani, H., Shirmohammadi, H., and Hamedi, G. H. (2018). Effect of Asphalt Binder Aging on Thermodynamic Parameters and Its Relationship with Moisture Sensitivity of Asphalt Mixes, Journal of Materials in Civil Engineering, Volume 30, Issue 11, November 2018, https://doi.org/10.1061/(ASCE)MT.1943-5533.0002453.
- Rashid, A. M., and Hossain, Z. (2016). Morphological and Nanomechanical Analyses of Ground Tire Rubber Modified Asphalts, Innov. Infrastruct. Solut. 1, 36 (2016). https://doi.org/10.1007/s41062-016-0036-5.
- Rashid, F., Hossain, Z., Bhasin, A. (2019). Nanomechanistic Properties of Reclaimed Asphalt Pavement Modified Asphalt Binders Using an Atomic Force Microscope. International Journal of Pavement Engineering. 2019 Mar 4;20(3):357-65.

- Roy, S. and Hossain, Z. (2021). Use of Molecular-Level Dissipated Energy of Asphalt Binders to Predict Moisture Effects on Pavements. International Journal of Pavement Engineering, 22(11):1351-62.
- Tarefder, R. A., Zaman, A. M. (2010). Nanoscale Evaluation of Moisture Damage in Polymer Modified Asphalts. Journal of Materials in Civil Engineering;22(7):714-25.
- Tsai, B., Coleri, E., Harvey, J. T., Monismith, C. L. (2016). Evaluation of AASHTO T 324 Hamburg-Wheel Track Device Test. Construction and Building Materials. Volume 114, pp. 248-260
- Van Oss C. J., Chaudhury M. K., Good R. J. (1987). Monopolar Surfaces. Advances in Colloid and Interface Science. 28:35-64
- Yan, C., Zhang, Y., Bahia, H. U. (2020). Comparison Between SCB-IFIT, Un-Notched SCB-IFIT, and IDEAL-CT For Measuring Cracking Resistance of Asphalt Mixtures. Construction and Building Materials, Volume 252, 20 August 2020, 119060 https://doi.org/10.1016/j.conbuildmat.2020.119060.
- Yang, S., Braham, A., Underwood, S., Hanz, A., Reinke, G. (2017). Correlating Field Performance to Laboratory Dynamic Modulus From Indirect Tension and Torsion Bar. Road Materials and Pavement Design, 18:sup1, 104-127, DOI: 10.1080/14680629.2016.1267438
- Zhang, J., Apeagyei, A. K., Airey, G. D., Grenfell, J. R. A. (2015). Influence of Aggregate Mineralogical Composition on Water-Resistance of Aggregate-Bitumen Adhesion. International Journal of Adhesion and Adhesives, Volume 62, October 2015, Pages 45-54.

APPENDIX A Compatibility Database

Table A.21: Nomenclature of Aggregates Used in This Study

Aggregate Type	Aggregate Source	Nomenclature
Sandstone	Duffield Quarry (Blackstone Construction)– Gum Log Quarry, Russellville, AR; 2 miles west on Hwy 326	SS1
Sandstone	APAC-Central - Jenny Lind,	SS2
Novaculite	Gravel Mountain Quarries, Bismarck, AR; 9 miles west on Hwy 347	NV1
Novaculite	Redstone Construction - Little Rock Quarry, Little Rock, AR; I-430	NV2
Limestone	Benton County Stone - Mill Creek Quarry, Bella Vista, AR; At Bella Vista	LS1
Limestone	APAC Central - Sharp's Quarry, Lowell, AR; Junction of Puppy Creek Road and Wagon Wheel Road at I-540	LS2
Dolomite	Martin Marietta - Propst Pit #4, Black Rock, AR; 4 miles north on Hwy 63	DM1
Dolomite	Vulcan Materials. Black Rock, AR; 3 miles north on Hwy. 63	DM2

Table A.22: Nomenclature of Asphalt Binders Used in This Study

Binder Type	Binder Source	Nomenclature
PG 64-22	Ergon Asphalt and Emulsion, Inc. Memphis, TN	S1B1
	Marathon Petroleum Corporation Memphis, TN	S2B1
	Coastal Energy Corporation Willow Springs, MO	S3B1
	Ergon Asphalt and Emulsion, Inc. Vicksburg, MS	S4B1
	Holly Frontier Refining & Marketing LLC Catoosa, OK	S5B1
	Lion Oil Company Memphis, TN	S6B1
PG 70-22	Ergon Asphalt and Emulsion, Inc. Memphis, TN	S1B2
	Marathon Petroleum Corporation Memphis, TN	S2B2
	Coastal Energy Corporation Willow Springs, MO	S3B2
	Ergon Asphalt and Emulsion, Inc. Vicksburg, MS	S4B2
	Holly Frontier Refining & Marketing LLC Catoosa, OK	S5B2
	Lion Oil Company Memphis, TN	S6B2
PG 76-22	Ergon Asphalt and Emulsion, Inc. Memphis, TN	S1B3
	Marathon Petroleum Corporation Memphis, TN	S2B3
	Coastal Energy Corporation Willow Springs, MO	S3B3
	Ergon Asphalt and Emulsion, Inc. Vicksburg, MS	S4B3
	Holly Frontier Refining & Marketing LLC Catoosa, OK	S5B3
	Lion Oil Company Memphis, TN	S6B3

Table A.3: Relative Compatibility Based on the Surface Free Energy (SFE) Data (A = Best, D = Worst)

Binder/ Aggregate	SS1	SS2	NV1	NV2	LS1	LS2	DM1	DM2
S1B1	A	B	D	D	B	A	A	A
S2B1	B	C	D	D	C	A	A	B
S3B1	A	B	C	C	B	A	A	A
S4B1	A	B	D	D	B	A	A	A
S5B1	B	B	D	C	B	A	A	B
S6B1	A	B	D	D	B	A	A	A
S1B2	B	B	D	D	B	A	A	A
S2B2	A	B	D	D	B	A	A	A
S3B2	A	B	C	C	B	A	A	A
S4B2	B	B	D	C	B	A	A	A
S5B2	B	B	D	D	B	A	A	B
S6B2	A	B	D	C	B	A	A	A
S1B3	A	B	D	D	B	A	A	A
S2B3	A	B	D	D	B	A	A	A
S3B3	A	A	B	B	A	A	A	A
S4B3	A	B	D	D	B	A	A	A
S5B3	B	B	D	D	B	A	A	A
S6B3	A	B	C	C	B	A	A	A

Notes:

1. Compatibility Ratio (CR): If CR > 1.5 then the rank is A (very good); if $1.5 \geq CR > 0.75$ then the rank is B (good); if $0.75 \geq CR > 0.5$ then the rank is C (poor); if CR < 0.5 then the rank is D (very poor).
2. If this table is used, make the best effort to use aggregate-binder systems with a rank between A and B.
3. Between the ranking methods of SFE (Table 3) and the Texas Boiling Test (Table 4), Table 4 is preferred since it is based on test results of loose mixture samples. On the other hand, Table 3 is based on test results of binders and aggregates separately. Another reason for preferring Table 4 is that this ranking system has 8 categories (1 to 8), whereas Table 3 has only four categories (A, B, C, and D).

Table A.4: Ranking of Aggregate-Binder Systems Based on the Texas Boiling Test (TBT) (ASTM D 3625) (a Lower Rank Indicates Better Compatible Mix)

Binder/ Aggregate	SS1	SS2	NV1	NV2	LS1	LS2	DM1	DM2
S1B1	7	4	8	8	4	4	5	4
S2B1	7	3	7	7	3	7	4	4
S3B1	7	2	7	6	4	4	3	3
S4B1	6	3	7	6	3	5	3	3
S5B1	5	3	6	8	2	6	2	3
S6B1	5	3	6	7	2	4	3	3
S1B2	5	2	7	4	4	3	4	3
S2B2	8	3	6	8	2	4	4	2
S3B2	6	2	6	6	2	3	2	3
S4B2	4	2	6	5	3	3	3	2
S5B2	6	3	4	5	2	3	2	5
S6B2	5	2	4	7	2	4	3	2
S1B3	6	2	7	4	2	4	2	2
S2B3	6	3	4	7	2	4	2	2
S3B3	6	2	5	7	1	3	2	2
S4B3	2	1	2	1	2	1	1	2
S5B3	5	2	3	5	2	2	2	3
S6B3	5	2	4	4	2	2	3	1

Notes:

1. Rank: 1 if % asphalt retention (x) ≥ 85; 2 if 85 > x ≥ 70; 3 if 70 > x ≥ 60;4 if 60> x ≥50; 5 if 50 > x ≥ 40; 6 if 40> x ≥ 30; 7 if 30 > x ≥ 20; 8 if x < 20.
2. A rank of 1 is the best compatible aggregate-binder system, and a rank of 8 is the worst compatible system.
3. If this table is used, make the best effort to use aggregate-binder systems with a rank between 1 and 4.
4. Between the ranking methods of SFE (Table 3) and the Texas Boiling test (Table 4), Table 4 is preferred since it is based on test results of loose mixture samples. On the other hand, Table 3 is based on test results of binders and aggregates separately. Another reason for preferring Table 4 is that this ranking system has 8 categories (1 to 8), whereas Table 3 has only four categories (A, B, C, and D).

Doc Express® Document Signing History

Contract: RSCH - TRC2102 - Effect of Aggregate-Binder Compatibility on P rformance of Asphalt Mix in Arkansas Document: TRC 2102 Final Report

Date	Signed By
01/07/2024	Zahid Hossain Arkansas State University - Jonesboro Electronic Signature (Submitted)
01/08/2024	Robin Russell Arkansas Department of Transportation Electronic Signature (Received by RFC)

Doc Express® Document Signing History

Contract: RSCH - TRC2102 - Effect of Aggregate-Binder Compatibility on P rformance of Asphalt Mix in Arkansas Document: TRC 2102 Final Report

Date	Signed By
02/27/2024	Sanghyun Chun Arkansas Department of Transportation Electronic Signature (Reviewed by PM)
03/05/2024	Jason Hughey Arkansas Department of Transportation Electronic Signature (Reviewed by Committee Chair)
05/28/2024	Sarah Tamayo Arkansas Department of Transportation Electronic Signature (Reviewed by Research)